2014

CHARACTERIZATION OF NIPAH VIRUS PATHOGENICITY IN VITRO AND IN VIVO AND PROTECTION FROM DISEASE USING A SINGLE DOSE RECOMBINANT VACCINE

Blair Lynn DeBuysscher
The University of Montana

CHARACTERIZATION OF NIPAH VIRUS PATHOGENICITY *IN VITRO* AND *IN VIVO* AND PROTECTION FROM DISEASE USING A SINGLE DOSE RECOMBINANT VACCINE

By
BLAIR LYNN DEBUYSSCHER

Bachelor of Science, Biology, Hillsdale College, Hillsdale, MI, 2008

Dissertation
presented in partial fulfillment of the requirements
for the degree of

Doctor of Philosophy
in Microbiology and Immunology

The University of Montana
Missoula, MT

September 2014

Approved by:

Sandy Ross, Dean of The Graduate School
Graduate School

Scott Wetzel, Co-Chair
Cellular, Molecular, and Microbial Biology

Heinz Feldmann, Co-Chair
Rocky Mountain Laboratories

Steve Lodmell
Cellular, Molecular, and Microbial Biology

Jack Nunberg
Montana Biotechnology Center

Keith Parker
Department of Biomedical & Pharmaceutical Sciences

DeBuysscher, Blair, Ph.D., Fall 2014 Molecular Biology and Biochemistry

CHARACTERIZATION OF NIPAH VIRUS PATHOGENICITY *IN VITRO* AND *IN VIVO* AND PROTECTION FROM DISEASE USING A SINGLE DOSE RECOMBINANT VACCINE

Co-Chairperson: Scott Wetzel
Co-Chairperson: Heinz Feldmann

Nipah virus is a zoonotic pathogen that infects a wide species range including humans. It was first discovered in Malaysia in 1998 during a large outbreak, but since has spread to Bangladesh and India causing almost yearly outbreaks in the region since 2001. The distinct geographic locations have led to two genetically varied strains. Infection of humans by Nipah virus leads to respiratory distress and acute encephalitis. Pathology caused by the virus is characterized by vasculitis, necrosis, and edema of small vessels of the lung and brain primarily. This work investigates differences of pathology and clinical signs in the hamster model between strains, aiming to explain differences seen in epidemiology reports. We also characterize infection of endothelial and smooth muscle cells, which make up the vasculature, and how they react to infection. After better understanding the pathology *in vivo* and *in vitro,* we developed and efficacy tested a single-dose Vesicular stomatitis virus based vaccine. Data from this work demonstrates that although the Bangladesh strain is delayed 2 days compared to the Malaysian strain they cause similar pathology in hamsters. We also show that Nipah virus replicated in smooth muscle cells but does not cause adverse effects. Finally this study presents a vaccine that is protective against Nipah virus pathology. Overall this work allows for future studies using the Bangladesh strain, better defines infection of primary vascular cells, and proposes a possible vaccine candidate for outbreak use.

ACKNOWLEDGMENTS

I would like to thank my mentor Dr. Heinz Feldmann for his continual support and advice throughout my time in his lab. The environment he has set up in our lab has taught me to think like a scientist as well as to strive for more. I am very thankful for his support in training the next generation of scientists for level 4 work. I will always be grateful for the opportunity to follow my dreams and work with awesome viruses under containment.

Thank you to Ricki, Elaine, and Joe for all the time they spent training me and helping with level 4 experiments and samples. Without your willingness to help others I would still be sitting in the lab doing titrations and transferring samples. I am also thankful for the advise, support, and heckling of ALL LV members current and past. If I was to name you all this thesis would be another 100 pages, which goes to show you how much of a community has shaped my Ph.D. Your constant willingness to bounce ideas around and teach protocols made for a great learning environment. Thanks Dr. Sonja Best for being a mentor through this process. A big thanks goes to my cubical mates (Elaine, Eva, Marko, and Julie) for listening to me vent and always reminding me that I could do it. Julie, without your encouragement cards and thoughtful surprise gifts I may not have made it thorough some of the tough times. Your smiling face reminded me there was sunshine in everything. Thank you Marko for being the other graduate student and being there for last minute lunches, support, and making me soft pretzels among other yummy baked goods.

Thank you to my Hamilton and Missoula family and friends: Jose, Martin, Anthony, Son(j)ia, Sara, Beth, Katherine, Whitney, Mike, Meghan, Ron, Kathy, Patty

Paul, Katy, Toby, Matt, Kamden, the Carmona's and Robinsons, the Goheen's, and Merick, Ernie, Bear, Zoe, and Baloo! My time in Montana and my life has been enriched with your company and support.

I would also like to thank Dr. Scott Wetzel for heading my committee and being my university liaison. I appreciate all the help getting GPP/ UM stuff figured out. A big thanks for keeping me on track (even if you had to hunt me down) and also sitting down with me whenever I needed to talk. Drs. Steve Lodmell, Jack Nunberg, and Keith Parker thank you for your time and expertise on this project and in my scientific education.

Finally I would like to thank my family: Mom, Dad, Carlie, Adam and Klayton!!!!! You guys have always been there for me from the beginning, including suffering through listening to the Hot Zone on vacation (thank you Wenzel family for humoring me too!!!!) and understanding and getting over me working in level 4. I would not have made it through this process without your constant support and encouragement. We may be far apart but your love makes it fell like we are closer than ever.

Ha Joe, you thought I forgot you! Words (or at least mine) cannot explain how much you have been an invaluable part of my time in Montana. I will never forget our endless hours in level 4 when I would talk your ear off and you would become my personal slave, pipetting till our hands cramped and we were fantasizing about food and peeing. I hope that whenever you see/read the Hunger Games you remember that first 40 entries. Thank you for shaping me into a scientist, I really appreciate all the hard work you put into getting "your 2nd Ph.D.". I am very grateful to be able to call you a friend!! We have had some great times from rope climbing freak-outs to leading, from no bike to

3, from Yellowstone to Glacier, from pre-doc to doctor and hopefully much more… Call me when you need a staff scientist ☺

TABLE OF CONTENTS

LIST OF FIGURES

LIST OF TABLES

CHAPTER 1 INTRODUCTION

Henipavirus

The family Paramyxoviridae of the order Mononegavirales consists two subfamilies Paramyxovirinae and Pneumovirinae. Paramyxovirinae include four genera, *Respirovirus, Morbillivirus, Henipavirus,* and *Rubulavirus* (1). Members of this family are enveloped negative- sense single stranded RNA viruses that cause disease in vertebrates. Hendra virus, Cedar virus and Nipah virus are part of the genus *Henipavirus*. Hendra virus and Nipah virus are highly virulent zoonotic pathogens. Cedar virus is newly discovered and is yet to be only found in the bat reservoir (2). These viruses are classified as select agents and must be worked with under biosafety level 4 conditions. They are pleomorphic in structure varying in size from 180- 1900nm, averaging 500nm (Figure 1-1c), making them longer than other paromyxovirses (3). Like other Paramyxoviruses, Henipaviruses, code 6 genes in a non-segmented genome as seen in Figure 1-1a. The genes encoded from 3' to 5' are the nucelocapsid (N), phosphoprotein (P), matrix (M), fusion (F), glycoprotein (G), and the large polymerase (L). The genomes of Nipah virus and Hendra virus are longer than those of the other paromyxoviruses being 18,246 and 18,234 nucleotides respectively but share a high sequence homology (4, 5).

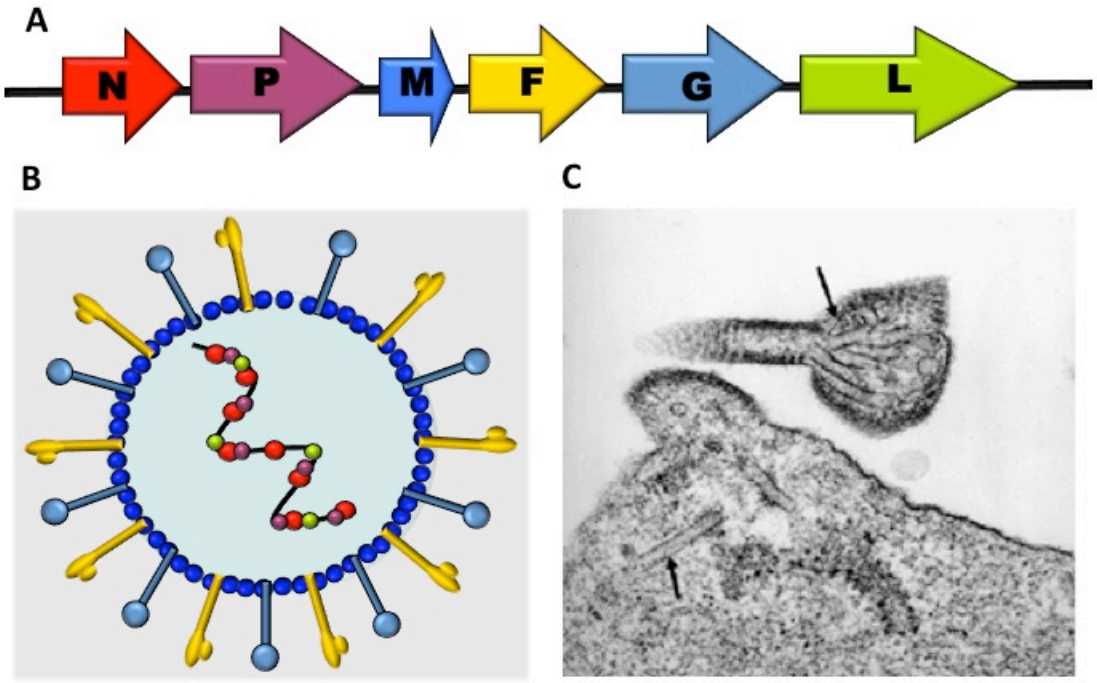

Figure 1-1: Schematic representation and electron micrograph of Nipah virus.

(A) Schematic retranslation of Niaph virus genome. Arrows represent open reading frames encoding the nucleocapsid protein (N), phosphoprotein (P), matrix protein (M), fusion protein (F), glycoprotein or attachment protein (G) and large protein (L) or RNA polymerase. (B) Representation of Niaph virus structure. The RNP complex is located in the center of the virus shown in red, purple, and green with the virion RNA in black. The matrix protein (dark blue) makes up virion architecture, underlying the viral envelope. The surface of the virion is covered with the attachment glycoprotein in light blue and the fusion protein in yellow. (C) Electron micrograph of Niaph virus budding from a cell. Micrograph reprinted with permission from Lippincott Williams (6). Copyright © 2013, Lippincott Williams, a Wolters Kluwer business

Nipah Virus Replication Cycle

Receptor binding and fusion

The receptor for Nipah virus was identified as the receptor tyrosine kinase, ephrin B2 (7, 8). Ephrin is a type I transmembrane protein that is the ligand for EphB4/B2. Ephrins are highly conserved ligands that function in cell-to-cell interactions, signaling, angiogenesis and neuronal axon guidance (9–11). Eprhrin B2 is expressed on vascular endothelial cells, with high expression in the lung and brain. Ephrin B3 expression is limited to the CNS and heart. Ephrin B2/B3 expression is consistent with Nipah virus tropism (7, 8, 10, 12, 13). Nipah virus was found to have high affinity for ephrin B2 with slightly less affinity for ephrin B3 (12, 14). Nipah virus has two surface proteins: the glycoprotein (G) and fusion (F) protein. G functions as the attachment protein binding ephrin B2/B3. G binding to its receptor triggers F, which acts to fuse the virus to the cell membrane independent of pH. However there is some evidence that macropinocytosis could also aid in cell entry (13).

Replication

Once the virus has fused with the cell membrane the ribonucleocapsid enters the cytoplasm of the cell and the viral mRNA acts as the template starting transcription (Figure 1-2) (15). Transcription is initiated at the promoter region in the 3' UTR. Each of the 6 genes have individual start and stop sequences with intergenic regions between genes (1). The Nipah genome only has one promoter thus if the polymerase complex (P/L) falls off the template re-initiation will only occur at the 3'UTR, this results in a differential gradient of transcription. This means that transcripts closer to the 3' end will be more abundant than ones towards the 5' end (16). This process results in accumulation

of viral proteins in the cytoplasm. After accumulation of unassembled nucleocapsid protein, replication of the genome begins producing a full-length (+) sense anti-genome, which is the template for the new (–) sense RNA (6). Once completed genomes are encapsidated by the nucleoprotein forming the ribonucleoprotein (RNP).

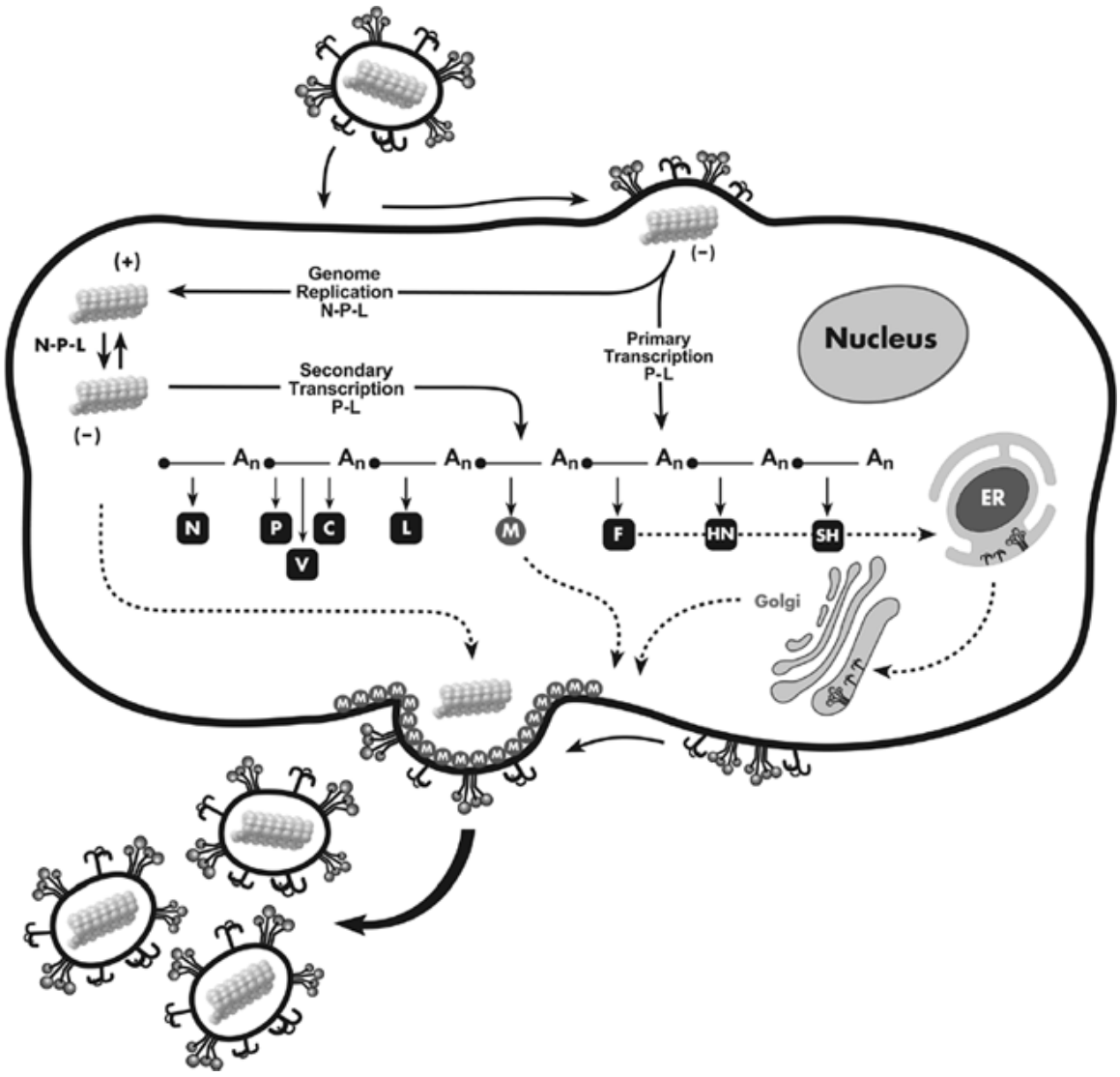

Figure 1-2: Replication schematic of paramyxovirus life cycle.

An incoming virion fuses with the plasma membrane and releases the RNP into the cytoplasm. mRNA is represented by solid lines with closed circles at the 5' end and An representing the 3' poly A tail. Dotted lines represent intracellular transport. Reprinted with permission from Lippincott Williams (6). Copyright © 2013, Lippincott Williams, a Wolters Kluwer business.

Budding and egress

Both glycoproteins are processed after translation, prior to their association with the membrane for incorporation into a new virion. G is synthesized in the endoplasmic reticulum (ER) then matured through the golgi, eventually trafficking to the cell membrane. F is also synthesized transported to the ER as an inactive precursor that is proteolytically activated in the trans-Golgi network then trafficked to the plasma membrane (6, 17, 18). Nipah budding is thought to be triggered by the accumulation of matrix protein; matrix protein alone can produce virus like particles (19). The matrix protein is trafficked to the nucleus for post-translational modification then returns to the membrane to bridge the glycoproteins in the membrane with the RNPs (6, 20). In Nipah replication, viral proteins associate with specific sites on the host cell membrane, where they pinch off and result in a virion with an envelope containing host-derived membrane that contains viral glycoproteins encapsulating matrix proteins and RNPs (15).

Nipah Virus Epidemiology

Discovery of Nipah virus

Malaysian outbreak

In 1998 there was an outbreak of respiratory sickness in swine in Malaysia. Soon after the agent jumped to the pig handlers causing similar respiratory symptoms as well as encephalitis. The outbreak originated in Northwestern peninsular Malaysia but quickly spread into the south as well as into Singapore (through pig exportation) (21, 22). At first the outbreak was misdiagnosed as Japanese encephalitis virus, which is endemic in rural Malaysia (23). The outbreak continued into 1999 infecting more than 250 humans with

over 100 fatalities (24). In mid-March 1999 the causative agent was identified as a Hendra-like virus and subsequently named Nipah virus after the home village of the patient the virus was isolated from (4, 25–27). Later sequencing of Nipah virus isolates showed that pig and human isolates are very similar thus the outbreak could have been caused by as little as 1 or 2 introductions (28, 29). Retrospectively, it is thought that Nipah virus may have emerged as early as 1997, when unexplained small scale pig deaths were reported as well as 6 causes of encephalitis that later tested positive for Nipah specific IgG (21).

The risk factors associated with this outbreak focused on direct contact or close proximity to pig or pig secretions (30, 31). This led to quarantining infected pig farms, evacuating people out of infected areas and public announcements about how to properly protect yourself when dealing with swine (23). Eventual containment of the outbreak was brought about by culling of over a million pigs in the infected areas as well as the discontinuing exportation until the outbreak subsided (22, 26, 31). These precautions eventually led to the end of the outbreak.

Bangladesh outbreaks

After the initial outbreak ending in 1999 Nipah virus was dormant in the human population until 2001 when it emerged on the Indian subcontinent. Since the first outbreak there have been almost annual small-scale outbreaks occurring in Bangladesh and India. Even though positive serology was identified no virus was isolated from the Bangladesh/ India outbreaks until 2004 when it was confirmed to be Nipah virus (32). Differing from the Malaysian outbreak, the Bangladesh outbreaks are small, still occurring, and do not involve pig farms. Bangladesh lacks large-scale pig farms, instead

individual families may have a small number of various species of animals. Sequencing of virus isolates from the numerous outbreaks have shown over 23 individual introductions with higher variation than the Malaysian isolates (33). In comparing the Bangladesh outbreaks over time it appears that the average case fatality is 70% (33). Another difference between the Malaysia and Bangladesh Nipah virus is that the Bangladesh outbreaks support human to human transmission with about 7% of individuals spreading disease to a median of 7 people (33).

Animal hosts

Natural animal hosts

During the Malaysian outbreak field investigations looking for an animal host were initiated. Due to its similarities with Hendra virus fruit bats of the family Pteropus were heavily focused on as a possible natural reservoir. In a study done in 2001 collecting blood for serologic data Yob et al. found a prevalence of 25% in fruit bats in Malaysia but no virus was isolated (34). Urine and fecal samples were also collected for sampling of Nipah virus in hopes of isolating virus (35). Nipah virus was later isolated from pooled urine (36). It was also demonstrated that bats intermediately shed virus even though they show no signs of disease (37, 38). Further study of Pteropus bats have shown henipavirus positive bats in Malaysia, Cambodia, Bangladesh, and Africa following the bats geographic range, suggesting the possibility of spread of the virus outside current endemic areas (34, 39–42).

As previously stated pigs played a large role in the Malaysian outbreak. Once Nipah virus entered a large pig farm the virus spread rapidly with a close to 100% infection rate. Incubation in these animals was 7-14 days and mortality was between 5-

15% (43). If signs of disease were seen they included neurologic signs in older pigs as well as increased abortions and respiratory signs in younger pigs. Other domestic animals tested positive in Malaysia but none as high in prevalence as pigs and bats. It is believed that theses animals, which include dogs, cats, and goats, became infected from pigs or bats and were dead end hosts (26, 34, 43, 44). Differing from the Malaysian outbreak there is thought to be no intermediate host during Nipah Bangladesh outbreaks.

Experimental animal models

Experimentally various species have been identified to support Nipah virus infection, replication, and disease. Guinea pigs were examined as a model and support viral replication; however, in general clinical presentation seemed to be mild to asymptomatic but death can occur (45). Infection in guinea pigs causes systemic vascular disease, fever, weight loss, and twitching. Another animal model for Nipah virus is the cat. This model mimics human disease showing signs of respiratory distress including fever and elevated respiratory rate, however there is no evidence of encephalitis in cats (46, 47). Cats present with clinical signs from day 4 to 8 with systemic vascular disease leading to death. Pigs have been infected experimentally and disease is similar to that which is seen with natural infection with high morbidity and low mortality (46, 48). However, like natural infection, experimentally some pigs are asymptomatic. If pigs do develop signs of infection it is often age dependent with older animals having neurologic signs and respiratory distress in younger animals (43, 46, 49).

The three animal models used the most in Nipah virus research include hamsters, ferrets, and nonhuman primates. Hamsters are a small animal model that mostly recapitulates human disease. These animals have clinical signs of both respiratory disease

as well as neurologic involvement (50) Hamsters have systemic vasculitits with pathology of the lung and brain often leading to death. Viral shedding is detectable and transmission is possible (51, 52). In the hamster model dose and route of infection affect disease outcome; low dose infections end in encephalitis around day 12 post challenge while high does infections are more respiratory and animals start to die around day 5 post challenge (53). Anther animal model that displays both respiratory and neurologic signs is the ferret. Infected ferrets present between days 6-10 post challenge with cough, depression, nasal discharge, and hind limb paralysis (54). Viral shedding does occur and disease is lethal. Another animal model for Nipah disease is the nonhuman primate. Both squirrel monkeys and African green monkeys have been infected and show clinical disease. Squirrel monkeys only show mild clinical diseases in about half of challenged individuals but infection can be lethal (55). The nonhuman primate model that more closely resembles human disease is the African green monkey. This model is close to human disease presenting with both respiratory ad neurologic symptoms about 7 days post challenge (56). This model is mostly lethal at high doses and characterized by pathology of the lung and brain, frothy discharge, viral shedding and endothelial syncytia.

Transmission

Transmission of Nipah virus Malaysia strain is thought to have occurred from bat to pig to human, mainly focusing on oral and urogenital secretions from pigs as the route of transmission (23, 30, 57). This transmission route is supported by the fact that educating people about proper personal protective equipment as well as culling pigs led to the end of the outbreak (26). There has however been some evidence that suggests

there could have been a few cases of infection passed from patient to healthcare worker. In a serologic study in Malaysia of 363 healthcare workers from hospitals that handled most Nipah patients, only 3 had positive Nipah IgG titers with no IgM or neutralization detectable (58). All 3 nurses described caring for Nipah infected patients for over a month. Of these 3, 2 described mild febrile illness prior to blood sampling. Another study also found 1 asymptomatic nurse with antibodies positive for Nipah (59). The finding of 4 health care workers with antibodies against Nipah virus suggests that person-to-person transmission may have occurred in Malaysia.

In the Bangladesh outbreaks it is thought that the virus is spread from bats to humans from drinking raw date palm sap or coming in direct contact with bat secretions (41, 60). One of the reasons that date palm sap is a possible transmission route is that Nipah virus outbreaks in Bangladesh coincide with the date palm harvest season, late December to early April (33). At this time, bark is shaved off the tree and a tap is inserted allowing sap to drip into open pots. Pots are collected daily and sap is sold for immediate consumption (raw) as well as processing into molasses (61, 62). Reports of bats visiting sap harvest locations were confirmed by infrared photography, which documented 185 bat visits in 20 nights with 84% of the bats directly contacting the sap (41). In case studies it has been found that there is a higher reporting prevalence of infected individuals having contact with or drinking raw date palm sap than not (63). However, Nipah virus has not been isolated from date palm sap. Several experimental studies have shown that Nipah virus is recoverable from various juices (mirroring fruit dropped from bats) and artificial date palm sap days after being spiked with virus (52, 64).

Also differing from the Malaysian outbreak, transmission in Bangladesh has been attributed to person-to-person contact (44, 65–67). In reviewing cases between 2001-2007 in Bangladesh, Luby et al. found that out of 122 patients questioned 51% became sick after having direct contact with an infected patient 5-15 days earlier (33). Human to human spread of virus is thought to be attributed to respiratory droplets released during coughing fits. In a later study it was identified that 7% of cases transmit infection, most often to health care workers or family members (68). Two outbreaks, one in 2001 in India and one in 2004 in Fardpur supported the largest number of person-to-person transmission as well as spaned up to 5 generations of person-to-person transmission (67, 69). There has also been documentation of corpse-to-human transmission of the virus (70). A few studies suggest nosocomial transmission and in one study swabs were taken of the walls and bed frame of a patients room and found to be positive 5 weeks after death, supporting environmental stability and nosocomial transmission (58, 67, 70, 71). Experimentally, the Bangladesh strain of Nipah virus has been identified in respiratory secretions and oral/ nasal swabs and has been documented to be transmitted by direct contact and, not as efficiently, by fomite in the hamster model (51, 72). Together these data support a more efficient person-to-person transmission of the Bangladesh strain over the Malaysian, with the lack of an intermediate host identified in Bangladesh.

Human disease

Clinical manifestations

Incubation periods for Nipah virus is estimated to be 4-45 days with most incubation periods lasting 2 weeks (73, 74)The average duration of illness in humans for Nipah virus is around 9 days (from fever to death) but has lasted anywhere from 2-30

days with some patients recovering (75). The age range of infected individuals is a large spread, 2-75 years, with variations in average age between outbreaks, most often middle age individuals are infected (73, 75, 76). In the case of the Malaysian outbreak the male to female ratio was highly skewed towards males, however this could be attributed to the route of infection and the male prevalence in pig handling (75). The male to female proportion throughout the Bangladesh outbreaks are still male skewed but are close to 50/50 (67, 73). Generally Nipah virus symptoms fit under two categories: respiratory distress or acute encephalitis. Major clinical symptoms of Nipah virus infection in humans are listed in Table 1-1. Generally, patients present with flu like symptoms including fever, headache, drowsiness, myalgia, and dizziness (73, 74). Other manifestations of Nipah virus infection include are flexia, fast resting heartbeat, high blood pressure, segmental myoclonus, and doll eye syndrome (6). The Malaysian strain of the virus had higher prevalence of acute encephalitis than the Bangladesh isolate (74). Neurologic symptoms are paired with MRI results of disseminated small discrete lesions in the white matter and to lesser extent the gray matter (74, 76, 77). Respiratory distress is characterized by difficulty breathing, coughing, shortness of breath, and atypical pneumonia (73).

Table 1-1: Common clinical symptoms and other features of Nipah virus infection.

General	Respiratory	Neurologic
fever	cough	convulsions
headache	shortness of breath	abnormal reflex
dizziness	respiratory difficulty	altered mental status
myalgia	abnormal chest radiographs	unconsciousness
severe weakness	Interstitial pneumonia	elevated lymphocytes in CSF
vomiting		Elevated protein in CSF
diarrhea		lesions in white and gray matter

Both outbreaks support relapsing encephalitis, often occurring in people with a primary infection that was acute or asymptomatic. Late-onset or relapsing infection can occur anytime from months to years later and is often associated with neurological sequel (74, 76, 78, 79). About 10% of survivors experience relapse but it is speculated that this could be an underestimate (79). Magnetic resonance imaging (MRI) findings from relapsing patients often showed a change from discrete small legions to more confluent wide spread lesions (74). Symptoms associated as high risk factors for a poor outcome are brain stem involvement, virus in the cerebrospinal fluid (CSF), and seizures (24, 74).

Pathology

Most of what we know about human pathology comes from the Malaysian outbreak, where necropsies were more common. Common pathologic findings central to disease include systemic vasculitis, endothelial destruction, and CNS involvement (76, 80). Specifically, Nipah virus pathology affects blood vessels of the CNS, lung, heart, and kidney. Typically small vessels (e.g. capillaries, venules) showed vasculitis, while medium to large vessels remained uninfected (75, 77). Vasculitis is characterized by destruction of the endothelium, mural fibroid necrosis and karyorrhexis (Figure 1-3). There are also reports of inflammatory infiltration, thrombosis, necrosis, and hemorrhaging in infected vessels. In some cases giant multinucleated syncytia, are seen in vessel walls and endothelial cells throughout infected organs. Syncytia formation is more prevalent in cases were duration of illness lasts from 6-15 days (75).

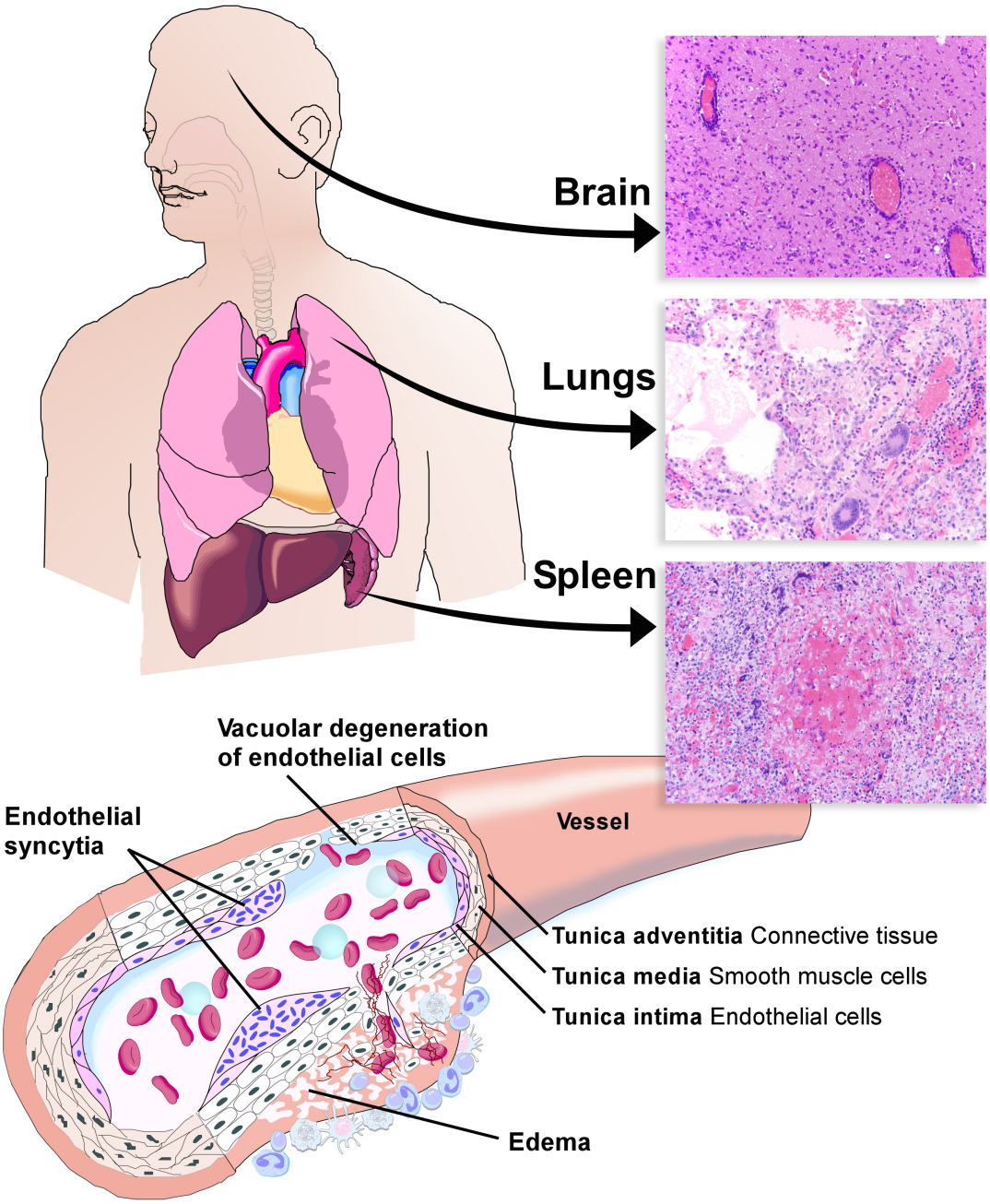

Figure 1-3: Cartoon representation of pathology caused by Niaph virus infection.

The major organs affected by Nipah virus pathology include the brain, lung and spleen. The images on the right are from the organs of experimentally infected animals showing

a representation of classic Nipah virus pathology. Vasculitis is central to infection and is characterized by edema, fibrin, perivascular inflammation, and endothelial syncytia.

The main infection induced pathology findings are in the CNS, paricularly brain. Again, vascular induced thrombosis was observed along with parenchymal necrosis. There are also appearances of some viral inclusions throughout both the white and gray matter. Matching MRI findings taken during infection, necrotic legions or plaques were observed with microcystic degeneration, microinfractions, and perivascular cuffing (75, 77, 80). Immunohistochemistry (IHC) staining of the CNS showed Nipah positive antigen staining in blood vessels as well as neurons that are associated with vasculitis or necrotic plaques (75). There is also positive staining in viral inclusions.

Other organs are also affected during infection. The lung is the next location of prominent virus induced pathology. Findings of vasculitis and necrosis are associated with small blood vessels. Syncytial cells are observed in alveolar spaces along with hemorrhaging causing pulmonary edema (75). Besides the lung and CNS pathology is observed in the spleen, lymph nodes, kidney and heart. Pathology documented in these organs consisted of vasculitis, fibroid necrosis, and some hemorrhaging (75). IHC staining for Nipah virus in these organs mainly focuses around blood vessels. Specifically in the endothelium and tunica media (smooth muscle cells surrounding vessels) (75).

Pathology of late-onset encephalitis differs significantly from acute pathology. In the case of late-onset encephalitis the few necropsies performed show no vasculitis in any organ (81). Pathology in the CNS is more predominant and disseminated compared to acute encephalitic patients (78, 81). The viral inclusions in relapse patients are larger and more extensive. Lesions of the parenchymal are more confluent and larger causing

neuronal loss and gliosis (59). Also differing from acute infection peracymal cuffing is limited and necrotic plaques are not found (75). Viral staining of these patients demonstrate prominent glial and neuronal staining that are more diffuse than acute patients with no blood vessel staining (75).

Cell tropism

Nipah virus pathologic features can be attributed to the tropism of Nipah virus. Nipah virus cell tropism is linked directly to receptor expression. Ephrin B2 and B3 are the receptors of the virus associating with the G of the virus. Ephrin B2 is found on arterial endothelial cells, smooth muscle cells, as well as neurons while ephrin B3 is more closely associated with the brain stem (10, 17). Ephrin expression levels vary in different organs and thus regulates Nipah virus infection (10). Ephrins are very conserved proteins, which probably accounts for the wide species range of Nipah virus (82). In cell culture, permissiveness of cells to Nipah virus has been linked to ephrin expression, however few cases of non-ephrin binding have been observed as well as the involvement of macropinocytosis (13, 82, 83). In general the virus favors vascular tropism, infecting endothelial cells and the tunic media as well as neuronal cells (80). Major organ and cell types found to be involved during Nipah virus infection are summarized in Table 1-2 (17).

Table 1-2: Organ and cells tropism of Nipah virus infection in Humans.

Organ	cell types infected
Brain	endothelial cells
	tunica media
	neurons
	rare- glical cells, ependyma
Lung	endothelial cells
	tunica media
	rare- bronchiolar epithelium
Spleen	Periarteriolar sheath cells
	macrophages
Kidney	endothelial cells
	tunica media
Heart	endothelial cells
	tunica media

Treatment and Prevention

Treatment

Since the discovery of Nipah virus there have been numerous attempts to discover a treatment for infection (Table 1-3). At the time of the Malaysian outbreak Ribavirin, a nucleoside inhibitor used to stop viral RNA synthesis, was made available to patients; this antiviral has been shown to be effective against other RNA viruses including Respiratory syncytial virus (84). The drug was given to 140 patients with 54 patients acting as controls. Patients in the Ribavirin group had a mortality rate of 32% compared to 54% in the control group, hospital stay and time on a ventilation system were also shorter in the treated group (85, 86). In an experimental setting Ribavirin limits replication in vitro (87–89). However, when Ribavirin was tested in the hamster model against Nipah virus, alone and in combination with Chloroquine, protection was not afforded (90, 91). Ribavirin was also evaluated in the African green monkey as a treatment option against Hendra virus and found to increase time to death, but not decrease mortality skewing disease to encephalitis over respiratory signs (92). Currently, Ribavirin is not used as a treatment option against Nipah virus.

Another treatment option proposed for Nipah virus are fusion inhibitory peptides. The peptides act to blocking fusion of the F protein with the cellular membrane. By using the conserved heptad repeat region in the fusion protein of Hendra virus, Nipah virus, or human parainfluenza virus 3 researchers have been able to reduce cell fusion in tissue culture as well as show plaque reduction against live Nipah virus (93–97). It is proposed that the fusion inhibitory peptides act after the fusion protein undergoes conformational

changes inhibiting its structural formation into a 6-helix coiled coil bundle, which is needed for fusion (97, 98).

Another strategy under development as a treatment against Nipah virus is antibodies. Early studies showed that passive transfer of polyclonal sera from vaccinated hamsters could be used to prevent death in naive hamsters given before Nipah virus challenge (99). Evolution of antibody therapy against Nipah virus focuses on monoclonal antibody development. First attempts used murine derived antibodies against NiV-F or NiV-G. Both F and G derived antibodies protected hamsters before challenge. The antibody against NiV-F protected100% of animals 1 hour after challenge and 50% if administered 24 or 48 hours after while the NiV-G antibody only protected 50% 1 hour after (100).

Next generation antibodies came from using a peptide display library and a human monoclonal antibody that could neutralize both Hendra and Nipah viruses (101). This antibody, m102.4, was then fully matured creating a full length human IgG antibody that is fully cross neutralizing against both viruses (102). This antibody was tested post challenge in the ferret model (Nipah virus challenge) and the African green monkey (AGM) model (Hendra virus challenge) and was found to be protective (54, 103). In ferrets the antibody was given 10 hours post challenge and showed protection (54). In the AGM m102.4 was given 10, 24, or 72 hours after challenge and again 48 hours after the first dose resulting in complete protection (103, 104).

Table 1-3: Treatments tested against Nipah virus infection.

Treatment	*in vitro*	Species	Efficacy	Reference
Ribavirin	Cell culture		• Reduced replication	(87–89)
		Human	• Reduced mortality	(85, 86)
		Hamster	• None	(90, 91)
		NHP	• None • Encephalitis skewed	(92)
Inhibitory peptides	Cell culture		• Reduced fusion • Reduced plaques	(93–97)
Sera transfer		Hamster	• Protection	(99)
Murine antibody		Hamster	• Protection	(100)
Humanized antibody m102.4	Cell culture		• Neutralization	(101, 102)
		Ferret	• Protection	(54)
		NHP	• Protection	(103)

Vaccines

As early as 2004 possible vaccine candidates were starting to be developed against Nipah virus infection (Table 1-4). Approaches focused on the surface glycoproteins G and F of Nipah virus. Due to biocontainment requirements some vaccine studies were performed without challenge. This study measured immune response to infection rather than efficacy. One such study was used a recombinant Newcastle disease virus expressing F or G as a vaccine vector. This vector was tested in mice and pigs using a prime boost strategy (105). Both vectors produced an antibody response as well as demonstrated neutralization suggesting the possibility of protection; however, animals in this study were never challenged. Another approach at protecting against Nipah virus disease focused on Venezuelan equine encephalitis replicon particles encoding G or F from Nipah virus (106). This vaccine was administered in 3 doses to mice and produced antibodies and neutralizing antibodies. Virus like particles (VLP) were also tested as a possible vaccine. This multi-dose vaccine was produced by expressing Nipah virus M, G, and F. The particles were fusogenic in nature and looked like wild type virions by electron microscopy. Antibody production and neutralization were measured after mice were immunized 3 times.

The next batch of vaccine candidates were tested in the hamster model testing for both immune response and efficacy. A DNA vaccine in two doses using codon optimized Nipah F or G in expression plasmid pCAGGS was perfrmed in mice (107). The presence of antibodies and neutralizing antibodies were used to support the possibility of efficacy. In a study using the hamster model, this approach did not protect animals from lethal Nipah virus challenge (DeBuysscher et. al, unpublished). Another candidate was created

using Vaccinia virus recombinants expressing Nipah virus G or F as well as a co-immunization with both F and G constructs in a prime boost strategy (99). Hamsters had high levels of neutralizing and non-neutralizing antibodies and were protected from infection with no detectable virus after challenge. This study also completed a passive transfer of sera from vaccinated hamsters to naïve animals; again protecting 100% of animals from disease, suggestion antibodies were important for protection. One of few single dose vaccines candidates include an adeno- associated virus (AAV) expressing G (108). This vector was tested in hamsters with 100% protection. After vaccination neutralizing antibodies were measured.

Another disease model used in some studies to test efficacy is the pig, which is the intermediate Nipah virus host. A recombinant Canarypox virus expressing F or G and was tested with a prime boost vaccination schedule (49). Vaccinated pigs were protected, having no evidence of viral shedding, only low levels of Nipah RNA were detected in the olfactory bulb, trigeminal ganglion, and trachea, however no virus was isolated and there was little pathology compared to controls. This vaccine also produced neutralizing antibodies. Other large animal model for Nipah infection that has been used for vaccine efficacy testing is the cat and ferret. A recombinant soluble glycoprotein (sG) of Nipah or Hendra viruses were produced and coupled with CpG and administered in multiple doses to cats and ferrets to test the efficacy (109–111). These studies found that the sG from Hendra virus was more cross-reactive, thus this antigen was focused on. Immunization with sG is thought to block receptor and to produce high levels of neutralizing antibodies. Ferrets challenged 20 days after immunization or 12 months after immunization were protected from disease (111). Two separate studies propose a non-replication

recombinant Vesicular stomatitis virus (rVSV) as a vector for Nipah vaccination (112–114). Both studies use a rVSV lacking its own glycoprotein and coding for Nipah virus F or G or a single-cycle F and G rVSV. Constructs protect hamsters or ferrets from disease and reduce virus replication in tissues. The constructs, when administered produce a strong immune response with neutralizing antibodies.

One vaccine was tested in the African green monkey model of Nipah virus infection. This vaccine was administered in multiple doses with a vector based on a measles recombinant system expressing Nipah G (115). This vaccine was tested in hamsters and African green monkeys in 2 doses and demonstrated protection against lethal outcome and disease.

Table 1-4: Vaccine candidates against Nipah virus infection.

Vaccine platform	Species	Vaccine schedule	Nipah virus challenge dose (route)	Efficacy	Ref.
Newcastle virus expressing either F or G	Mice Pigs	Prime with 1 boost	N/A	• T-cell response • Neutralizing antibodies • Long lasting	(105)
Venezuelan equine encephalitis virus expressing G or F	Mice	Prime with 2 boosts	NA	• Neutralizing antibodies	(106)
VLPs comprised of G, F and M	Mice	Prime with 2 boosts	NA	• Neutralizing antibodies	(116)
DNA vaccination (pCAGGS G or F)	Mice Hamsters	Prime with 1 boost	NA	• Neutralizing antibodies • No protection in hamsters	(107)

Vaccinia virus (VV) expressing G and/or F	Hamster	Prime with 1 boost	$1x10^3$ PFU (intraperitoneal)	• Protection • Passive antibody-protects	(99)
Adeno associated virus (AAV) expressing G	Mice Hamster	Single immunization	1e4 PFU, Nipah or Hendra	• 100% Nipah • 50% Hendra • Antibodies in mice	(108)
Recombinant canarypox virus expressing G or F	Pigs	Prime with boost	$2.5x10^5$ PFU (intranasal)	• Reduction in virus • Inhibition of viral shedding	(49)
Soluble Nipah or Hendra G	Cats ferrets	Prime with boost Prime with 2 boosts	$5x10^4$ $TCID_{50}$ (oronasal) $5x10^2$ $TCID_{50}$ (subcu.)	• Protection • Non-sterile immunity	(109–111)
Recombinant vesicular stomatitis virus (VSV) expressing G or F	Mice Hamsters Ferrets	Single immunization	N/A	• Neutralizing antibodies • Protection in hamsters	(112–114)
Recombinant measles virus expressing G	Hamster NHP	Prime with 1 boost	N/A	• Protection in hamsters • No clinical signs in NHP	(115)

CHAPTER 2 AIMS

Goal: To understand pathogenesis of Nipah virus and to create a vaccine to protect against Nipah virus infection and disease.

Specific Aim 1: Comparison of the pathogenicity of Nipah virus isolates from Bangladesh and Malaysia in the Syrian hamster.

We hypothesize that infection and disease caused by Nipah Bangladesh will be more severe that Nipah Malaysia. In this aim we will establish the hamster as a model for Nipah Bangladesh as well as compare infection and pathogenicity of Nipah Bangladesh and Nipah Malaysia.

Specific Aim 2: Defining the mechanisms of pathogenicity of Nipah virus in smooth muscle and endothelial cells.

We hypothesized that Nipah virus infects and replicates in endothelial and smooth muscle cells, leading to viral pathogenesis and cell destruction. In this aim we plan to further characterize the role of these two important cell types for Nipah infection and pathogenicity both *in vivo* and *in vitro*.

Specific Aim 3: Development and characterization of a recombinant vesicular stomatitis virus based Nipah vaccine.

We hypothesize that a replicating recombinant vesicular stomatitis virus based vector expressing Nipah proteins (antigens) is an effective vaccine candidate. In this aim we will use the hamster model to test the immunogenicity and efficacy of a new Nipah vaccine candidate.

CHAPTER 3 COMPARISON OF THE PATHOGENICITY OF NIPAH VIRUS ISOLATES FROM BANGLADESH AND MALAYSIA IN THE SYRIAN HAMSTER

Abstract

Nipah virus is a zoonotic pathogen that causes severe disease in humans. The mechanisms of pathogenesis are not well described. The first Nipah virus outbreak occurred in Malaysia, where human disease had a strong neurological component. Subsequent outbreaks have occurred in Bangladesh and India and transmission and disease processes in these outbreaks appear to be different from those of the Malaysian outbreak. Until this point, virtually all Nipah virus studies *in vitro* and *in vivo*, including vaccine and pathogenesis studies, have utilized a virus isolate from the original Malaysian outbreak (NiV-M). To investigate potential differences between NiV-M and a Nipah virus isolate from Bangladesh (NiV-B), we compared NiV-M and NiV-B infection *in vitro* and *in vivo*. In hamster kidney cells, NiV-M-infection resulted in extensive syncytia formation and cytopathic effects, whereas NiV-B-infection resulted in little to no morphological changes. *In vivo*, NiV-M-infected Syrian hamsters had accelerated virus replication, pathology and death when compared to NiV-B-infected animals. NiV-M infection also resulted in the activation of host immune response genes at an earlier time point. Pathogenicity was not only a result of direct effects of virus replication, but likely also had an immunopathogenic component. The differences observed between NiV-M and NiV-B pathogeneis in hamsters may relate to differences observed in human cases. Characterization of the hamster model for NiV-B infection allows for further research of the strain of Nipah virus responsible for the more recent outbreaks in humans. This model

can be used to study NiV-B pathogenesis, transmission, and countermeasures that could be used to control outbreaks.

Author Summary

Nipah virus causes severe disease in humans and outbreaks have occurred in two geographic regions, Malaysia and Bangladesh, and viruses have been isolated during outbreaks from both of these regions (NiV-M and NiV-B, respectively). The original outbreak of Nipah virus occurred in Malaysia and caused severe encephalitis in humans. All subsequent outbreaks of Nipah virus have occurred in Bangladesh or India and disease has been characterized as having a strong respiratory component. Nipah virus is a public health concern that can cause up to 100% lethality in humans and there is no approved treatment or vaccine. Current research should focus on understanding disease progression and pathogenicity. We compared NiV-M and NiV-B infection and disease progression using the Syrian hamster model. We found that NiV-M is more destructive in cultured hamster cells and has faster onset of cytopathogenicity compared to NiV-B. This is also true in hamsters, where although both viruses are pathogenic and cause a similar disease, pathology caused by NiV-M infection is accelerated. These data show that there is a difference in disease progression between the two strains of Nipah virus and will allow for a more detailed understanding of the events leading to disease caused by these viruses.

Introduction

Nipah virus is a member of the family *Paramyxoviridae*, genus *Henipavirus*, and was discovered in 1998–99 to be the etiological agent responsible for an outbreak of severe respiratory disease in pigs (4) and encephalitis in humans in Malaysia (74). All

subsequent outbreaks of Nipah virus have occurred in Bangladesh or India, beginning in 2001, and have occurred on an almost annual basis (117). Genetic data demonstrate that the isolates from Malaysia (NiV-M) and Bangladesh (NiV-B) represent two distinct Nipah virus strains (28, 117). Nipah virus outbreaks have case fatality rates of up to 100% and there are no approved vaccines or treatments and these viruses have been categorized as a biosafety level 4 (BSL4) agents. Nipah virus differs from other paramyxoviruses in its ability to infect a wide range of mammals including bats (36), dogs (4, 26), horses (118), pigs (4), and cats (4, 80). Wildlife surveillance at the time of the first outbreaks, along with several subsequent studies, has identified fruit bats of the family *Pteropodidae* as the natural reservoir of Nipah virus (32, 34, 36, 119).

During the first Nipah virus outbreak in Malaysia, NiV-M caused over 265 cases of encephalitis with 105 human deaths, resulting in a case fatality rate of 40% (4). Common clinical manifestations of Nipah virus infection included fever, headache, respiratory disease, encephalitis and loss of consciousness (75, 120). Fatal human cases of NiV-M infection were characterized by pathology involving the respiratory tract, central nervous system (CNS), heart, kidney and spleen (75). NiV-M infection causes vasculitis characterized by destruction of the endothelium, syncytia formation, thrombosis and necrosis, with infiltration of inflammatory cells throughout affected organs. In the lungs of infected humans, pulmonary edema, alveolar hemorrhage and pneumonia were documented as well as occasional multinucleated giant cells found in alveolar space (75). During this outbreak, the disease predominantly affected the nervous system with prominent signs of brain stem dysfunction. Magnetic resonance imaging of the brains of infected individuals showed focal lesions throughout the white matter (75).

In a study examining 94 Nipah virus-infected patients in Malaysia, only 6% showed abnormal chest radiographs, and of these, only one presented with a cough (74). Also, cases of late onset or relapsing encephalitis were documented during the Malaysia outbreak (74). During the Malaysian outbreak, pigs predominantly showed signs of respiratory disease and were determined to be an intermediate host (24, 27).

Epidemiologically, reports of infection with NiV-B differ from that of NiV-M infection in several aspects. Clinically, NiV-B infection resulted in a higher percentage of respiratory disease and a higher case fatality rate, reaching up to 100%, compared to NiV-M infection (120). This disparity could reflect the differences in availability of health care and in reporting (73). Disparities, however, could also be caused by intrinsic differences in the pathogenicity of NiV-M and NiV-B. NiV-B is transmitted from bats to humans by multiple routes including the ingestion of contaminated date palm sap (60), and can subsequently be transmitted nosocomially (71), or by human-to-human transmission (44, 65–67). Common clinical signs and symptoms of NiV-B infection included fever, altered mental status, headaches, cough, and difficulty breathing (73, 121). During the Bangladeshi outbreaks, acute respiratory distress was noted in many patients (73, 122). Febrile neurologic illnesses were also documented in some outbreaks of NiV-B, with lesions found in the gray and white matter of the brain (69, 121, 123). In one study looking at 92 patients, 69% had difficulty breathing and 62% had a cough (73). Limited studies have been conducted to describe the pathology in NiV-B infected patients.

In contrast to most other paramyxoviruses, Nipah virus has a broad species tropism and there are few suitable animal models that recapitulate human disease.

Experimentally cats, guinea pigs, ferrets, pigs, non-human primates, and Syrian hamsters have been shown to support NiV-M viral replication resulting in clinical signs of infection (47, 56, 124). The Syrian hamster is the only small rodent model that closely mimics multiple aspects of human disease (47, 48, 50, 80). When infected intraperitoneally (i.p.) or intranasally (i.n.) with NiV-M, hamsters develop respiratory disease and/or encephalitis. The pathological changes that occur in the hamster are similar to those described in humans. The presence of vasculitis, necrosis, and inflammation is seen in both the human and hamsters. Viral antigen and disease pathology is observed in lung, kidney and heart tissue (50, 53). Similar to human infections that lead to encephalitis, hamsters show antigen positive neurons, necrosis, and vasculitis in the CNS (50). These similarities in infection between humans and hamsters make the Syrian hamster a suitable model for the study of Nipah virus pathogenesis.

This study was designed to compare NiV-B and NiV-M infections in a hamster-derived cell line, followed by a comparison of the pathogenesis and immune responses to infection by both virus strains in the Syrian hamster. Our results demonstrated that hamster cells are permissive for infection by both virus strains, with NiV-M causing increased syncytia formation and cytopathic effect (CPE) compared to NiV-B. *In vivo*, NiV-B infection resulted in a delayed disease progression compared to NiV-M infection. Overall NiV-M is more cytopathic *in vitro* and causes an accelerated disease *in vivo*, compared to NiV-B.

Materials and Methods

Ethical statement

All work with Nipah virus, potentially infectious materials, and infected hamsters was completed in the BSL4 facility at the Rocky Mountain Laboratories, Division of Intramural Research, National Institute of Allergy and Infectious Diseases, National Institutes of Health. All standard operating procedures applied were approved by the Institutional Biosafety Committee (IBC). All animal experiments were approved by the Institutional Animal Care and Use Committee of the Rocky Mountain Laboratories and performed following the guidelines of the Association for Assessment and Accreditation of Laboratory Animal Care, International (AAALAC) by certified staff in an AAALAC-approved facility.

Virus propagation

NiV-B and NiV-M were provided by the Special Pathogens Branch of the Center for Disease Control and Prevention, Atlanta, GA, USA. NiV-M was isolated from a human case (cerebrum) in 1999 and passaged on Vero E6 cells a total of four times before used in experiments (125). NiV-B was isolated from a throat swab of a lethal human infection from Bangladesh in 2004 and passaged in Vero E6 cells a total of three times (28). Viruses were propagated on Vero E6 cells in Dulbecco's Modified Eagle's medium (DMEM) (Sigma) supplemented with 10% fetal calf serum, 2 mM l-glutamine, 50 IU/mL penicillin and 50 µg/mL streptomycin (Life Technologies). Supernatants were collected and clarified by low-speed centrifugation and stored in liquid nitrogen.

Virus titration

For plaque assays, Vero C1008 (European Collection of Cell Cultures) were grown to confluency in 6-well plates. Media was replaced with 250 µL of serial 10-fold dilutions of virus in DMEM and incubated for 1 hr at 37°C, rocking every 15 min. The virus inoculum was replaced with 2 mL of a 1:1 mixture of 2× minimal essential medium (MEM) and 1.6% low-melt agarose (Life Technologies). The cells were then incubated for 3 d at 37°C, 5% CO_2 before staining with 2 mL of a 0.25% crystal violet solution in 10% formalin for 3 hr at room temperature. The stain and overlay were then removed from the wells and the plaques were enumerated.

To determine the 50% tissue culture infectious dose ($TCID_{50}$), monolayers of Vero C1008 cells were grown in 96-well plates and 100 µL of serial 10-fold diluted samples in MEM containing 2% FBS, were added to the wells. Cells were then incubated for 5 d at 37°C, 5% CO_2 and then scored for CPE.

Cell lines and *in vitro* infections

Baby hamster kidney cells (BHK-21) from the American Type Culture Collection were propagated in MEM (Sigma) supplemented with 10% fetal calf serum, 2 mM l-glutamine, 50 IU/mL penicillin and 50 µg/mL streptomycin (Life Technologies). Nipah virus infections were performed in 48-well plates when cells reached 95–100% confluency. Infections were performed by replacing medium with 250 µL of diluted virus (multiplicity of infection (MOI) of 0.1 and 0.01) in MEM, 2% FBS. After 1 hr, the inoculum was replaced with MEM supplemented with 2% FBS. Supernatants were collected at 1 hr, and 1, 2, and 3 days post infection (dpi) for virus titration. Cells were stained using the Kwik Diff Kit (Thermo scientific) to visualize syncytia according to the

instructions of the manufacturer. Cells were monitored for CPE with a light microscope and images were captured using a Nikon DS-Fi1 camera.

Inoculation of hamsters and sample collection

Groups of 5 to 6 week old female Syrian hamsters (Harlan) were inoculated with the indicated doses of NiV-M or NiV-B diluted in sterile DMEM and administered via the i.p. route in a total volume of 500 µL. Control animals received the equivalent volume of sterile DMEM by the same route. Two groups were inoculated i.n. with 105 TCID50 per hamster of either NiV-M or NiV-B diluted in sterile DMEM. Fifty microliters of virus preparation was delivered to each nare using a pipette. Hamsters were weighed and scored daily for clinical signs for two weeks. When signs of disease no longer existed, animals were monitored but no longer weighed. The health of animals was assessed and scored according to the following criteria: 0 = no signs of disease; 1 = ruffled fur; 2 = ruffled fur & weight loss <5%; 3 = ruffled fur, hunched posture & weight loss >5%; 4 = ruffled fur, hunched posture & weight loss >10%; 5 = ruffled fur, hunched posture, weight loss >15%, or encephalitic signs, or hemorrhagic signs, or paralytic signs or dyspnea; 6 = ruffled fur, hunched posture, weight loss >20%, or encephalitic signs, or hemorrhagic signs, or paralytic signs or dyspnea; 7 = death. Euthanasia occurred at a score of 5 and above. At the time of euthanasia, animals were bled (EDTA- and heparin-treated vacutainer tubes) via cardiac puncture. Necropsies were performed to collect lung, spleen, heart and brain tissue. Tissues were placed in lysis buffer RLT (Qiagen) for RNA extraction, or 10% formalin for histopathology and immunohistochemistry (IHC) analysis.

RNA extraction and quantitative real-time RT-PCR (qRT-PCR)

Tissues (30 mg pieces) were homogenized in RLT buffer and removed from the BSL4 using approved standard operating procedures. Total RNA was extracted using RNeasy kit (Qiagen), according to the manufacturers' instructions. Whole blood was collected and inactivated in AVL buffer and removed from the BSL4 using approved standard operating procedures. Total RNA was extracted using QIAamp viral RNA kit (Qiagen), according to the manufacturers' instructions.

The RNA was quantified on a nanodrop 8000 spectrophotometer (Thermo Scientific). Real-time quantitative RT-PCR (qRT-PCR) was performed on a rotor-gene 6000 instrument (Corbett Life Science) using QuantiFast probe reagents (Qiagen) targeting the NiV-M or NiV-B nucleocapsid protein gene. Primers and probes used were: NiV-B sense (5′-GTTCAGGCCAGAGAAGCTAAATTT-3′), NiV-B antisense (5′-CCTCTTCGTCGACATCTTGATCA-3′), NiV-M sense (5′-GTTCAGGCTAGAGAGGCAAAATTT-3′), NiV-M antisense (5′-CCCCTTCATCGATATCTTGATCA-3″), NiV-B probe (5′-6FAM-CTGCAGGAGGTGTGCTCATCGGAGG-TAMRA-3′) and NiV-M probe (5′-6FAM-CTGCAGGAGGTGTGCTCATTGGAGG-TAMRA-3″). qRT-PCR components were used at the concentrations recommended by the manufacturer and 5 μL of RNA was added to each reaction and the following thermocycling parameters were used: 50°C for 10 min, 95°C for 5 min, and 40 cycles of 95°C for 5 s, 60°C for 10 s. Dilutions of RNA extracted from a known titer of each Nipah virus were run in triplicate to generate a standard curve from which sample $TCID_{50}$ equivalents were extrapolated. Hamster immune gene expression was determined as previously described (126). Briefly, RNA

was extracted from tissues and qRT-PCR was performed as described above using gene-specific primers and probes under multiplex conditions. The fold-change in each gene was calculated by normalizing the change in C_T (ΔC_T) to the C_T values for RPL18 (as an internal reference gene) for each sample and comparing this to the CT values of uninfected hamsters ($2^{-\Delta\Delta CT}$).

Histopathology and immunohistochemistry

Tissues were fixed in 10% neutral buffered formalin for 7 d with one volume change, then transferred out of the BSL4 using approved standard operating procedures. Tissues were then placed in cassettes and processed with a Sakura VIP-5 Tissue Tek, on a 12 hr automated schedule, using a graded series of ethanol, xylene, and ParaPlast Extra. Embedded tissues were sectioned at 5 µm and dried overnight at 42°C prior to staining with hematoxylin and eosin (H&E).

Specific Nipah virus IHC was performed using an anti-Nipah virus N protein rabbit primary antibody at a 1:5000 dilution (kindly provided by L. Wang, CSIRO Livestock Industries, Australian Animal Health Laboratory, Australia) (54). The tissues were then processed using the Discovery XT automated processor (Ventana Medical Systems) with a DAPMap (Ventana Medical Systems) kit.

Statistics

Statistical analyses were performed on the data form the $TCID_{50}$ and qRT-PCR experiments using a 2-way ANOVA with a Bonferroni's post-test. To determine whether there were significant differences in the time to death between the viruses, we performed a log-rank test. The mean and SEM is represented and significance (* = $p<0.05$, ** = $p<0.01$ and *** = $p<0.001$) is reported where appropriate.

Results

NiV-M causes increased cytopathology in BHK-21 cells, compared to NiV-B

To determine the cellular responses and replication kinetics of the two Nipah virus strains in a hamster cell line, we infected BHK-21 cells with either NiV-M or NiV-B at MOIs of either 0.01 or 0.1. As early as 1 dpi, syncytia formation was apparent in all NiV-M-infected cultures. By 3 dpi, and at both MOIs, NiV-M-infected cells showed extensive CPE and nearly complete destruction of the cell monolayer (Figure 3-1A). NiV-B-infected cells showed little CPE at any of the time points sampled, regardless of the inoculation dose. At 3 dpi, NiV-B-infected cells began to form small syncytia. At both MOIs, NiV-M replicated sooner and reached higher virus titers in the supernatant at earlier time points compared to NiV-B (Figure 3-1B and C). At the lower MOI, NiV-M reached a titer that was 4 logs higher at 3 dpi than NiV-B (Figure 3-1B), whereas end titers were similar for both Nipah virus strains at the higher MOI, with a faster progression for NiV-M (Figure 3-1C).

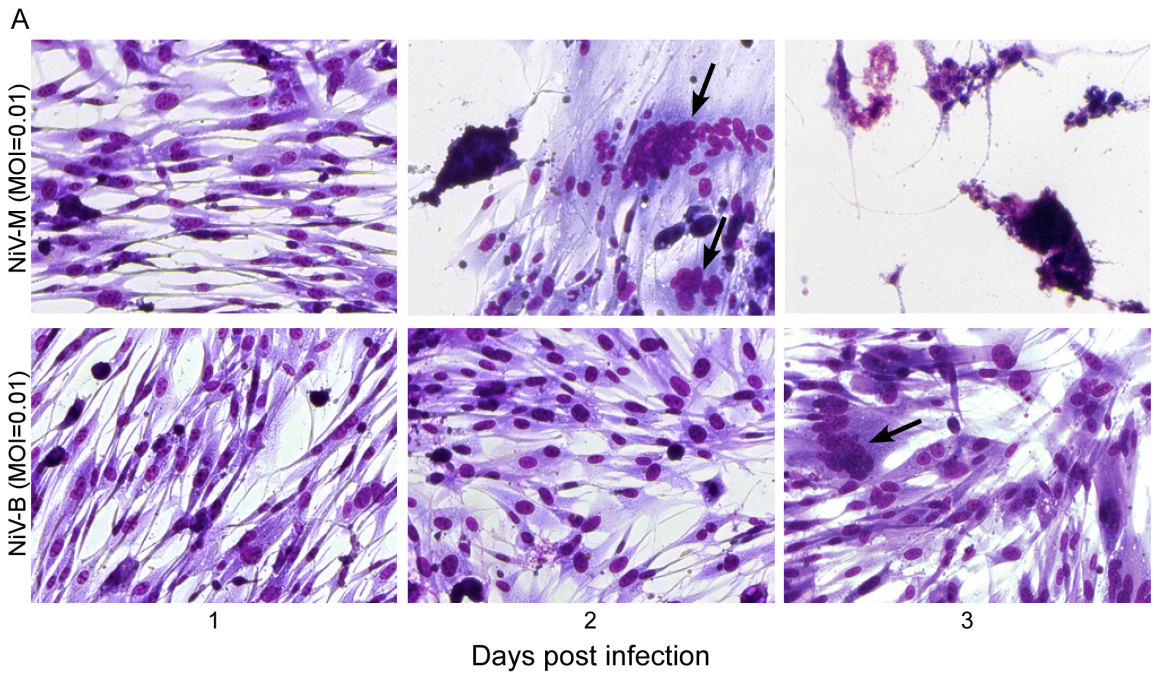
A
NiV-M (MOI=0.01)
NiV-B (MOI=0.01)
1
2
3
Days post infection

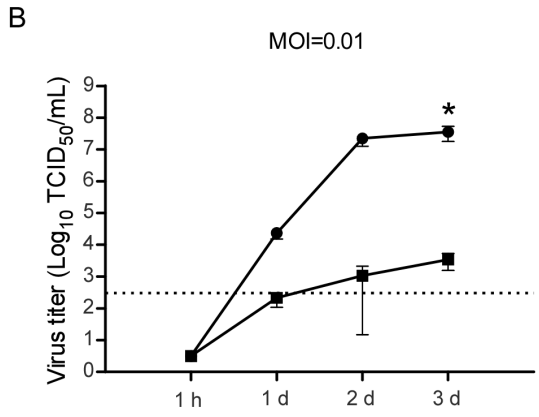
B
MOI=0.01
Virus titer (Log10 TCID50/mL)
0
1
2
3
4
5
6
7
8
9
*
1 h
1 d
2 d
3 d

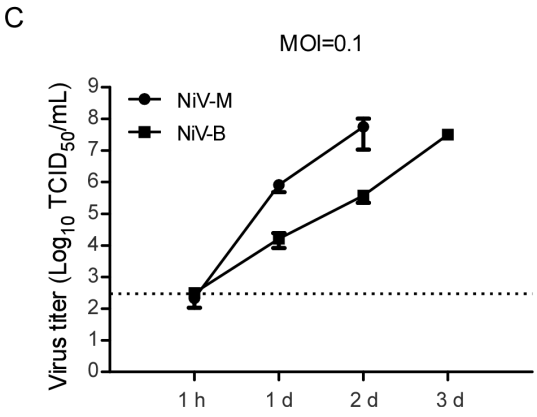
C
MOI=0.1
NiV-M
NiV-B
Virus titer (Log10 TCID50/mL)
0
1
2
3
4
5
6
7
8
9
1 h
1 d
2 d
3 d

Figure 3-1: NiV-M replicates more efficiently and causes increased cytopathogenicity in hamster cells compared to NiV-B.

To study the cytopathogenicity of these Nipah viruses, BHK-21 cells were infected with NiV-M or NiV-B at an MOI of 0.01 and stained using the Kwik Diff Kit at 1, 2, and 3 dpi. Arrows point to multinucleated giant cells (A). To examine the viral growth kinetics, BHK-21 cells were infected with Nipah virus at an MOI of 0.01 (B) or 0.1 (C) and supernatants were collected at the indicated time points. Supernatants of NiV-M at an MOI of 0.1 at 3 dpi were not collected due to extensive destruction of the cell monolayer. Virus was titrated on Vero C1008 cells and the results are expressed as the mean of three replicates and error bars indicate the SEM. The dotted line denotes limit of detection for the assay. A 2-way ANOVA with Bonferroni's post test was used to compare the viruses (* = $p<0.05$) (B and C).

Disease progression during NiV-B infection of hamsters is delayed compared to NiV-M infection

To date, NiV-B infection has not been examined in an animal model. To assess the suitability of the hamster as a model for NiV-B infection, as well as to compare the two strains, hamsters were inoculated i.p. with 10-fold serial dilutions of Nipah virus from 10^5 to 1 $TCID_{50}$ (Figure 3-2). Animals were evaluated for clinical signs of disease on a daily bases according to a scoring system outlined in the Materials and Methods section. Only one hamster showed abnormal clinical signs on the day prior to euthanasia, which consisted of ruffled fur. All other hamsters did not display abnormal clinical signs until the day euthanasia was necessary. Hamsters challenged with either virus strain showed clinical signs of respiratory distress and/or neurologic dysfunction leading to a score that required euthanasia. Signs of respiratory disease included labored abdominal breathing and hunched posture; neurological dysfunction included imbalance, partial paralysis and seizures. Similar to previous studies with NiV-M, respiratory distress was observed only in animals infected at the highest doses (10^4 and 10^5 $TCID_{50}$/animal) (53). The majority of animals inoculated with the lower doses of Nipah virus (10^0 through 10^3 $TCID_{50}$/animal) displayed neurologic dysfunction prior to euthanasia. One animal infected with NiV-M at the highest dose (10^5 $TCID_{50}$) and two animals infected with NiV-B (one inoculated with 10^4 and one with 10^5) presented with both respiratory and neurologic dysfunction, while the rest of animals had either respiratory or neurological signs of distress that required euthanasia. NiV-M-infected animals showing severe respiratory signs of disease were euthanized between 5–7 dpi, whereas animals displaying neurological disorders were euthanized between days 5–11. Disease

progression in NiV-B-infected animals was generally slower, and animals displaying severe respiratory distress or neurological dysfunction were euthanized on 8–9 dpi or 8–14 dpi for NiV-M and NiV-B infection, respectively (Table 3-1). The slower disease progression in NiV-B-infected animals was reflected in the overall survival curves with 80% lethal disease outcome even at the highest dose of infection Figure 3-2:Hamsters inoculated with NiV-B show delayed disease progression compared to NiV-M-infected hamsters.and Table 3-1. The LD_{50} for NiV-M and NiV-B was 68 and 528 $TCID_{50}$, respectively. At both 10^3 and 10^5 $TCID_{50}$, there was a statistically significant difference in the time to death between the two virus strains, with death occurring approximately two days later for NiV-B infected animals at each dose (Table 3-1). To determine if the delay in survival is associated with the route of infection, we inoculated hamsters i.n. with 10^5 $TCID_{50}$ of either NiV-M or NiV-B. The mean time to death was delayed by two days in hamsters inoculated with NiV-B compared to NiV-M (Figure 3-2). Both routes of inoculation showed a two-day delay in NiV-B compared to NiV-M, although the mean time to death was later in both virus groups with the i.n. compared to i.p. route.

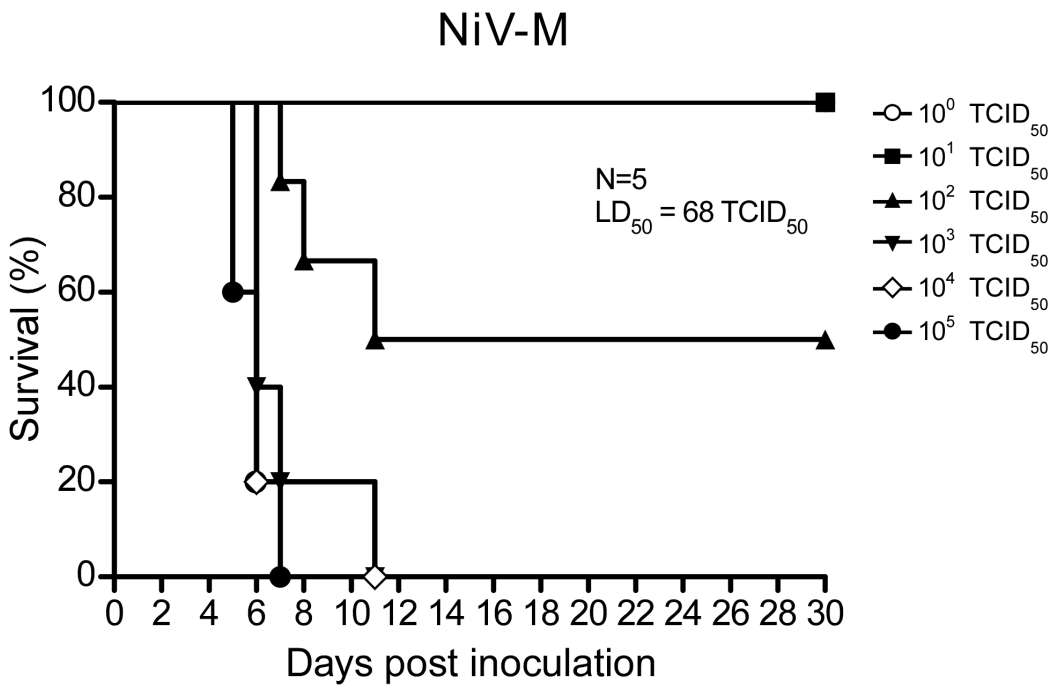
NiV-M
Survival (%)
Days post inoculation
N=5
LD50 = 68 TCID50
10^0 TCID50
10^1 TCID50
10^2 TCID50
10^3 TCID50
10^4 TCID50
10^5 TCID50

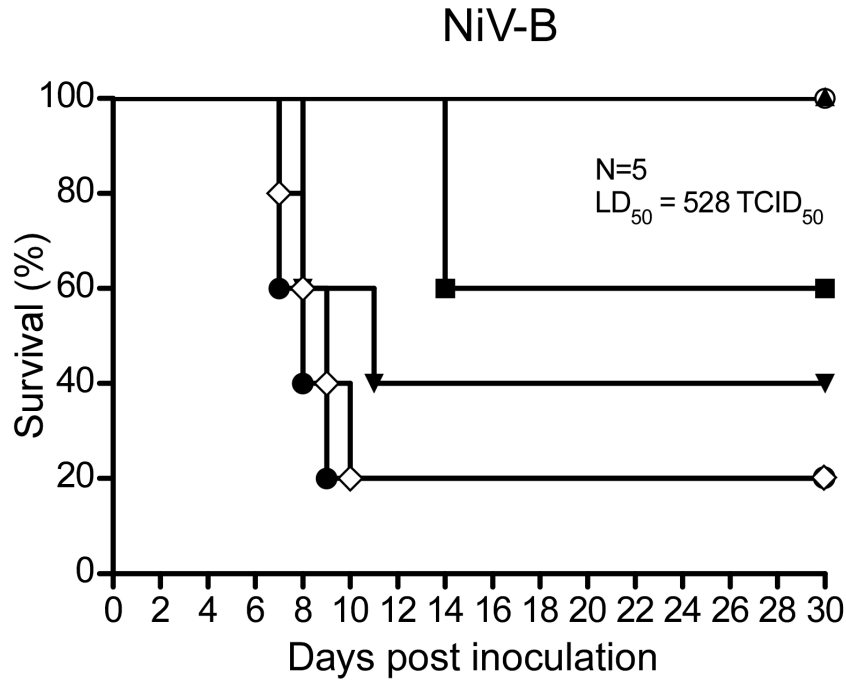
NiV-B
Survival (%)
Days post inoculation
N=5
LD50 = 528 TCID50

Figure 3-2:Hamsters inoculated with NiV-B show delayed disease progression compared to NiV-M-infected hamsters.

Groups of 5 hamsters were inoculated i.p. with 10-fold serial dilutions of virus from 10^5 to 1 $TCID_{50}$. The hamsters were monitored for 30 dpi for survival.

Table 3-1: Clinical signs and outcome of hamsters inoculated with NiV-M or NiV-B.

Inoculum	Dose ($TCID_{50}$)	Survival (%)	Mean time to death (days)[a]
NiV-M	1×10^{0}	100	N/A
	1×10^{1}	100	N/A
	1×10^{2}	40	8.7±1.7
	1×10^{3}	0	7.2±1.9* [b]
	1×10^{4}	0	7±2
	1×10^{5}	0	5.8±0.7** [c]
NiV-B	1×10^{0}	100	N/A
	1×10^{1}	60	14±0
	1×10^{2}	100	N/A
	1×10^{3}	40	9±1.4* [b]
	1×10^{4}	20	8.5±1.1
	1×10^{5}	20	7.75±0.8** [c]

[a]Excluding survivors.
[b]Significant difference between NiV-M and NiV-B at dose 10^3 $TCID_{50}$,
*$p<0.05$: Log-rank test.
[c]Significant difference between NiV-M and NiV-B at dose 10^5 $TCID_{50}$,
**$p<0.01$: Log-rank test.
doi:10.1371/journal.pntd.0002024.t001

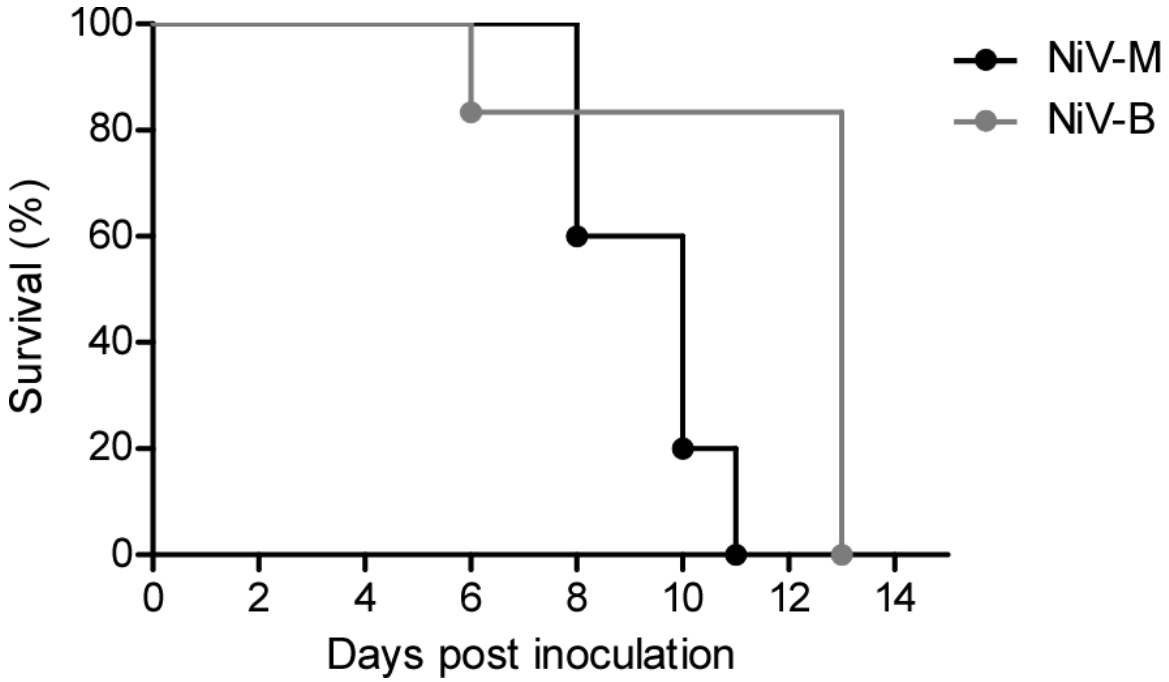

Figure S 1: Hamsters inoculated intranasally with NiV-B show delayed disease progression compared to NiV-M-inoculated hamsters.

Groups of 5 hamsters were inoculated i.n. with 10^5 $TCID_{50}$. The hamsters were monitored for survival. A log- rank test was used to compare survival curves (* = $p<0.05$). NiV-B infected animals had a mean time to death of 11.6 days and NiV-M infected animals 9.4 days.

Both Nipah viruses replicate in hamster lung, brain and spleen tissue

To compare the pathogenesis of NiV-M to NiV-B, groups of hamsters were inoculated with 10^5 $TCID_{50}$ of either Nipah virus and tissues were collected on 1, 3 and 5 dpi for both virus groups, and 7 dpi for NiV-B. Based on the time to death at this dose from our survival experiment, 7 dpi tissues were not collected for NiV-M-inoculated animals for this pathology experiment. Viral RNA was detected using Nipah virus N-specific qRT-PCR (Figure 3-3). In NiV-M-inoculated animals, replication was detected at an earlier time point than NiV-B replication. As early as 1 dpi, viral RNA was detected in lungs, brain and spleen tissue of some NiV-M-infected animals. NiV-B-infected animals had detectable levels of viral RNA at 1 dpi in lung tissue of some hamsters, and in the spleen by 3 dpi. Both strains showed an increase in viral RNA over time in the lungs, brain and spleen, with the highest overall titers in the lungs at the last time point sampled. We assessed viremia in hamsters inoculated with either virus by qRT-PCR. Levels of viral RNA were barely detectable and viral RNA was undetectable in some animals at each time point (data not shown).

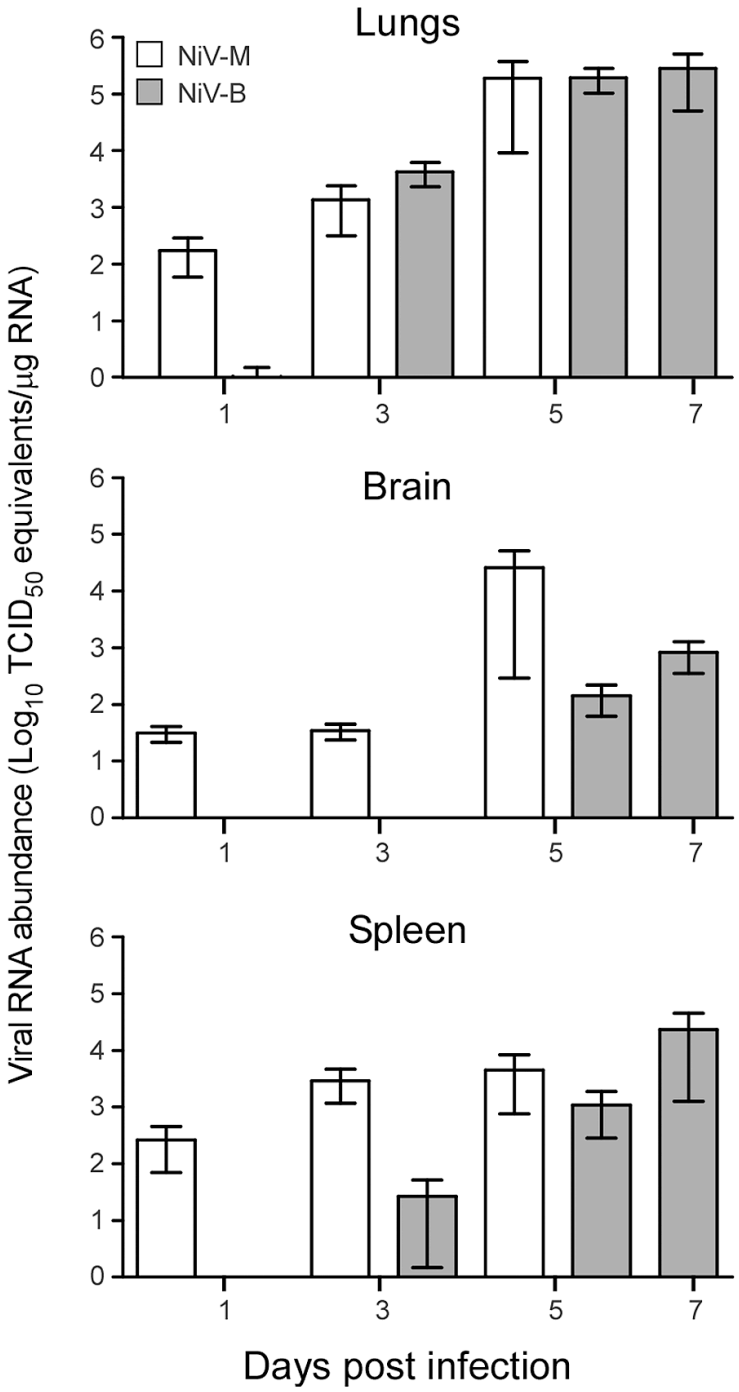
Lungs
NiV-M
NiV-B
Brain
Spleen
Viral RNA abundance (Log10 TCID50 equivalents/μg RNA)
Days post infection
0
1
2
3
4
5
6
1
3
5
7

Figure 3-3: NiV-B replication is delayed in hamster organs compared to NiV-M replication.

Hamsters were inoculated with 10^5 $TCID_{50}$ of Nipah virus and 9 animals/group were euthanized at 1, 3, 5, and 7 (for NiV-B only) dpi and tissues were collected. Total viral RNA was extracted and Nipah virus N-specific viral RNA was quantified by qRT-PCR. Gray bars represent NiV-B and white NiV-M. Bars represent the mean and error bars represent the SEM.

Host gene expression in lung, brain and spleen tissue of hamsters is differentially regulated during Nipah virus infection

To examine the kinetics of the host immune response to Nipah virus infection, and compare responses between NiV-M and NiV-B infections, the expression level of a subset of cytokine and chemokine mRNAs were examined by qRT-PCR in the lungs, brain and spleen (Figure 3-4). Throughout the infection, the largest overall response was seen in the lungs. At 1 dpi, a statistical difference in the upregulation of interleukin-4 (IL-4), interleukin-6 (IL-6), tumor necrosis factor (TNF), and interferon-γ (IFNγ) was observed between NiV-M and NiV-B infections, with higher expression of these genes in response to NiV-M. A similar result was measured at 3 dpi for IFNγ in the lungs (Figure 3-4). At 3 dpi, IL-4, IL-6 and TNF were upregulated similarly in response to both virus strains and remained upregulated throughout the course of infection. Upregulation of the gene for myxovirus resistance protein-2 (Mx2) in the lungs was detected only at the last time point for both virus strains. IFNγ-induced protein 10 (IP-10) mRNA increased starting at 1 dpi and remained upregulated in the lungs throughout the course of infection, peaking at 3 dpi in NiV-M-infected hamsters and 5 dpi in NiV-B-infected hamsters. IL-4, IL-6 and TNF were also upregulated in brain (Figure 3-4). There was a significant increase in Mx2 transcription in the spleens of NiV-M-infected hamsters at 3 dpi compared to NiV-B. In the brain, IL-4, IL-6 and TNF were slightly upregulated over control animals. IL-4, IL-6, TNF, and IFNγ mRNAs were downregulated in the spleen.

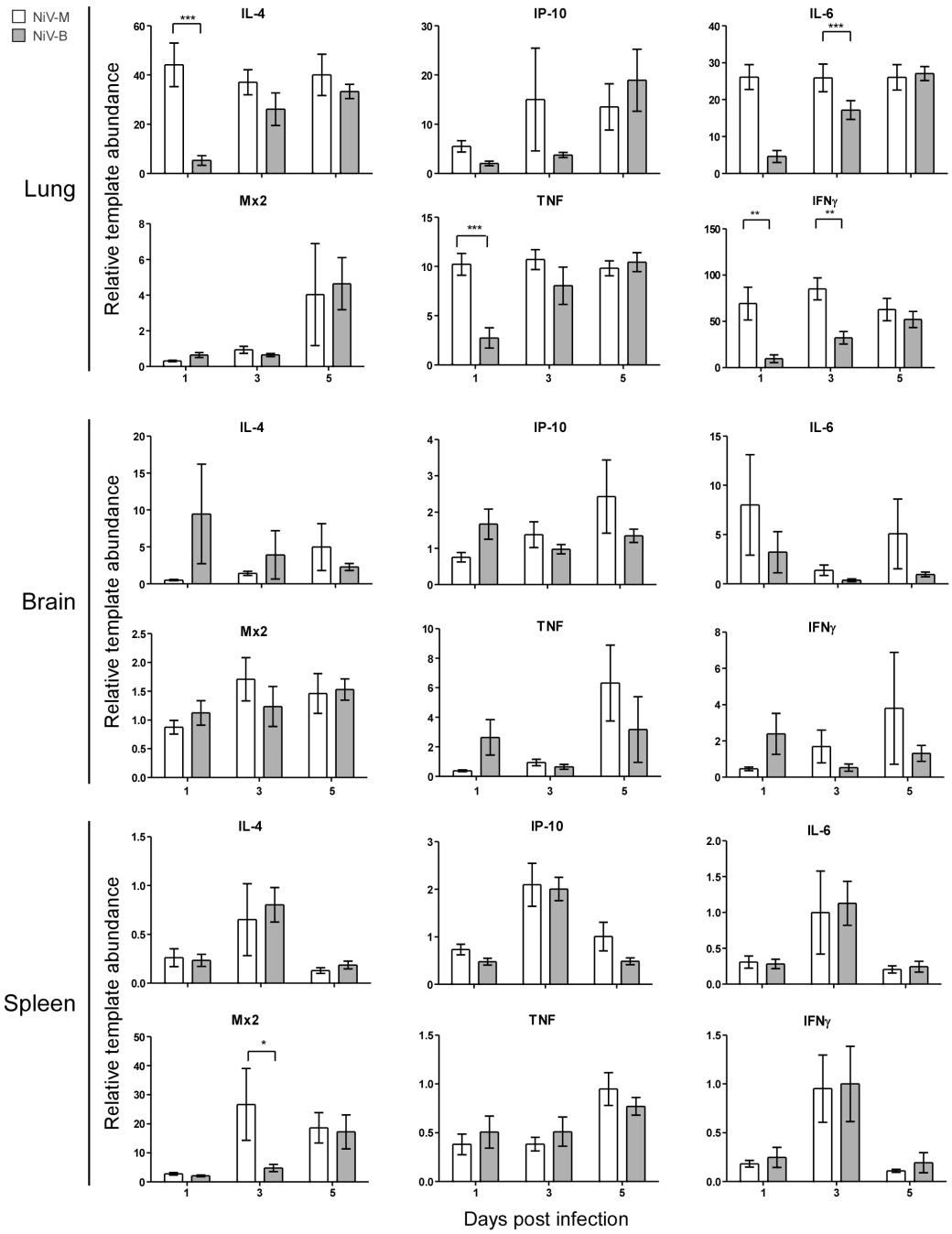
NiV-M
NiV-B
Lung
Brain
Spleen
Relative template abundance
IL-4
IP-10
IL-6
Mx2
TNF
IFNγ
Days post infection

Figure 3-4: Host gene expression in lung, brain and spleen tissue of hamsters is differentially regulated during infection with Nipah viruses.

Quantitative RT-PCR for IL-4, IP-10, IL-6, Mx2, TNF and IFNγ was performed on lung, brain and spleen tissues from groups of 9 hamsters inoculated with 10^5 $TCID_{50}$ of NiV-M (white bars) or NiV-B (gray bars) at the indicated time points. Data are shown as the fold-change of each gene over uninfected controls and normalized to an internal reference gene (RPL18). Error bars represent the SEM. A 2-way ANOVA with Bonferroni's post-test was used to determine statistical significance between viruses (* = $p<0.05$, ** = $p<0.01$ and *** = $p<0.001$).

Histopathological changes occurred earlier in NiV-M-infected hamsters compared to NiV-B-infected animals

To compare the pathology between the two strains, hamsters were inoculated with 10^5 $TCID_{50}$ of NiV-B or NiV-M and tissues were examined histologically. Pathology was observed for both infections and was composed of a mild to moderate multifocal, subacute, bronchointerstitial pneumonia with vasculitis on 5 dpi for NiV-M and NiV-B infection (Figure 3-5). By 7 dpi in NiV-B-infected animals, the pneumonia progressed to marked, multifocal to coalescing, subacute bronchointerstitial pneumonia with vasculitis, necrosis, edema, and fibrin deposits. The pneumonia in both groups, on day 5 dpi for NiV-M infection and 7 dpi for NiV-B infection, was characterized by effacement of terminal bronchioles and adjacent alveoli by small to moderate numbers of macrophages, neutrophils, lymphocytes and plasma cells. Multifocal vasculitis was observed with disruption of the arterial tunica media by small numbers of neutrophils and lymphocytes. Syncytial endothelial cells were found in affected small to medium caliber vessels. Hamsters from the final time points had moderate to marked lesions in the lungs and demonstrated a loss of pulmonary architecture with replacement by cellular and karyorrhectic debris with small to moderate amounts of hemorrhage, fibrin deposits and edema. IHC revealed viral antigen in alveolar capillary endothelium, small and medium caliber arteriolar endothelium, and in mononuclear inflammatory cells starting at 3 dpi for NiV-M infection and 5 dpi for NiV-B infection (Figure 3-5B). The presence of viral antigen was strongly associated with areas of inflammation. No pathological changes were observed in the CNS of hamsters infected at the high dose used in the pathology study.

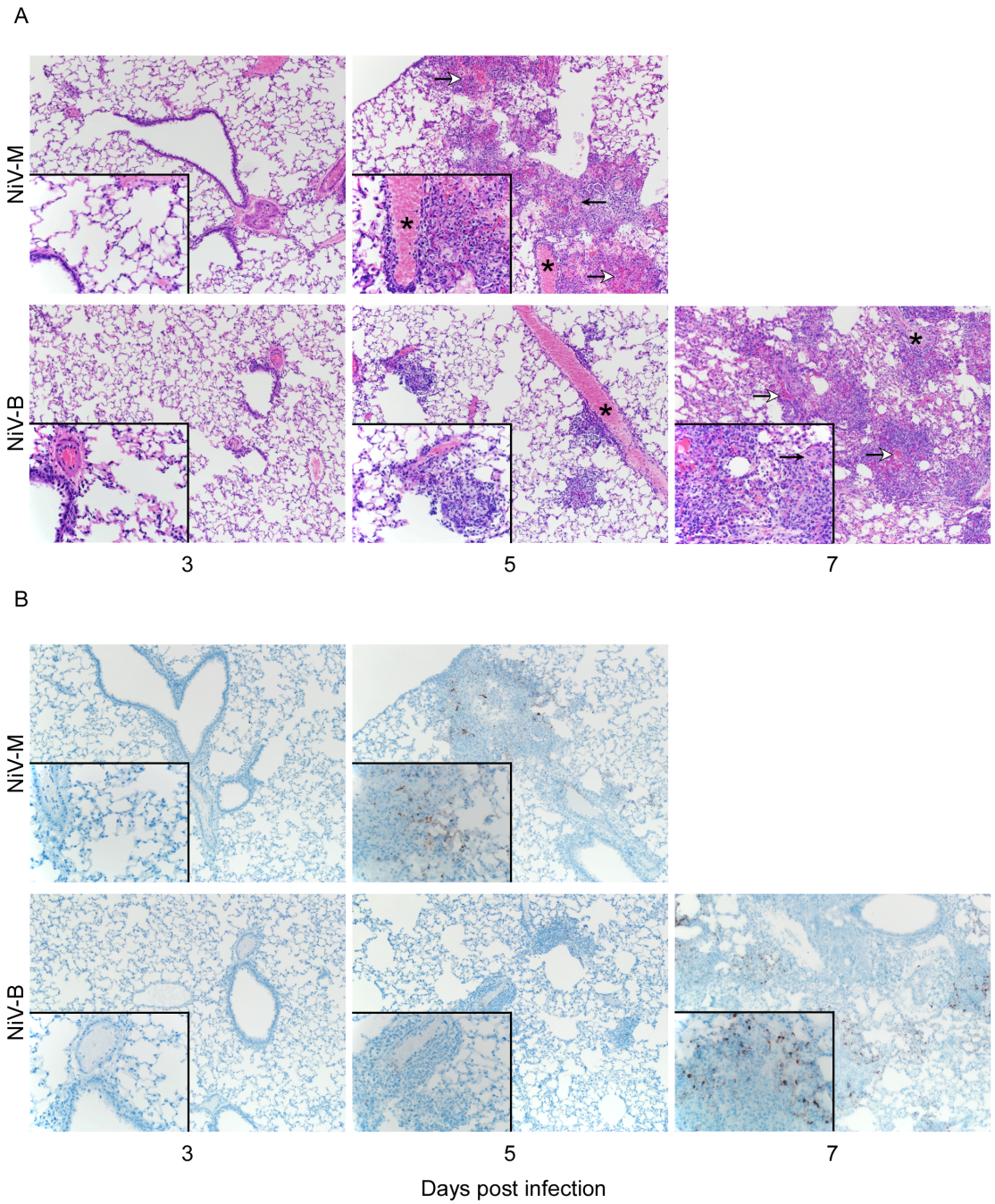
A
NiV-M
NiV-B
3
5
7
B
NiV-M
NiV-B
3
5
7
Days post infection

Figure 3-5: NiV-M infection results in accelerated pathology compared to NiV-B infection in hamsters.

Nipah virus inoculated hamsters were euthanized at 3, 5 and 7 dpi (for NiV-B only) and lung sections were stained with H&E (A) and for Nipah virus nucleocapsid protein (IHC) (B) Images were taken at a magnification of 100× and 400× (insets). Asterisks denote arteries with vasculitis as demonstrated by recruitment of inflammatory cells with effacement of the tunica intima and tunica media. Open arrows denote areas of acute hemorrhage and closed arrows indicate fibrin deposits.

Discussion

Nipah virus is a zoonotic pathogen that causes encephalitis and pulmonary disease with a high case fatality rate and is classified as a category C pathogen by the NIAID's pathogen priority list (120). Two strains of Nipah virus, NiV-M and NiV-B, have been isolated from geographically and temporally separated outbreaks (28). Human outbreaks caused by these strains differ in disease progression and epidemiologically (121). The Syrian hamster has been established as a disease model for NiV-M infection (50, 53), but NiV-B infection studies have not been reported for any animal model. The goal of this study was to compare the replication, pathogenesis, and immune response to infection with NiV-M and NiV-B using *in vitro* and *in vivo* methods. BHK-21 cells infected with NiV-M showed more severe damage and supported higher virus replication compared to NiV-B-infected cells. Hamsters infected with NiV-B had a delay in disease progression and increased survival rates compared to NiV-M infected animals.

In vitro, BHK-21 cells were permissive for infection by both NiV-M and NiV-B. NiV-M replicated to higher titers in the supernatant at an earlier time point, and infection resulted in widespread syncytia formation causing extensive CPE. Widespread CPE was not observed in NiV-B-infected BHK-21 cells, although a few syncytia were present at later time points. The differences observed in virus replication and syncytia formation could be attributed to either higher viral replication causing more syncytia, or more syncytia formation resulting to higher virus load. Differences in replication efficiency including protein production, viral assembly and budding could explain the higher virus production and large number of syncytia observed in NiV-M infected cultures. Conversely, differences in fusion kinetics could account for disparate amounts of

syncytia that then lead to variation in virus replication. The high amount of fusion and syncytia formation in cells could result in the infection of cells that were not initially infected at the low MOIs used in our experiments. This could lead to higher overall levels of virus production. Previous studies using paramyxoviruses have demonstrated that viral spread can occur by cell-cell fusion; the surface proteins of Nipah virus are present at the cell junctions and have been shown to initiate fusion and spread of virus (127–129). Slower fusion kinetics could lead to less and slower formation of syncytia observed in NiV-B infected cells. The affinity of Nipah virus glycoprotein to its receptors, ephrin B2 and B3, as well as the ability of the glycoprotein to trigger the fusion protein could also affect fusion rates. Further experiments need to be completed to examine the relationship between replication and syncytia formation.

In our experiments, we chose i.p. as the route of inoculation due to the more uniform disease progression and outcomes described in previous Nipah virus studies (50). It is likely that i.p. inoculation would more readily allow for the detection of subtle differences between strains that may not be detectable in a less uniform infection route, such as i.n. When infected with NiV-M or NiV-B, hamsters developed clinical signs of disease similar to human infection (30, 50, 74, 75). The onset of disease and death in hamsters was rapid and occurred between 5–14 dpi, which corresponds to human cases, where symptoms start to develop between 7–10 dpi (24, 84, 130). We observed earlier replication of NiV-M than NiV-B in all organ types sampled, although, once NiV-B RNA was detected, it reached similar values within two days. Earlier replication of NiV-M in tissues corresponded with earlier pathologic changes and accelerated disease and death compared to NiV-B infection. In humans, CNS pathology is documented, but in our

comparative pathology experiment, we did not observe pathology in the CNS. This is likely attributed to the high dose of inoculum for the pathology experiment (10^5 $TCID_{50}$) and route of inoculation (i.p.). However, we did observe pathology in the lungs consisting of multifocal subacute bronchointerstitial pneumonia with vasculitis. The pneumonia was characterized by inflammation in the terminal bronchioles and alveoli spaces, necrosis, hemorrhage, fibrin deposits, edema and syncytia in endothelial cells. In human cases, fibrinoid necrosis, vasculitis, pulmonary edema, alveoli hemorrhaging, and syncytia were documented (24, 75, 84). It is probable that hamsters inoculated with this high dose (10^5 $TCID_{50}$) succumbed to infection due to inflammation, edema, and widespread vasculitis in the lungs that caused interstitial pneumonia. Even with low levels of viral antigen, pathology was severe enough to cause a fatal outcome.

The typical dose that humans are infected with, as well as the route of infection is not known. In hamsters, both virus strains caused respiratory distress and/or neurological dysfunction in a dose-dependent manner. Based on previous data in hamsters, it is likely that dose and route of infection might play a role in Nipah virus outcome in humans (53). Disease progression could be altered by the transmission route, which could include fomite (51, 71), oral ingestion (60, 131), and respiratory droplets (51, 58, 132). In this study, inoculation of hamsters with NiV-B resulted in a delay in disease progression and the LD_{50} was approximately a log higher compared to NiV-M. However these data are contrary to what has been reported in humans, where NiV-B results in higher case fatality rates compared to NiV-M. Since we did not observe a difference in disease that would explain differences in the epidemiological data for the two Nipah virus strains, factors other than the intrinsic pathogenicity likely contribute to the disparities in the

documented epidemiological data. The suboptimal health care, lack of supportive care and inconsistencies in reporting could account for higher documented case fatality rates and differences in disease manifestations during NiV-B outbreaks (73).

Cytokine and chemokine mRNAs were quantitated in the hamsters over the course of infection and several immune genes were upregulated in the lung, brain, and spleen, although there was a slight downregulation of some genes in the spleen. NiV-M induced an earlier and more robust immune response compared to NiV-B, which eventually reached similar levels to hamsters infected with NiV-M. Early TNF activation during NiV-M infection may contribute to recruitment of inflammatory cells, as observed in the lungs of infected hamsters by histopathology. The upregulation of IP-10 in the lungs coincided with lymphocyte recruitment, appearance of vascular damage, and necrosis in the lungs. IP-10 upregulation has been documented in other Nipah virus studies, specifically focusing on endothelial cells (133, 134). Teruya-Feldstein et al reported that high levels of IP-10 are found in necrotic tissue and in areas of vascular damage associated with Epstein-Barr virus-positive lymphoproliferative processes in mice (135). They demonstrated a correlation between IP-10 regulation, tissue necrosis, and vascular damage during viral infection. Similarly, IP-10 is upregulated in the airways of patients with pulmonary diseases such as tuberculosis and plays a role in recruitment of activated T cells (136). IL-6 gene expression was increased earlier in the lung in NiV-M compared to NiV-B infected hamsters. IL-6 activates T cells (137) and the recruitment of T cells likely contributed to the widespread vasculitis associated with Nipah virus infection and disease. Recruitment of lymphocytes could also be a way for Nipah virus to disseminate throughout the host, as it has recently been published that lymphocytes and

monocytes can carry virus without becoming infected and release virus at distant sites from the original infection (83, 138). In the lungs, IL-4 was also upregulated, following similar kinetics than IL-6. IL-4 promotes differentiation of B cells, and is upregulated is indicative of the activation of a Th2 response (139). However, during disease, specific antibody production would not occur fast enough, since animals succumb to infection before significant antibody production can likely occur. Due to the use of the hamster as a model, we are limited in the amount of reagents available for a detailed examination of the immune response and future work is needed to get a more complete picture of the immune response to Nipah virus infection. In general NiV-M infection caused earlier induction of immune genes which probably corresponds to the earlier pathology observed. It is possible that the strong early immune response in Nipah virus-infected animals might contribute to disease via an immunopathogenic mechanism.

In conclusion, there is a delay in NiV-B-induced disease progression compared to NiV-M, specifically in time to death, virus replication, pathology and immune responses. NiV-M is more cytopathic *in vitro* and more pathogenic *in vivo*. Viral antigen staining was low in tissues, although the pathologic changes were extensive and the inflammatory response was robust, suggesting disease progression may not only be a result of direct effects of the virus, but likely has an immunopathogenic component. The experimental data presented herein characterizes the hamster as a suitable small animal model for NiV-B infection, showing clinical signs, viral tropism, and pathologic changes similar to those observed in humans. These data are important to further the understanding of Nipah virus infection and pathogenesis. By applying the hamster model for NiV-B this allows for

future studies in transmission, pathology and therapeutics, specifically focusing on the Nipah virus strain responsible for recent outbreaks.

Acknowledgments

This work is published in full in PLoS NTD 2013;7(1):e2024. doi: 10.1371/journal.pntd.0002024 (140). http://www.plosntds.org/article/info%3Adoi%2F10.1371%2Fjournal.pntd.0002024

The authors would like to thank Tina Thomas, Rebecca Rosenke and Dan Long (Rocky Mountain Veterinary Branch, Division of Intramural Research (DIR), NIAID, NIH) for histopathology work, Friederike Feldmann and Elaine Haddock (DIR, NIAID, NIH) for BSL4 technical assistance and Anita Mora (DIR, NIAID, NIH) for graphics.

Author Contributions

Conceived and designed the experiments: BLD JP. Performed the experiments: BLD JP DS EdW VJM HF. Analyzed the data: BLD JP DS EdW VJM HF. Wrote the paper: BLD JP HF.

CHAPTER 4 CHARACTERIZATION OF CELL-TYPE SPECIFIC INFECTION OF NIPAH VIRUS *IN VITRO* AND *IN VIVO*

Abstract

Nipah virus infects humans and animals causing respiratory distress and encephalitis. Infection with Nipah virus is systemic causing wide spread vasculitis. Previous studies have identified vascular endothelial and smooth muscle cells as targets of infection. In this study we provided further evidence for infection *in vivo* in these cells as well as characterized pathology in endothelial cells and lack thereof in smooth muscle cells. To further define effects of infection on these cells we used primary human cells *in vitro.* Experiments in culture revealed that both cell types are permissive to infection and can produce high virus titers. Similar to the situation *in vivo* in humans and animals there was little change in smooth muscle cell morphology following infection. We discovered that smooth muscle cells unlike endothelial cells do not express measureable amounts of Nipah virus receptor on the surface, which prohibited fusion and viral spread. These data suggest that smooth muscle cells get infected ephrin-independently and act as a continuous source for virus production.

Introduction

Nipah virus is a zoonotic pathogen causing respiratory distress as well as encephalitis in humans. It is a member of the genus *Henipavirus* in the family *Paramyxoviridae.* Since its discovery in 1998 in Malaysia and Singapore, Nipah virus has been found to be the cause of almost yearly outbreaks on the Indian subcontinent. The natural reservoir of the virus is the pteropid fruit bat (32). During the Malaysian outbreak the pig was identified as an intermediate host amplifying and spreading the virus to

humans (118). In Bangladesh, where current outbreaks occur, Nipah virus is transmitted from bats to humans and then from human to human (72).

Clinical infection in humans is characterized by fever, cough, dyspnea, headache and loss of consciousness. Average duration of illness is 9 days, resulting in mortality in about 70% of patients (75). Autopsies of patients have found common hallmarks of Nipah virus disease including systemic vasculitis, endothelial destruction, and CNS involvement (76, 80). More specifically, Nipah virus causes vasculitis of small blood vessels of the CNS, lung, heart, and kidney. The endothelium of medium to large vessels seems to be refractory for Nipah virus infection (62). Vessels infected with Nipah virus show inflammation with leukocyte infiltration, thrombosis, necrosis, as well as hemorrhages (80). Vasculitis of these vessels is often described as destruction of the endothelium with fibrinoid necrosis. Part of the destruction of the endothelium is the formation of giant multinucleated cells, called syncytia.

The two main target organs of Nipah virus infection are brain and lung. Infection of the CNS produces viral inclusions throughout the white and gray matter resulting in degeneration and perivascular cuffing (75, 77, 80). Immunohistochemistry (IHC) of the brain for Nipah virus antigen results in positive staining of blood vessels and neurons that are associated with vasculitis and necrotic plaques (56, 77). Pathologic changes in the lung are also characterized by vasculitis and necrosis in small blood vessels. Syncytia can been found in alveolar spaces causing pulmonary edema. Viral antigen staining is seen in the endothelium and tunica media of blood vessels as well as in the alveolar spaces of the lung (140).

Pathologic findings correspond to Nipah virus receptor expression. The receptors for Nipah virus has been identified as the receptor tyrosine kinase ephrin B2 and B3 (7, 8, 12). The receptor is a highly conserved transmembrane ligand that normally functions in cell-to-cell signaling, angiogenesis and neuronal axon guidance (9, 11). The highly conserved receptor is thought to account for the broad species tropism of Nipah virus (82). Expression of ephrin B2 is localized to arterial endothelial cells, smooth muscle cells and neurons with high expression in the lung and brain, while ephrin B3 expression is restricted to the brain stem and heart (7, 8, 10, 12, 17). The expression levels of ephrins are regulated in organs and during various times in the cell cycle, thus limiting Nipah virus infection to organs with high expression (10).

In cell culture, various cell lines have been evaluated for permissibility to Nipah virus infection as well as ephrin expression. In most cases infection has been directly linked to ephrin expression; however a few cases of ephrin-independent infection have been reported including the possibility of macropinocytosis (13, 82, 83).

The goal of this study was to characterize virus replication and cytotoxicity in both endothelial cells and smooth muscle cells during Nipah virus infection. We first detected Nipah virus infection in the endothelium and tunica media *in vivo* in tissue derived from infected hamsters and African green monkeys. Subsequently, we found that both primary cultures of human endothelial and smooth muscle cells are permissive to infection resulting in cytotoxicity in endothelial but not smooth muscle cells. The non-cytotoxic phenotype was associated with the low to no ephrin expression decreasing viral cell-to-cell spread and syncytia formation. Overall our results suggest that Nipah virus can infect smooth muscle cells by an ephrin-independent manner and serve as a source

for virus propagation without cell destruction. We also demonstrate that primary human endothelial and smooth muscle cells are a suitable *in vitro* system mirroring vascular *in vivo* infection.

Materials and Methods

Ethical statement

All work with Nipah virus and potentially infectious materials and animals was completed in the BSL4 facility at the Rocky Mountain Laboratories, Division of Intramural Research, National Institute of Allergy and Infectious Diseases, National Institutes of Health. The Institutional Biosafety Committee (IBC) approved all standard operating procedures applied. Animal experiments were approved by the Institutional Animal Care and Use Committee of the Rocky Mountain Laboratories and performed following the guidelines of the Association for Assessment and Accreditation of Laboratory Animal Care, International (AAALAC) by certified staff in an AAALAC-approved facility.

Cells and Virus

Vero C1008 cells (European Collection of Cell Cultures, Salisbury, UK), primary human microvascular lung endothelial cells (EC) (Lonza), and primary human pulmonary artery smooth muscle cells (SMC) (Lonza) were purchased and propagated according to manufactures reconditions. HeLa cells expressing ephrin B2 or ephrin B3 were kindly provided by Chris Broder (Uniform Services University, MD). Nipah virus (Malaysian strain) was kindly provided by the Special Pathogens Branch of the Center for Disease Control and Prevention, Atlanta, GA, USA. Virus were propagated on Vero E6 cells in

Dulbecco's Modified Eagle's medium (DMEM) (Sigma) supplemented with 10% fetal calf serum, 2 mM l-glutamine, 50 IU/mL penicillin and 50 μg/mL streptomycin (Life Technologies) and supernatants were clarified by low-speed centrifugation and stored in liquid nitrogen.

Tissue staining

Historical tissue blocks from Nipah virus infected hamster (140) and African green monkey (AGM) (104) were analyzed for effects of infection on endothelial and smooth muscle cells. Embedded tissues were stained with hematoxylin and eosin (H&E). Specific Nipah virus IHC was performed using an anti-Nipah virus nucleocapsid rabbit primary antibody at a 1:5000 dilution (kindly provided by L. Wang, CSIRO Livestock Industries, Australian Animal Health Laboratory, Australia) (54). The tissues were then processed using the Discovery XT automated processor (Ventana Medical Systems) with a DAPMap (Ventana Medical Systems) kit. Tissues were also stained for with 1:100 anti-smooth muscle actin mouse monoclonal (Millipore) and 1:700 anti-CD31 (LifeSpan BioSciences) for identification of smooth muscle cells and endothelial respectively.

In vitro infection

Nipah virus infection was performed on cells in 48-well plates when cells had reach 90-95% confluence. Growth media was removed and diluted virus was added in 250 μL of fresh media (multiplicity of infection (MOI) of 5, 0.1, and 0.01). After 1 hr, the inoculum was replaced with fresh media. Supernatants were collected at 1 hr, and for every day after infection up to 20 days for virus titration. On a separate plate, cells were infected as above and stained using the Kwik Diff Kit (Thermo scientific) to visualize syncytia according to the instructions of the manufacturer. Cells were monitored for

cytopathic effect (CPE) with a light microscope and images were captured using a Nikon DS-Fi1 camera. Cells were grown on 8-well chamber slides and infected as above at an MOI of 5. These cells were fixed at the designated time points in formalin for 24 hours then the formalin was replaced and the samples were removed from BSL-4 for immunofluorescence.

Virus visualization

Vero C1008 cells were grown to confluence in 96-well plates in normal growth media. Ten-fold serial diluted samples in Dulbecco's Modified Eagle's medium (DMEM) (Sigma) supplemented with 2% fetal calf serum, 2 mM l-glutamine, 50 IU/mL penicillin and 50 µg/mL streptomycin (Life Technologies) were added to the well. Cells were then incubated for 5 days at 37°C, 5% CO_2 and the scored for CPE.

For viral protein expression, SMC were infected with Nipah virus at MOI 1, and 0.01 and cells were collected in SDS buffer 2 days later. Cells were centrifuged and the cell pellet was used for 10% SDS-polyacrylamide gel electrophoresis. Proteins were transferred to a PVDF membrane (GE healthcare, UK) and probed with Nipah N specific rabbit sera (kindly provided by L. Wang, CSIRO Livestock Industries, Geelong, Australia).

Chamber slides, for immunofluorescence, were infected with Nipah virus at an MOI of 5 then fixed at the designated time point in 10% formalin overnight. Formalin was then exchanged and slides were taken out of BSL4. After fixation, slides were washed in PBS then incubated in 0.2% triton x100 for 7 minutes followed by blocking in PBS/4% BSA for 10 minutes. Slides were then incubated in Nipah N specific rabbit sera

followed by anti-rabbit alexa 488. ProLong Gold antifade reagent with DAPI (Invitrogen) was applied to the slides and all slides were visualized by confocal microscopy.

Ephrin expression

Endogenous expression of ephrin was quantified in cell culture by flow cytometry. Cells were collected for flow cytometry and washed using PBS containing 15 mM EDTA. Cells were incubated with recombinant Human EphB4 (the ligand to Nipah virus receptor ephrin B2/ B3) labeled with human FC (R&D) for 1 hr, washed then incubated with anti-human IgG (H+L) alexa 647 (Life Technologies) and fixed in 4% paraformaldehyde (PFA). Flow cytometry was performed using an LSR II (BD Biosciences) and data were analyzed using FlowJo software (Treestar Inc.).

Lentivirus infection and co-cultures

SMC and EC were transduced with lenti viruses expressing red fluorescent protein (RFP) or green fluorescent protein (GFP) (Cellomics Technology) respectively per the manufactures protocol. Briefly, cells were incubated in growth media with 6 µg polybrene, and lentivirus stock for 24 hrs at 37°C followed by regular growth media exchange. Fluorescing SMC and EC cells were mixed in culture before Nipah virus infection (MOI 5). Cells were visualized for syncytia formation, CPE, and virus infection by Kwik Diff Kit and IFA.

Ephrin transfections and infections

SMC were transfected with human ephrin B2 in a CMV promotor driven expression plasmid (Sino Biological Inc.) or Nipah virus fusion (F) and glycoprotein (G) using the Nucleofector kit for primary smooth muscle cells (Lonza). Cultured cells at

$5x10^5$ in Nucleofector solution were mixed with DNA (1 μg ephrin, and 1 μg of F and 1 μg G) then loaded into a cuvette. The Nucleofector device was used with program A033 after which media was added to cells and cells were plated in 12-well plates. In the case of F and G transfection, cells were mixed with EC the day after transfection and then stained with Kwik Diff Kit 24 hrs later. After 2 days, ephrin B2 transfected cells, were transferred into BSL-4 and infected at MOI 5 with Nipah virus. Cells were observed for 2 days and stained by Kwik Diff Kit.

Results

Nipah virus infects smooth muscle and endothelial cells of the lung vasculature with distinct cytopathogenicity

Nipah virus infection in hamsters and African green monkeys (AGM) is characterized by systemic infection with vasculitis. In order to better understand the cellular targets of Nipah virus infection we focused on the vasculature of the lung, one of the target organs of infection. Historic tissue blocks of hamsters and AFMs lungs were used to identify vascular cells infected with Nipah virus. The hamster tissue was derived from animals 5 days after intraperitoneal infection with 1000 LD_{50} of Nipah virus and AGM tissues was derived from animals 10 days after intratracheal infection with $1x10^5$ PFU of Nipah virus. Tissues were stained for Nipah virus nucleocapsid as well as endothelial marker CD31 and smooth muscle actin to visualize infection in the vascular endothelial and tunica media. Stained sections showed Nipah virus positive cells surrounding small arteries in both hamsters and AGMs (Figure 4-1). Closer inspection showed antigen positive cells within the actin smooth muscle layer and the endothelium. Pathology observed in the tissues originated in the endothelial layer with syncytia

formation only observed in the endothelium of infected animals. Pathology was absent in the tunica media (Figure 4-1). These data are similar to what has been reported from human infections.

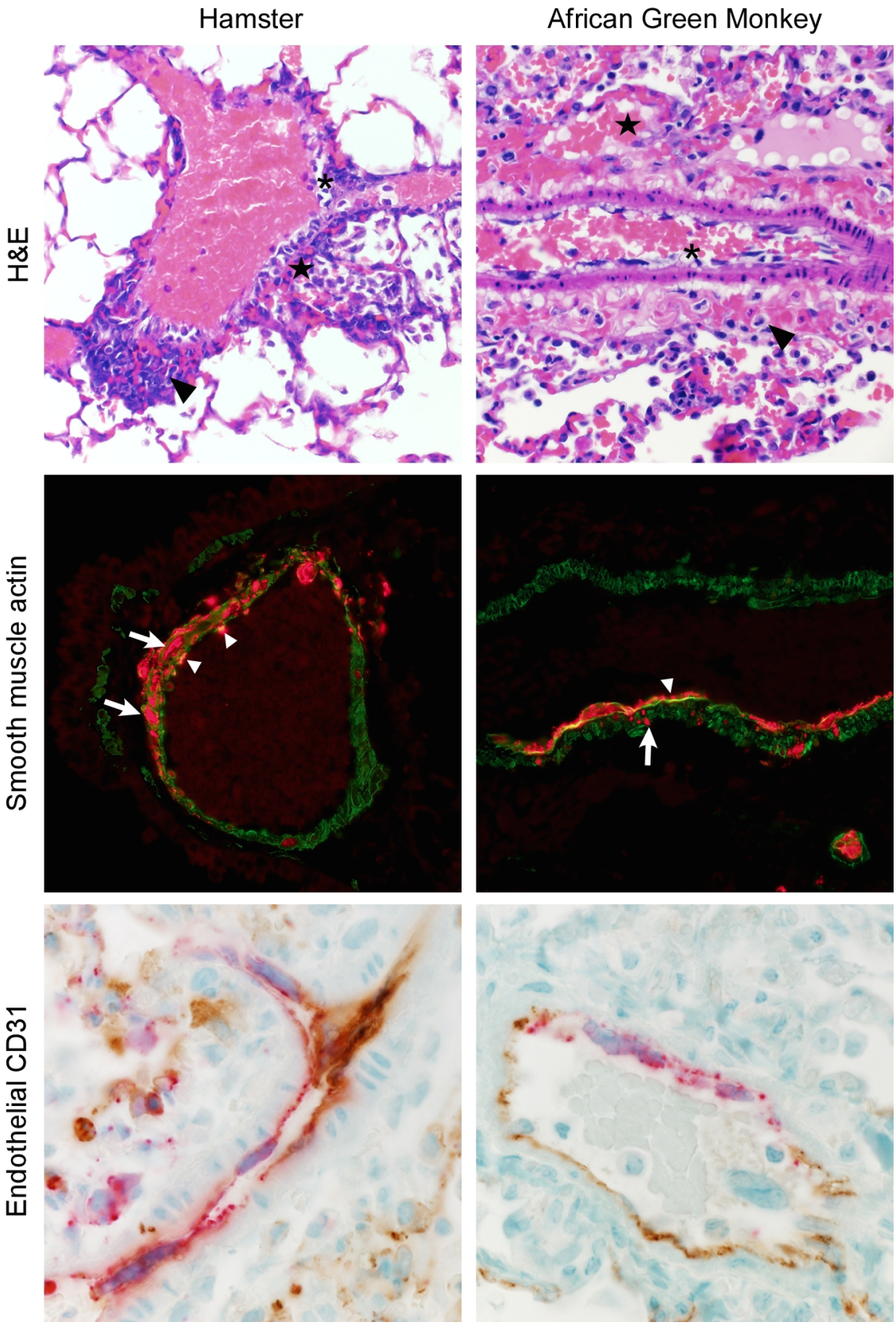
Hamster
African Green Monkey
H&E
Smooth muscle actin
Endothelial CD31

Figure 4-1: *In vivo* lung sections confirm Nipah virus antigen in endothelial and smooth muscle cells.

Lung tissue from hamsters (left column) and African green monkeys (right column) were sectioned and stained. The top row is stained with H&E. Asterisks denote vascular degeneration of EC, stars denote hemorrhage and arrowheads denote perivascular inflammation. The middle row shows staining for anti-smooth muscle actin in green and virus necleocapsid in red. Arrows point to infected SMC and arrowheads to infected EC. The last row is tissue stained for anti-CD31 in brown and viral nucleocapsid in red.

Primary human endothelial and smooth muscle cells support Nipah virus replication

To determine effects of Nipah virus infection on endothelial and smooth muscle cells *in vitro,* we used primary human microvascular endothelial cells from the lung (EC) as well as human pulmonary artery smooth muscle cells (SMC). We infected monolayers of both cells with Nipah virus at an MOI of 5, 0.1, and 0.01 and collected supernatants starting 1 hour after infection and continuing until extensive cytopathic effect (CPE) was observed (for EC) or primary cell viability decreased (for SMC). Cells were observed for CPE, syncytia formation, or other morphologic changes throughout the experiment. As early as 1 day following infection EC cells started to undergo morphologic changes including formation of syncytia (Figure 4-2A). By day 3, most EC cells were dead and peeled off the plate, showing complete destruction of the monolayer by Nipah virus infection. In contrast, SMC cells did not show any CPE or morphologic changes over 3 weeks in culture (Figure 4-2A).

To assess the ability of Nipah virus to infect SMC, as seen *in vivo*, we collected cells 2 days after infection to test for Nipah protein expression (B). Western blot analysis using an anti-Nipah N polyclonal serum confirmed infection and replication in SMC. Viral growth kinetics from primary cells confirmed that both EC and SMC supported Nipah virus replication (Figure 4-2). At both, high and low MOI, EC produced high viral loads, reaching peak titers already by day 1 or 2; these cells showed complete CPE on day 3 post infection. In contrast, SMC showed lower viral titer at early time points after infection compared to EC but reached similar high titer a few days later. Titers in SMC remained relatively high over an extended period of time with no obvious CPE. These

data demonstrate that both endothelial and smooth muscle cells can be infected *in vitro* mimicking the distinct pathology seen in infected animal models and human cases.

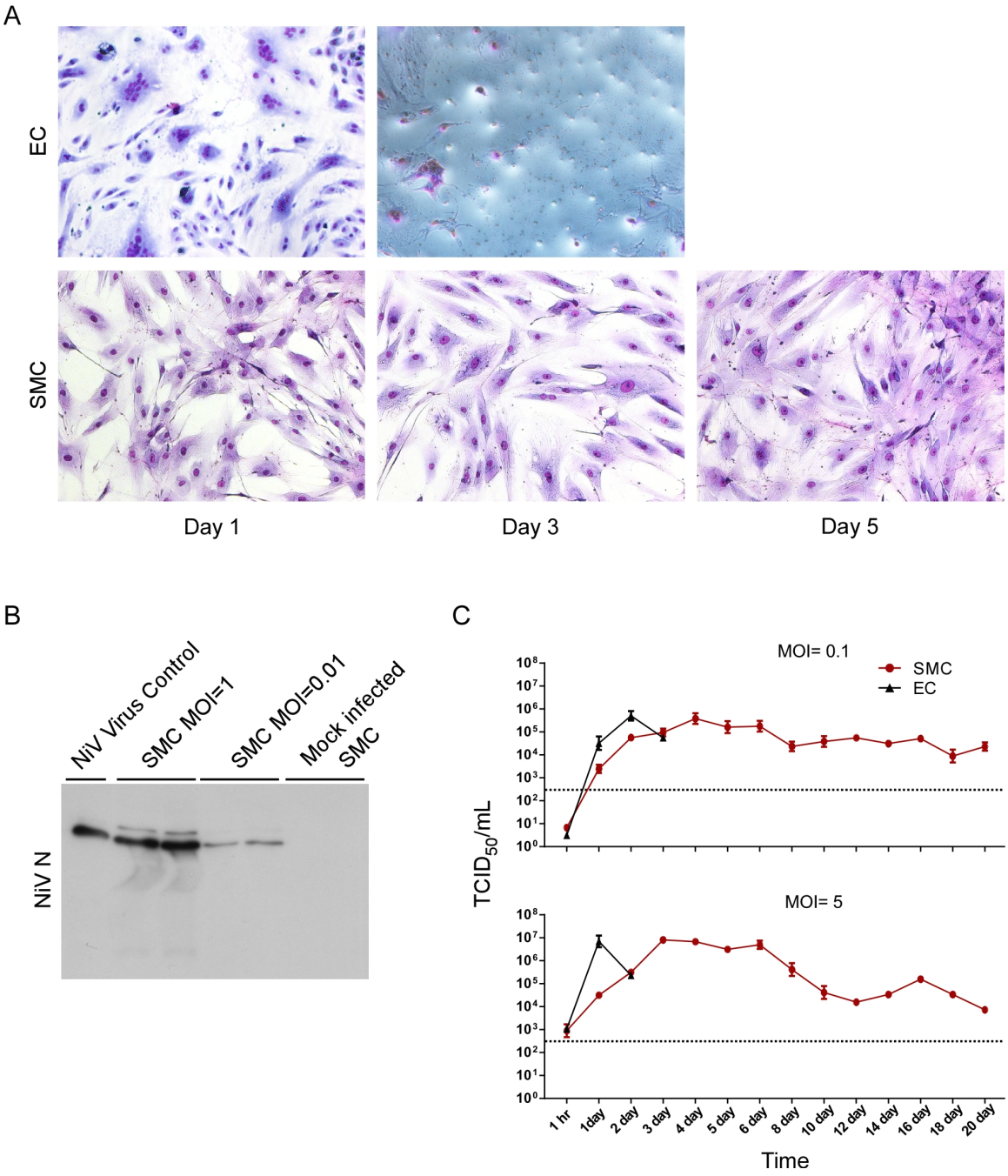
A
EC
SMC
Day 1
Day 3
Day 5
B
NiV Virus Control
SMC MOI=1
SMC MOI=0.01
Mock infected SMC
NiV N
C
MOI= 0.1
SMC
EC
MOI= 5
TCID50/mL
Time
1 hr
1 day
2 day
3 day
4 day
5 day
6 day
8 day
10 day
12 day
14 day
16 day
18 day
20 day

Figure 4-2: Human primary endothelial and smooth muscle cells are permissive to Nipah virus infection.

(A) Morphologic effects of Nipah virus infection on cells. EC and SMC were infected at an MOI of 0.1 and morphologic changes were visualized with the Kwik Diff Kit on days 1, 3, and 5 post infection. (B) Protein expression of Nipah virus nucleocapsid. SMC were infected at MOI 1 and 0.01 or mock infected and collected for western blot analysis 2 days post infection. Nipah virus proteins were used as a positive control in lane 1. (C) Quantification of viral replication in primary cells. Cells were infected at a MOI of 1 or 0.1 and supernatants were collected at the designated time points. Viral progeny in the collected supernatant was measured by a $TCID_{50}$ assay.

Smooth muscle cells have limited cell-to-cell spread compared to endothelial cells

To further characterize cell susceptibility including identifying number of initially infected cells and fusion capacity in cultures, we performed an immunoflourscent time course study in EC and SMC. Cell monolayers were infected at an MOI of 5 for an hour, washed and incubated until fixed at the designated times shown (Figure 4-3), then stained with anti-Nipah N polyclonal serum. Expression of Nipah viral nucleoprotein was first observed at 8 hours post infection (hpi) in EC and by 10 hpi in SMC. By 12 hpi EC samples showed the first evidence of syncytia formation followed by large syncytia and 100% infection by 14 hpi and cell destruction over the next 2-4 hours (Figure 4-3). In contrast to EC, SMC infection remained focal with little to no syncytia formation and a lack of cell-to-cell virus spread (Figure 4-3). These data suggest differences in virus entry, replication and/or maturation limiting Nipah virus infection to individual smooth muscle cells in contrast to a fulminant infection throughout the EC monolayer.

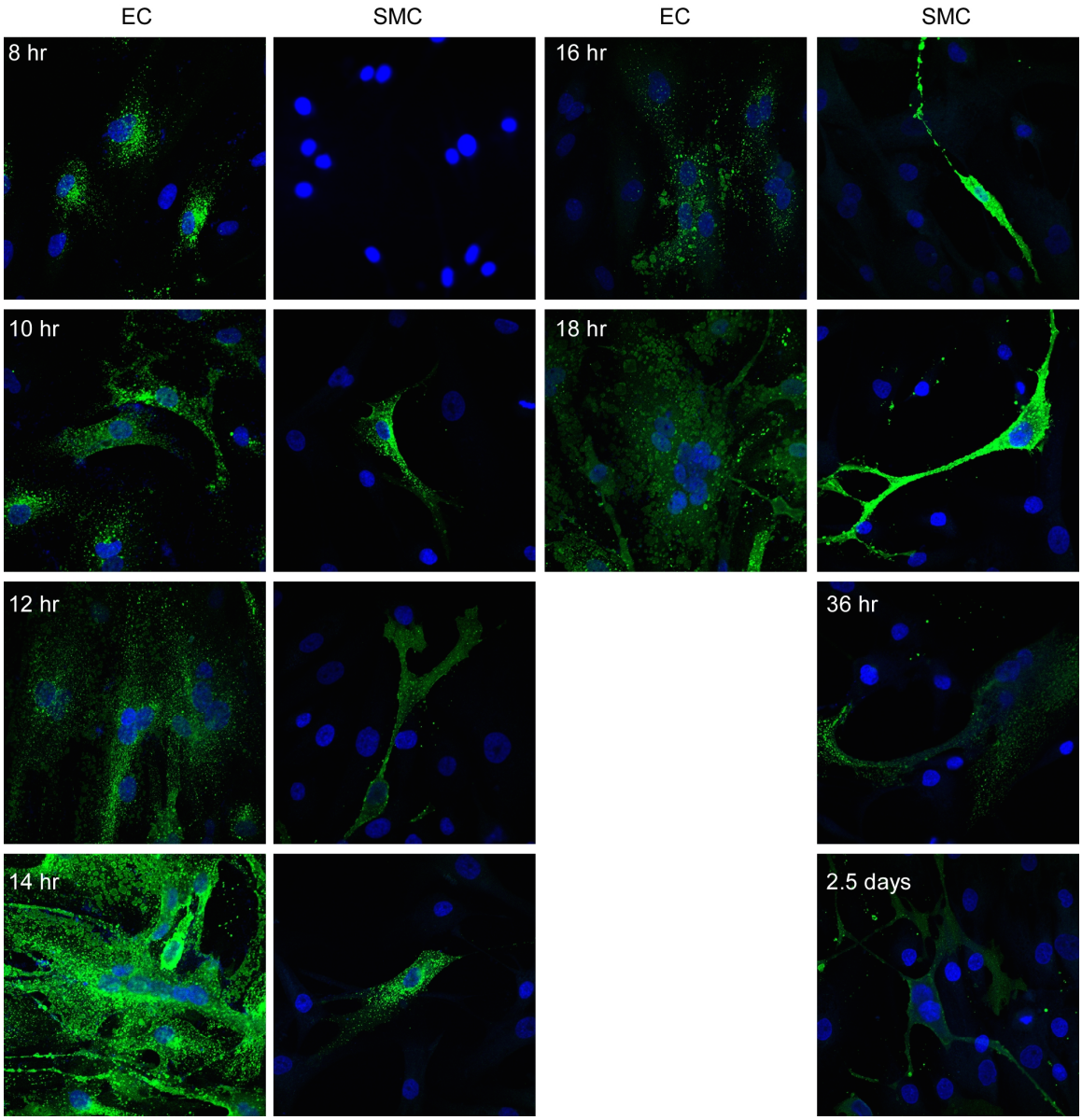

Figure 4-3: Visualization of Nipah virus infection over time in endothelial and smooth cells.

EC and SMC cultures were infected at a MOI of 5 and samples were fixed in formalin at the designated time point (8 hrs through 2.5 d post infection). Cells were permeabilized with triton x100 then stained with an anti- Nipah virus nucleocapsid antibody (green) and DAPI (blue).

Primary smooth muscle cells have minimal ephrin B2/B3 surface expression

Since infection of SMC is very inefficient, even with a high MOI, and the virus shows little ability to spread from cell-to-cell by initiating fusion, we hypothesized that SMC might express little or no ephrin B2/3. In order to test this hypothesis we used flow cytometry to measure ephrin expression on the cell surface. Cells were grown to confluency and then incubated with recombinant human EphB4-FC (the receptor for ephrin ligand). Analysis of both Vero and EC, which both are susceptible to cytolytic replication of Nipah virus, expressed measurable amounts of ephrin on their cell surface (Figure 4-4). In contrast, SMC showed little to no measureable ephrin surface expression. The lack of a functional receptor explains the low percentage of infected SMC seen *in vivo* and *in vitro*.

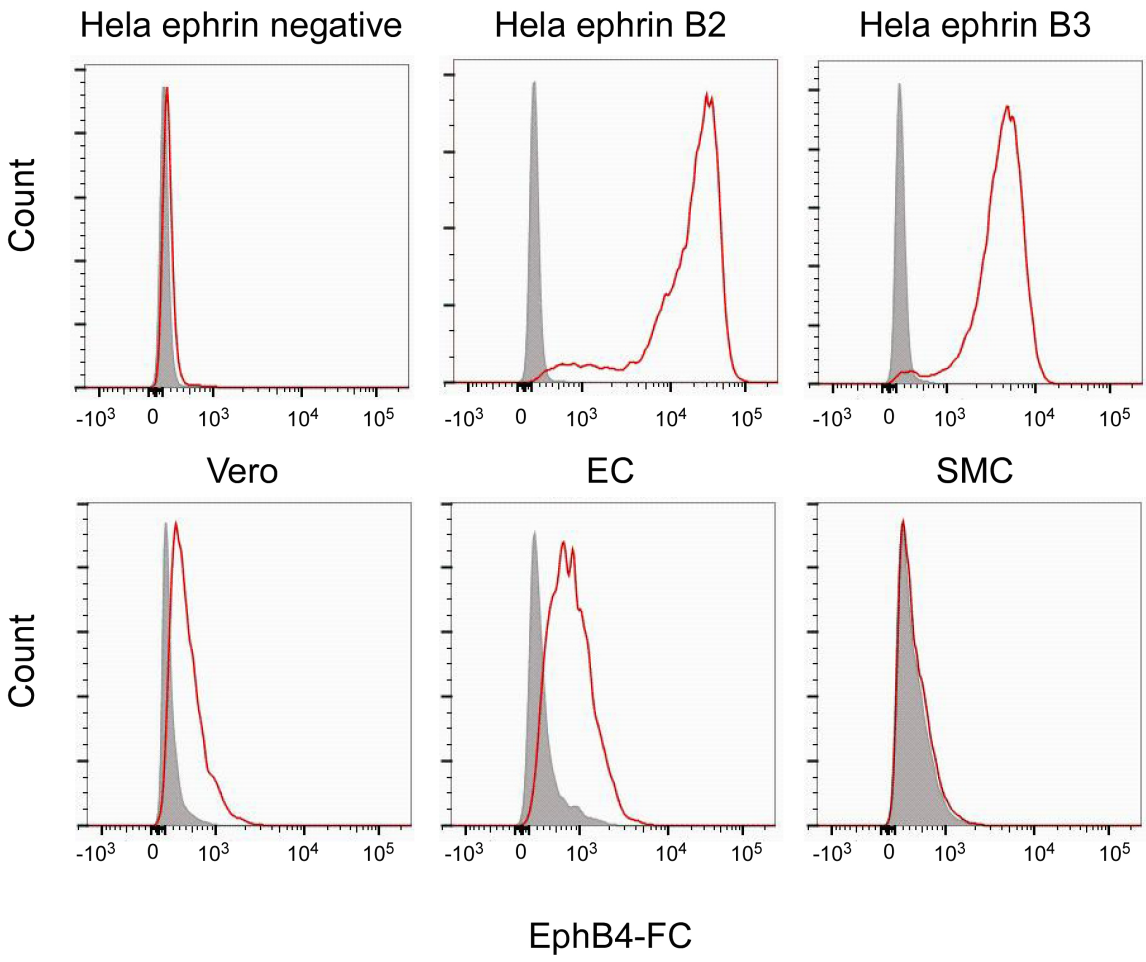

Figure 4-4: Smooth muscle cells show little ephrin expression on the cell surface compared to more susceptible cells.

Cells were collected and surface stained for ephrin expression by flow cytometry using recombinant EphB4-FC. Tinted histograms represent negative controls and colored lines represent replicates. HeLa cells were used as negative control cells and HeLa cells stabling expressing either ephrin B2 or B3 were used as positive controls.

Ephrin expression promotes spread of Nipah virus in smooth muscle cells

To test whether SMC are capable of fusing we transfected them with Nipah virus fusion and glycoprotein and mixed them with EC, with the notion that the glycoproteins on the SMC surface would fuse with the naïve EC expressing RFP. Alone, the transfected SMC did not fuse, but in combination with EC, wide-spread syncytia were observed (Figure 4-5A,B). The involvement of EC in the syncytium (Figure 4-5C) was confirmed by the presence of RFP which was expressed only in EC (Figure 4-5D); which could only fuse by binding SMC expressing Nipah virus glycoproteins.

To further confirm the fusogenic capacity of SMC and EC we co-cultured the cells and then infected them with Nipah virus (Figure 4-5,F). For this experiment, cells were fluorescently labeled using a lentivirus system, SMC-RFP and EC-GFP, in order to distinguish the cell types. In the co-cultures, we observed some cases where fusion occurred between SMC and EC (Figure 4-5F) resulting in a colocalization of flourscent proteins (RFP and GFP) and with viral proteins (white) in the cytoplasm. Fusion was not observed in uninfected mixed cultures (Figure 4-5E). These data show that SMC are capable of fusing with cells that express ephrin on their surface.

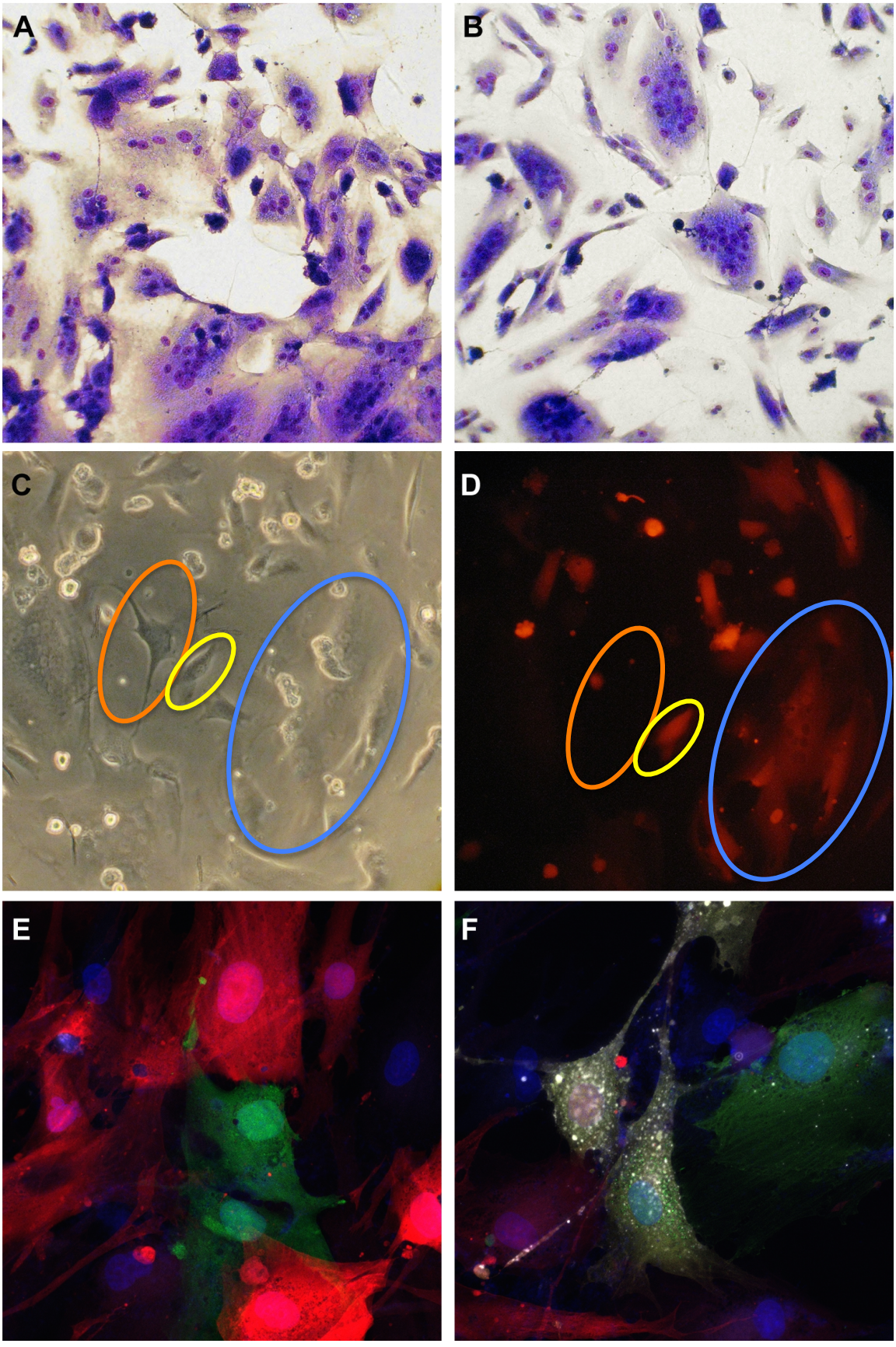
A
B
C
D
E
F

Figure 4-5: Smooth muscle cells expressing Nipah glycoproteins are able to fuse with naïve endothelial cells in mixed culture.

(A) Glycoprotein transfection of SMC enables fusion with EC. SMC cultures were transfected with Nipah virus fusion and glycoprotein using nucleofector then mixed with naïve EC. Cells were visualized with Kwik Diff Kit and demonstrate syncytia formation 24 hrs after mixing. (B) Infected smooth muscle cells mixed with naïve labeled endothelial cells results in labeled syncytia. EC were transduced with lenti-RFP prior to being mixed with SMC. SMC were infected at an MOI of 5, incubated for an hour, washed and mixed with EC expressing RFP. One day after –culturing syncytia were observed. An example of a SMC is outlined in orange, EC in yellow, and a syncytium in blue for better visualization. (C) Visualization of virus infection and syncytia in mixed culture of smooth muscle and endothelial cells. SMC and EC were transduced with lentivirus constructs expressing either GFP or RFP, respectively. After expression was confirmed cells were mixed followed by infection with Nipah virus at an MOI 5 (right panel) or mock infection (left panel). Cells were fixed 12 hrs after infection and stained with anti-Nipah nucleocapsid antibody (white) and dapi (blue). Syncytia composed of both SMC and EC are yellow in color.

Ephrin expression in smooth muscle cells rescues characteristic Nipah virus cytopathic effect and syncytia formation

To further confirm the role of ephrin for cytolytic Nipah virus replication in SMC, we transfected SMC with a plasmid expressing either ephrin B2 or an irrelevant protein (GFP) prior to infection. Plasmid transfection did not result in morphologic changes (Figure 4-6). Two days post transfection SMC were infected with Nipah virus at an MOI of 5 and observed for morphologic changes as an indicator for Nipah virus replication and spread. As early as 24 hpi small-scale syncytia started to form in SMC (Figure 4-6). At 48 hpi transfected cells were fused and started to show typical CPE. This experiment demonstrates that Nipah virus cytotoxicity in SMC can be achieved through expression of ephrin B2 on the cell surface.

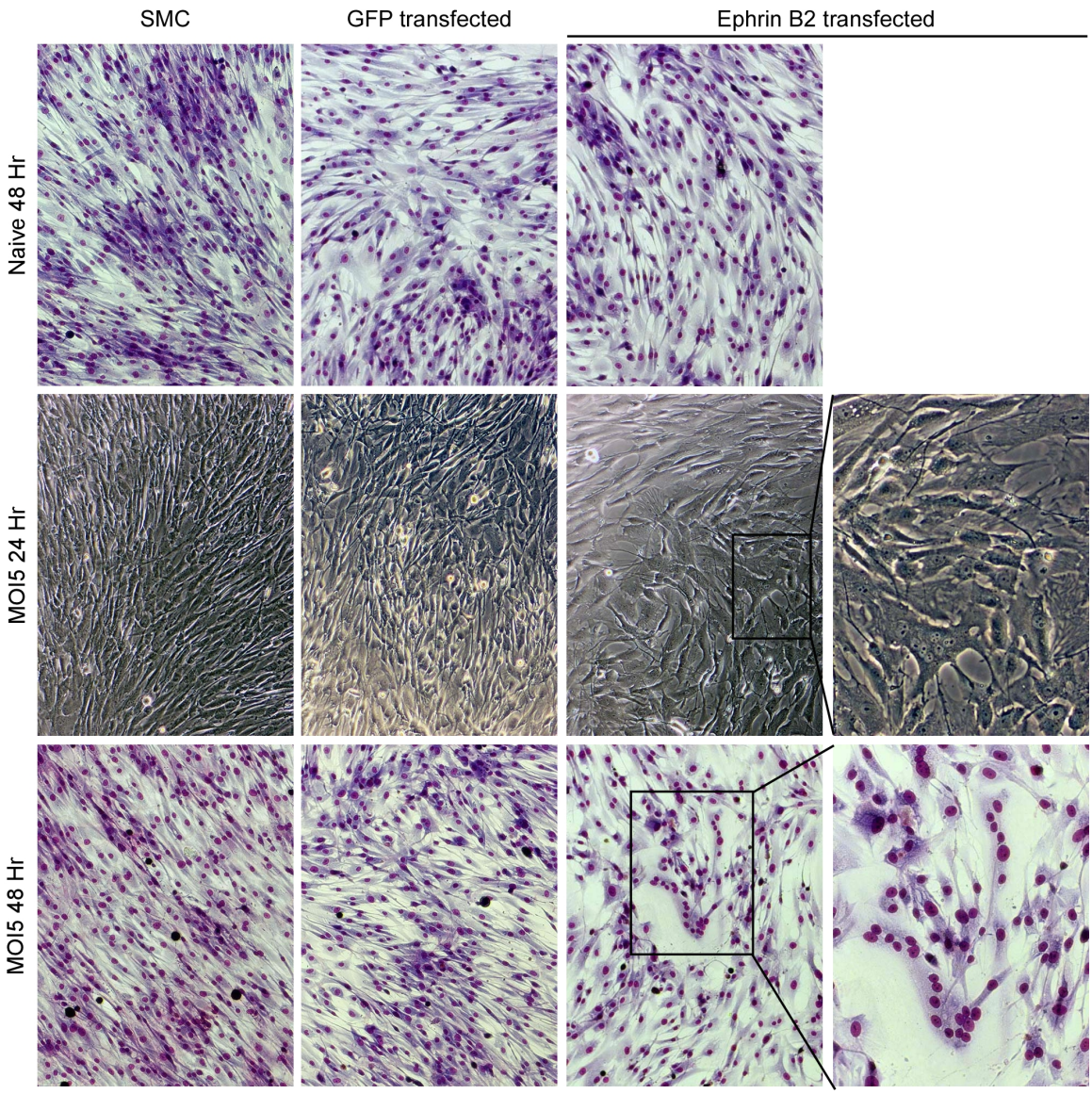

Figure 4-6: Ephrin expression on the surface of smooth muscle cells rescues Nipah virus induced cytopathology including syncytia formation.

SMC were either transfected with a GFP or ephrin B2 expression plasmid using nucleofactor reagent. The left panel shows naïve, the middle GFP transfected and the right 2 panels ephrin B2 transfected SMC. Cells are shown non-infected (top row) or after 24 (middle row) and 48 hr (bottom row) post infection. Cells were visualized by light microscopy at 24 hrs and then stained with Kwik Diff Kit at 48hrs post infection.

Discussion

Nipah virus is a zoonotic pathogen that causes encephalitis and respiratory distress in humans. Since its discovery in 1998 in Malaysia Nipah virus has been responsible for multiple smaller outbreaks in Bangladesh and India (121). The basic understanding of Nipah virus pathology in humans is solely derived from a few early autopsies; most of what we know about pathology is from studying disease in animal models. The most commonly used models for Nipah virus that recapitulate human disease are the hamster and the African green monkey (50, 56). A hallmark finding of pathology reports from infected humans and experimentally infected animals is the presence of viral antigen in the vasculature (141). Specifically, both endothelial cells lining the luminal side of the vessels as well as the tunica media surrounding the vessel walls have been reported as sites of viral replication (17). However, little is known about their role in virus spread and pathology. The goal of this study was to better define the role of endothelial cells and smooth muscle cells during Nipah virus infection.

In vivo we observed Nipah virus antigen systemically throughout the vasculature of infected animals. Focusing on the lung, staining of hamster and AGM tissue identified positive for viral antigen in the endothelium and the smooth muscle layers surrounding vessels. We observed syncytia formation and pathology particularly in endothelial cells, whereas smooth muscle cells seemed to be less infected with no obvious pathology. Antigen staining of smooth muscle cells seemed to be localized to SMC of the tunica media both in proximity to infected EC as well as in areas of uninfected EC. Indicating that both EC and SMC can become infected independently of each other. Taken together

our data confirms infection of endothelial and smooth muscle cells but raises the question why there is different cytopathology.

To study possible explanations for differences in cytopathology between these cell types we created an *in vitro* system using primary human cells. Human lung endothelial cells (EC) and human smooth muscle cells (SMC) were selected as surrogates for human vessels. Both primary cells were permissive to Nipah infection and replicated virus to high titers. Interestingly, smooth muscle cells once infected did not undergo morphologic changes, which mirror the situation *in vivo*. Unlike SMC, EC showed widespread cytopathology including syncytia formation within hours of infection.

Interestingly it appeared that the SMC were persistently infected for the lifetime of the primary cell culture, producing virus at high titer throughout. This phenomenon could allow for continuous viral production with little host cell consequence, thus acting as a virus production factory. Other viruses like rat virus (a parvovirus), encaphlamyocarditis virus, cytomegalovirus and Epstein-Barr virus have the capacity to infect SMC (142–146). Infection of SMC by Epstain-Barr virus and encaphlamycardiditis virus leads to a lytic infection, proving that infection of SMC can contribute to pathogensis of a viral infection (145, 146). In contrast, infection of SMC by cytomegalovirus and rat virus leads to viral latency or persistence (142–144, 147). The survival of infected SMC during viral infection in these systems leads to persistence similar to our results for NiV infection. *In vivo,* viral replication in SMC appears to be controlled by destruction of the surrounding EC, causing inflammatory cell recruitment and necrosis of the surrounding tissue, eventually destroying the vascular architecture and thus also affecting SMC.

To further identify the mechanisms of Nipah infection of these cells we stained infected cells over the lifetime of the primary culture for Nipah virus antigen. EC exhibited 100% infection with mass syncytia formation in as short as 16 hpi. In contrast, staining of SMC cultures revealed low level infection (about 10%) throughout with little evidence of virus spread and no obvious cytopathogenicity. The differences in percentage of infected cells between primary cells could account for the differences in CPE; however, it does not account for the lack of syncytia formation. Previous studies demonstrate that Nipah virus spread from cell-to-cell is accomplished by surface expression of the Nipah glycoproteins of infected cells which than leads to fusion with neighboring uninfected cells by interaction with the receptor, ephrin B2 or B3 (127, 148, 149). The non-fusigenic nature of these cells could be contributed to either ephrin expression or an inability of the cells to fuse. Other explanations of viral spread include viral production and spread from EC, from viral penetration through the damaged endothelium, or through capillaries. Since we see SMC infected independent of EC infection spread from EC or from damage to EC is unlikely.

Due to the low number of cells initially infected at a high MOI we choose to first pursue receptor expression. Our experiment indicated that EC express ephrin on the cell surface, while SMC showed little to no receptor surface expression. This supported our hypothesis that there is a lack of receptor on the surface of SMC limiting viral infection, spread and syncytia formation. How the original cells became infected in the absence of the measurable surface receptor is yet unknown. Biologically smooth muscle cells express ephrin during cell differentiation and maturing, and thus some cells in our cultures could be of varying maturity (11, 150). This is, however, unlikely due to

selection of cells for primary culture by using numerous mature smooth muscle markers. It could also be that the amount of ephrin is lower than detection of our assay or that only on a small percentage of cells in the population express it. Another explanation could be that Nipah virus in SMC uses a different mechanism for viral entry. Early studies of Nipah entry identified macropinocytosis as a possible entry mechanism for Nipah virus (13). Another explanation could be the presence of a second receptor for Niaph virus entry in SMC. For example, measles virus, a member of the same family, can use either CD46 or SLAM as its cell entry receptor (151).

To further study the impacts of ephrin expression and the ability of SMC to fuse we co-cultured either infected or glycoprotein transfected SMC with naïve EC. This experiment resulted in fusion between SMC and EC demonstrating that SMC are capable of expressing Nipah virus glycoproteins on the surface thus leading to fusion with EC. We also transfected naïve SMC with human ephrin B2 followed by viral infection, which resulted in productive Nipah virus replication and cytopathogenicity including syncytia formation. Together these data demonstrate that the lack of host cell damage in smooth muscle cells can be linked to the absence of receptor expression.

In this paper we investigated infection of EC and SMC by Nipah virus both *in vitro* and *in vivo.* We found that both in tissue as well as cell culture smooth muscle cells are productively infected; however, little SMC derived pathology is observed in either case. We show that primary human SMC and EC can act as a surrogate system for Nipah virus infection of the vasculature. By studying infection of this *in vitro* system, we postulated that SMC could serve as a reservoir for Nipah virus production and or persistence, much like infection with rat virus and cytomegalovirus. Previous research of

SMC and EC interactions show that direct EC damage by virus infection can lead to proliferation of SMC (152, 153). SMC express ephrin on their cell surface during developmental stages and thus proliferation could account for differences in susceptible of SMCs to Nipah virus infection . Even though previous papers have identified SMC as a target of Nipah virus infection, this is the first study to specifically research the effects of Nipah virus infection on SMC. Further research will have to identify potential secondary receptors on target cells that lack ephrins such as SMC. A better understanding of the mechanisms of Nipah virus infection will promote the development of new therapeutic approaches against this serious regional public health threat.

Acknowledgments

This work was supported by the Division of Intramural Research (DIR), National Institutes of Allergy and Infection Diseases (NIAID), National Institutes of Health (NIH). The authors would like to thank Dan Long, Rebecca Rosenke, and Tina Thomas (Rocky Mountain Veterinary Branch, DIR, NIAID, NIH) for histopathology work, and Anita Mora (DIR, NIAID, NIH) for graphics.

Conflict of Interest

All authors declare no conflict of interest.

CHAPTER 5 SINGLE-DOSE LIVE-ATTENUATED NIPAH VIRUS VACCINES CONFER COMPLETE PROTECTION BY ELICITING ANTIBODIES DIRECTED AGAINST SURFACE GLYCOPROTEINS.

Abstract

Background: Nipah virus (NiV), a zoonotic pathogen causing severe repiratory illness and encephalitis in humans, emerged in Malaysia in 1998 with subsquent outbreaks on an almost annual basis since 2001 in parts of the Indian subcontinent. The high case fatality rate, human-to-human transmission, wide-ranging reservoir distribution and lack of licensed intervention options are making NiV a serious regional and potential global public health problem. The objective of this study was to develop a fast-acting, single-dose NiV vaccine that could be implemented in a ring vaccination approach during outbreaks.

Methods: In this study we have designed new live-attenuated vaccine vectors based on recombinant vesicular stomatitis viruses (rVSV) expressing NiV glycoproteins (G or F) or nucleoprotein (N) and evaluated their protective efficacy in Syrian hamsters, an established NiV animal disease model. We further characterized the humoral immune response to vaccination in hamsters using ELISA and neutralization assays and performed serum transfer studies.

Results: Vaccination of Syrian hamsters with a single dose of the rVSV vaccine vectors resulted in strong humoral immune responses with neutralizing activities found only in those animals vaccinated with rVSV expressing NiV G or F proteins. Vaccinated animals with neutralizing antibody responses were completely protected from lethal NiV disease, whereas animals vaccinated with rVSV expressing NiV N showed only partial protection.

Protection of NiV G or F vaccinated animals was conferred by antibodies, most likely the neutralizing fraction, as demonstrated by serum transfer studies. Protection of N-vaccinated hamsters was not antibody-dependent indicating a role of adaptive cellular responses for protection.

Conclusions: The rVSV vectors expressing Nipah virus G or F are prime candidates for new 'emergency vaccines' to be utilized for NiV outbreak management.

Introduction

Nipah virus (NiV; family *Paramyxoviridae*, genus *Henipavirus*) was discovered to be the causative agent of an outbreak of viral encephalitis in pig farmers in Malaysia in 1998. This initial large outbreak has been followed by smaller nearly annual outbreaks in Bangladesh and India (62, 74). Disease in humans is characterized by respiratory distress and/or encephalitis, with histopathologic changes in the lung and brain showing multinucleated giant cells throughout the microvasculature (62, 74, 80). NiV is highly pathogenic in humans and has reached up to 100% case fatality rates (average 70%) (154). Transmission of NiV from its natural reservoir, *Pteropus* fruit bats, to pigs and humans has been documented, as well as human-to-human transmission (34, 44, 67).

Currently there are no approved vaccines or therapeutics for human use against NiV infections. Although a public health concern to regional, national and even international authorities, a widespread campaign to vaccinate a large percentage of the at-risk human population against NiV infection currently seems unfounded. Outbreaks are rare, result in relatively few cases, are focal and isolated, and human-to-human transmission is generally confined to health care workers and family members engaging in close contact with exposed individuals, thus, rather favoring a ring vaccination

approach. Therefore, a vaccine that produces a rapid and robust immune response after a single immunization with the potential for peri-exposure application ('emergency vaccine') would be most beneficial.

Current vaccine approaches for protection from NiV infection have focused on the use of NiV glycoprotein (G) and/or fusion protein (F) as immunogens in various platforms, including DNA vaccines, subunit vaccines, non-replicating vectors, as well as replicating vectors (49, 54, 99, 105–113, 115, 116, 155, 156). Efficacy of most of the previously tested vaccine candidates required a prime/boost(s) approach, which would not favor their use in an emergency situation for rapid dissemination during an outbreak.

In order to develop a vaccine appropriate for ring vaccination, we generated live-attenuated recombinant vesicular stomatitis viruses (rVSVs) encoding individual NiV proteins using the established reverse genetic system for VSV (157). The VSV system has been used to generate vaccine candidates for many disease-causing viruses (158–161). As a fast-acting single-dose vaccine, rVSV-based vaccines have been reported to elicit effective humoral and cellular immune responses, as well as to protect peri-exposure (159, 162).

Herein, we tested the protective efficacy of three rVSVs expressing either the nucleoprotein (N), F or G of the Malaysian strain of NiV. Following a single dose, the vaccine vectors expressing G and F fully protected Syrian hamsters from lethal NiV challenge, whereas the N expressing vector conferred only partial protection. Using passive serum transfer, we further determined that full protection is conferred by glycoprotein (F, G)-specific antibodies, most likely the neutralizing fraction, elicited by the rVSV vaccines. However, other components of the immune system, such as cellular

responses, also contribute to protection as demonstrated by partial efficacy and lack of protection in passive transfer studies in the case of the N expressing vaccine vector.

Materials And Methods

Cells and Viruses.

Vero C1008 cells (European Collection of Cell Cultures, Salisbury, UK) and baby hamster kidney cells expressing the bacteriophage T7 promoter (BHK-T7) (kindly provided by Dr. Naoto Ito, Gifu University, Japan (163)) were used. NiV (Malaysian strain) was kindly provided by the Special Pathogens Branch, Center for Disease Control and Prevention, Atlanta, and propagated as previously described (140).

Generation of rVSV Vectors.

The plasmid pVSVXN2 (kindly provided by J. Rose, Yale University, New Haven) was modified as previously described to encode the open reading frame (ORF) for *Zaire ebolavirus* (ZEBOV) glycoprotein (GP) in place of that encoding the VSV glycoprotein (G) (164, 165). NiV F, G, or N ORFs from the Malaysian strain of NiV, were amplified similarly and cloned into pVSVXN2ΔG/ZEBOV-GP downstream of ZEBOV-GP (Figure 5-1A). BHK-T7 cells were transfected using *trans*it-LT1 Transfection Reagent (Mirus, Madison, WI) along with individual plasmids encoding the VSV N, P, and L ORFs and the modified VSV genomic plasmids as shown in Figure 5-1A. Cells were incubated at 37°C for 7 days, at which time supernatant was collected and passaged once on fresh Vero cells. Cultures were monitored daily for cytopathogenic effect (CPE) and supernatants or cells were collected for sequence confirmation and analysis of protein

expression. The rescued viruses are referred to as rVSV-ZEBOV-GP-NiVF, rVSV-ZEBOV-GP-NiVG and rVSV-ZEBOV-GP-NiVN.

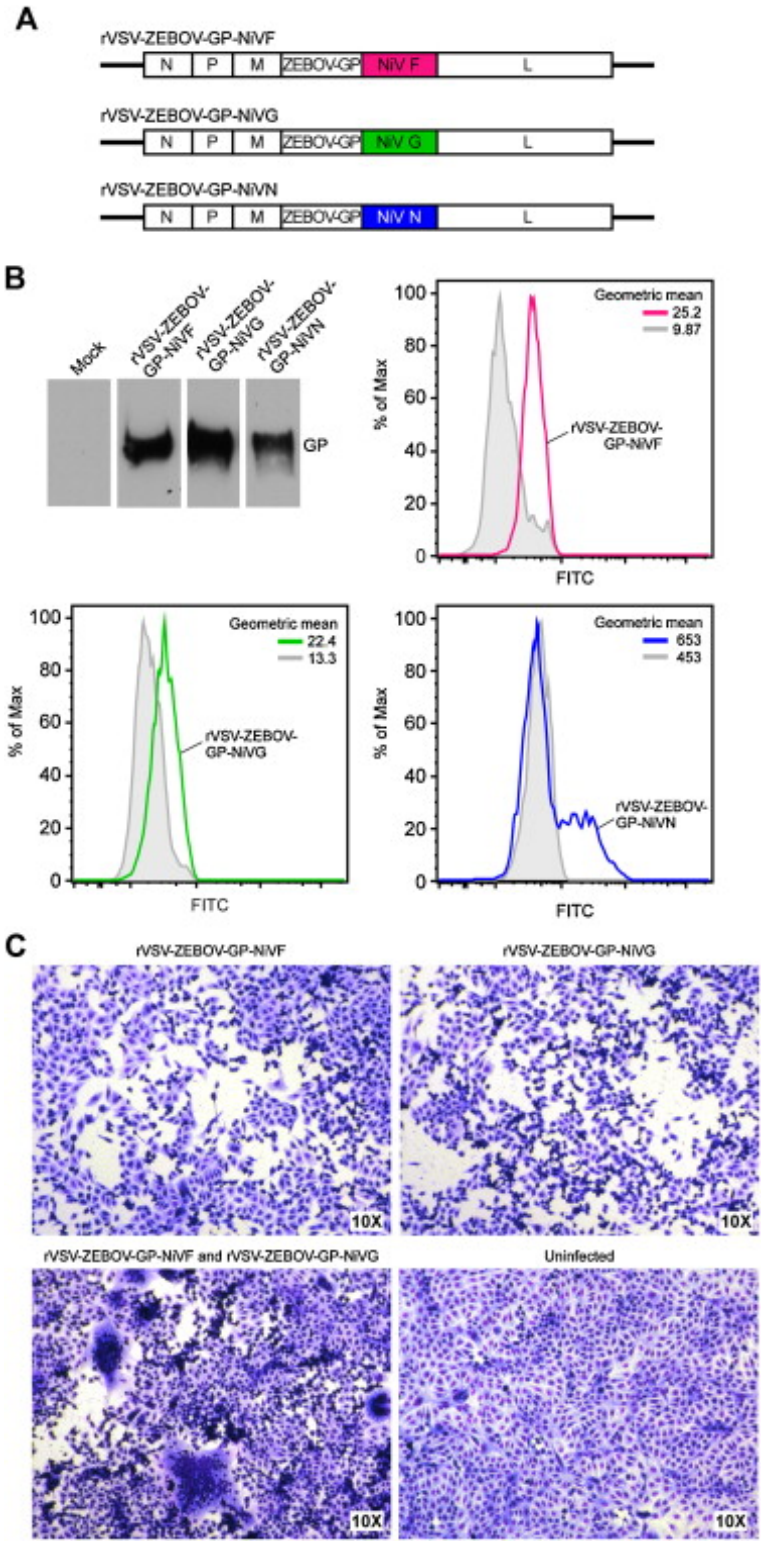
A
rVSV-ZEBOV-GP-NiVF
N
P
M
ZEBOV-GP
NiV F
L
rVSV-ZEBOV-GP-NiVG
NiV G
rVSV-ZEBOV-GP-NiVN
NiV N
B
Mock
rVSV-ZEBOV-GP-NiVF
rVSV-ZEBOV-GP-NiVG
rVSV-ZEBOV-GP-NiVN
GP
% of Max
Geometric mean
25.2
9.87
FITC
22.4
13.3
653
453
C
10X
Uninfected

Figure 5-1: Construction and characterization of recombinant VSV *(*rVSV*)* vectors expressing NiV glycoprotein *(*G*),* fusion protein *(*F*),* or nucleoprotein *(*N*).*

(A) Schematic representation of the vaccine constructs. rVSV-ZEBOV-GP-NiV constructs were engineered by cloning NiV protein open reading frames into the vector directly downstream of the ZEBOV-GP, which replaced VSV-G. (B) Verification of foreign protein expression. ZEBOV-GP expression was verified by western blot analysis of rVSV vector-infected cell lysates using the anti-ZEBOV-GP antibody 43.3.7. Expression of NiV proteins was verified by flow cytometry. Cells were infected with the different NiV protein-expressing rVSV vaccines (colored lines) or uninfected (gray lines) and surfaced stained with antibodies specific for the respective protein, anti-G 1187 and anti-F 835. In the case of N expression (colored line), cells were fixed in 4%PFA, then permeabilized using saponin, followed by intracellular N-specific antibody staining. (C) Verification of fusogenic activity of F and G. Vero C1008 cells were infected with rVSV-ZEBOV-GP-NiVF, rVSV-ZEBOV-GP-NiVG, or co-infected with rVSV-ZEBOV-GP-NiVF and rVSV-ZEBOV-GP-NiVG at an MOI of 0.1, incubated for 2 days and stained with the Kwik Diff Kit. Medium (DMEM) alone was used as a negative control.

Analysis of Protein Expression.

Vero cells were infected with the different rVSVs at a multiplicity of infection (MOI) of 1. Two days later, cell culture supernatants were collected, centrifuged, and the resulting pellet was subjected to 10% SDS-polyacrylamide gel electrophoresis. Proteins were transferred to a PVDF membrane (GE healthcare, UK) and ZEBOV-GP was detected using the monoclonal antibody 43.3.7 (kindly provided by A. Takada, Hokkaido University, Sapporo, Japan). Flow cytometry was performed to detect NiV F, G and N expression. Virus-infected Vero cells (12 h post infection) were collected and washed in PBS containing 15 mM EDTA. For surface staining, cells were incubated with the primary antibodies anti-G 1187 (148) and anti-F 835 (kindly provided by Hector Aguilar-Carreno, Washington State University, USA), followed by incubation with goat anti-rabbit antibodies conjugated to Alexa 488 (Life Technologies) and fixed in 4% paraformaldehyde (PFA). For intracellular staining, cells were fixed in 4% PFA for 10 min, then washed and incubated in buffer containing 0.2% saponin (Sigma) for 10 min. After permeabilization, cells were incubated with an anti-NiV N rabbit antiserum (54) (kindly provided by L. Wang, CSIRO Livestock Industries, Geelong, Australia), followed by the above mentioned goat anti-rabbit antibodies in the presence of saponin. Flow cytometry was performed using an LSR II (BD Biosciences, San Jose, CA) and data were analyzed using FlowJo software (Treestar Inc., Ashland, OR). To measure the fusogenic activity of expressed NiV F and G, Vero cells were grown in 48-well plates and infected with individual rVSVs or co-infected with rVSV-ZEBOV-GP-NiVF and rVSV-ZEBOV-GP-NiVG for 1 h at a MOI of 0.1. After 2 days, cells were stained and fixed with the Kwik Diff kit (Thermo Scientific).

Immunization and Challenge of Syrian Hamsters.

Groups of 10, 4-5 week old, Syrian hamsters (Harlan, Indianapolis, IN) were vaccinated intraperitoneally (i.p.) with 10^5 plaque forming units (PFU) of the specified rVSV vectors, or mock-vaccinated with DMEM in a total volume of 500 µL. Two days prior to NiV challenge (day 26 post vaccination), blood was collected by retro-orbital bleeding for analysis of antibody responses. After 28 days, animals were challenged i.p. with 1000 LD_{50} (6.8×10^4 $TCID_{50}$) of NiV and monitored for clinical signs of disease. Necropsies were performed on four animals from each group 5 days post challenge to measure viral load, attempt virus isolation, and assess histopathology. Brain, lung, and spleen tissues were collected and placed in RLT lysis buffer (Qiagen, Valencia, CA) for RNA extraction, and in 10% formalin for histopathology and immunohistochemistry (IHC) analysis. The remaining six animals were used to monitor survival for 42 days post challenge.

Immune Response to Vaccination.

Antibody responses were measured by enzyme-linked immunosorbent assay (ELISA) as described previously (51). Neutralizing titers were determined by a neutralizing tissue culture infections dose 50% ($NTCID_{50}$) assay.

Histopathology and Immunohistochemistry.

Hamsters tissues were collected and processed as described previously (140). Embedded tissues were sectioned and stained with hematoxylin and eosin (H&E) or the above mentioned anti-NiV N rabbit antiserum at a 1:5000 dilution for immunohistochemistry (IHC) (54).

Quantitative Real-Time RT-PCR (qRT-PCR) and Virus Titration.

Tissues were processed for qRT-PCR as described previously targeting the NiV N (140). Defined dilutions of NiV RNA were used in triplicate to generate a standard curve from which sample $TCID_{50}$ equivalents were extrapolated. NiV isolation and titration was performed as previously described (51). A similar method was used in a qRT-PCR assay targeting VSV N with the Fwd primer: CGGAGGATTGACGACTAATGC, Rev primer: CGAGCCATTCGACCACATC and probe: FAM- CGC CAC AAG GCA G-MGB.

Passive Transfer of Antibodies.

Groups of 18, 4-5 week old, hamsters were vaccinated i.p. with 10^5 PFU of the specified rVSV vaccine vectors. After 28 days, animals were exsanguinated via cardiac puncture, serum was inactivated by gamma-irradiation (5 Mrads) and measured for antibody titers by ELISA and $NTCID_{50}$ assay as described above. Positive sera were pooled from each group. Groups of six naïve hamsters were given 1 mL of serum i.p. 1 day prior to, and 1 day post i.p. challenge with 1000 LD_{50} (6.8×10^4 $TCID_{50}$) of NiV and monitored for clinical signs for 42 days.

Ethics and Biosafety.

All work with NiV was completed in the BSL4 facility at the Rocky Mountain Laboratories, NIAID, NIH under standard operating procedures approved by the Institutional Biosafety Committee. All animal experiments were approved by the Institutional Animal Care and Use Committee and performed following the guidelines of the Association for Assessment and Accreditation of Laboratory Animal Care, International (AAALAC) by certified staff in an AAALAC-approved facility.

Results

Rescue of replication-competent rVSV vectors

To generate rVSVs expressing NiV proteins, the F, G, or N ORFs were amplified and individually inserted into pVSVXN2ΔG/ZEBOV-GP downstream of the ZEBOV-GP gene as previously described (165) (Figure 5-1A). Individual genome constructs were transfected together with the VSV helper plasmids into BHK-T7 cells and the supernatants were passaged once onto fresh Vero cells. Cultures demonstrating CPE were verified for viral protein expression using western blotting of whole cell lysates for the detection of ZEBOV-GP, and flow cytometry for the detection of NiV F and G on the cell surface and NiV N intracellular. All three rescued rVSVs expressed ZEBOV-GP, and the individual viruses also expressed either NiV F, G, or N (Figure 5-1B). To verify the structural and functional integrity of surface expressed NiV F and G, their fusogenic activity was tested by co-infecting a monolayer of Vero cells with rVSV-ZEBOV-GP-NiVF and rVSV-ZEBOV-GP-NiVG. We observed large-scale cell-to-cell fusion resulting in multinucleated syncytia formation, a phenomenon that requires the presence of functional NiV F and G on the cell surface (Figure 5-1C).

Immunization with rVSV vectors elicits strong specific antibody responses

The humoral immune response to vaccination was assessed in Syrian hamsters, a well-established NiV animal disease model (50, 53). Groups of 10 hamsters were immunized with a single i.p. dose of 10^5 PFU of the different rVSV vectors (rVSV-ZEBOV-GP-NiVF, rVSV-ZEBOV-GP-NiVG or rVSV-ZEBOV-GP-NiVN) and rVSV-ZEBOV-GP as the control. After 26 days, blood samples were obtained and tested for NiV-specific antibodies by ELISA using antigen prepared from whole inactivated NiV particles. In

contrast to the animals in the control group (rVSV-ZEBOV-GP), all other vaccinated animals showed high levels of antibodies titers ranging from 1600 to ≥3200 (Table 1). In addition, we tested all sera for the presence of neutralizing antibodies against NiV. As expected, vaccination of hamsters with rVSV-ZEBOV-GP or rVSV-ZEBOV-GP-NiVN did not result in the generation of neutralizing antibodies (Table 1). In contrast, all animals from the groups vaccinated with rVSV-ZEBOV-GP-NiVF and rVSV-ZEBOV-GP-NiVG generated neutralizing antibody titers ranging from 80 to ≥640 (Table 5-1).

Table 5-1: Humoral immune responses to foreign proteins 26 days after rVSV vaccination as measured by ELISA (whole inactivated NiV particle antigen) and $NTCID_{50}$ assay (against live Nipah virus).

	ZEBOV-GP		NiV F		NiV G		NiV N	
Animal	ELISA Titer	Neut. Titer	ELISA Titer	Neut. Titer	ELISA Titer	Neut. Titer	ELISA Titer	Neut. Titer
1	<20	<20	≥3200	160	≥3200	640	1600	<20
2	<20	<20	≥3200	80	≥3200	320	≥3200	<20
3	<20	<20	≥3200	160	≥3200	≥640	≥3200	<20
4	<20	<20	≥3200	80	≥3200	≥640	≥3200	<20
5	<20	<20	≥3200	320	≥3200	≥640	≥3200	<20
6	<20	<20	≥3200	180	≥3200	320	≥3200	<20
7	<20	<20	≥3200	320	≥3200	≥640	1600	<20
8	<20	<20	≥3200	320	≥3200	≥640	≥3200	<20
9	<20	<20	≥3200	320	≥3200	320	1600	<20
10	<20	<20	≥3200	320	≥3200	≥640	1600	<20

Vaccination confers protection against lethal Nipah virus infection

The animals (10 per group) from the immune response study above were subsequently challenged i.p. with 1000 LD_{50} of NiV. For the protection study we added a group of six hamsters that was mock-vaccinated (DMEM). Six animals in each group were monitored for survival. Animals in both control groups, DMEM and rVSV-ZEBOV-GP, developed clinical signs of disease between days 5 and10 post challenge, resulting in respiratory distress with varying degree of neurologic dysfunction, and were euthanized according to the approved protocol (Figure 5-2A). All animals in the groups vaccinated with rVSV-ZEBOV-GP-NiVF and rVSV-ZEBOV-GP-NiVG were completely protected from clinical disease with no significant weight loss (Figure 5-2A and B). Hamsters vaccinated with rVSV-ZEBOV-GP-NiVN were partially protected (two of six animals) with no clinical signs of disease, while the remaining four animals had to be euthanized 9 days post challenge (Figure 5-2A, and B).

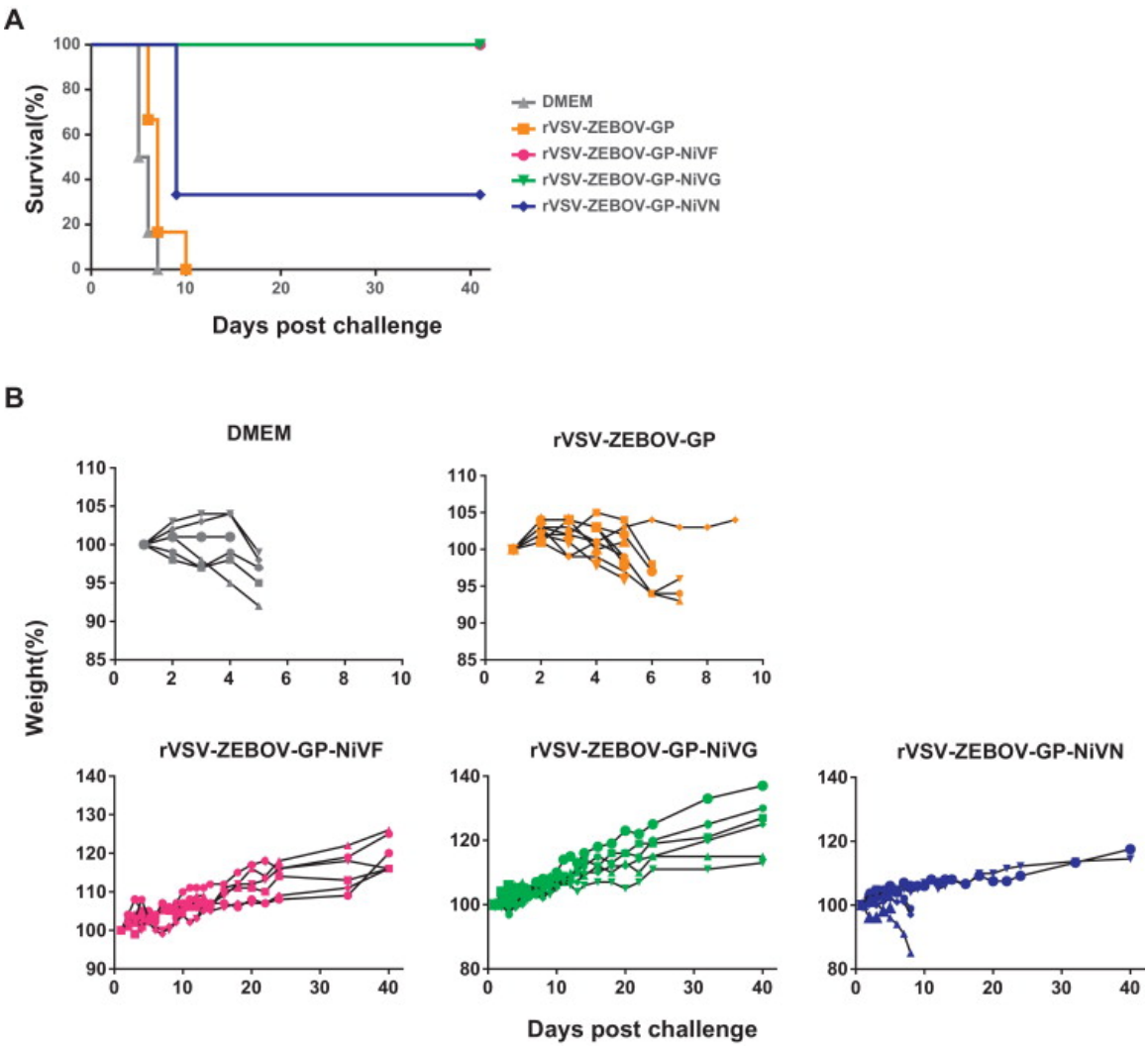

Figure 5-2: Survival of vaccinated hamsters following Nipah virus challenge.

Groups of six hamsters were vaccinated i.p. with 10^5 PFU of rVSV-ZEBOV-GP, rVSV-ZEBOV-GP-NiVF, rVSV-ZEBOV-GP-NiVG, rVSV-ZEBOV-GP-NiVN or mock vaccinated (DMEM) 28 days prior to challenge with 1000 LD_{50} of NiV. (A) The percentage of animals surviving over time. (B) Body weight loss over time. Weights are shown as percentage of starting body weight.

Vaccinated animals showed reduced viral loads and less pathology

In order to determine the impact of vaccination on virus replication, we collected brain, lung and spleen tissues 5 days post NiV challenge from four hamsters of each group described above for NiV load determination and isolation. Viral loads were determined using a NiV N-specific qRT-PCR assay (Figure 5-3). All NiV-vaccinated animals had lower organ levels of viral RNA compared to the animals in the control groups (>10^3 $TCID_{50}$ equivalent/mg tissue), with rVSV-ZEBOV-GP-NiVF and rVSV-ZEBOV-GP-NiVG vaccinated animals showing organ loads <1 $TCID_{50}$ equivalent/mg tissue. rVSV-ZEBOV-GP-NiVN vaccinated animals showed a greater than 2-log reduction in viral organ loads compared to the rVSV-ZEBOV-GP vaccinated controls. In order to confirm that the positive immunohistochemistry described below (Figure 5-4) represents replication of the challenge virus (NiV) rather than N expressed by the vaccine vector (rVSV-ZEBOV-GP-NiVN), we performed a VSV N-specific qRT-PCR assay. No VSV N RNA could be detected in lung tissue of the rVSV-ZEBOV-GP-NiVN vaccinated animals. NiV isolation was only successful from control animals (rVSV-ZEBOV-GP group).

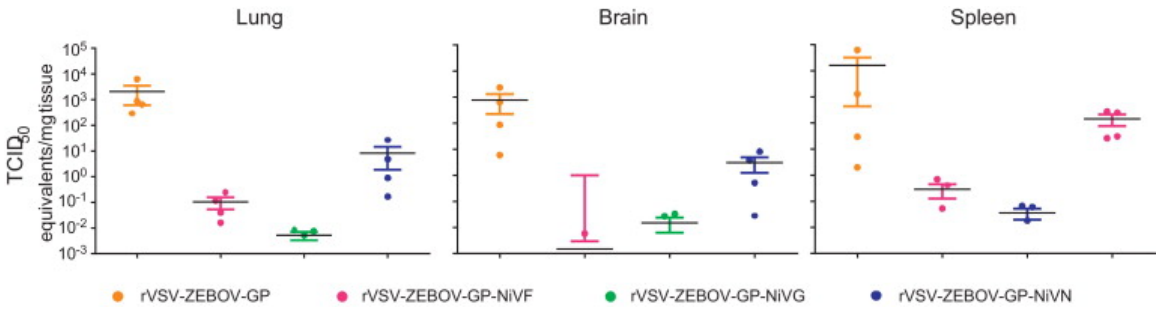

Figure 5-3: Vaccination reduces Nipah virus load in tissues.

Tissues (brain, spleen, lung) were collected in RLT buffer from four animals per group on day 5 after challenge and homogenized prior to total RNA extraction. Quantitative RT-PCR using an N-specific primer and probe set was used to determine $TCID_{50}$ equivalents by extrapolating from a standard curve from a NiV seed stock of known titer. Individual animals are represented by dots and horizontal lines represent the mean, error bars indicate standard error of the mean (SEM).

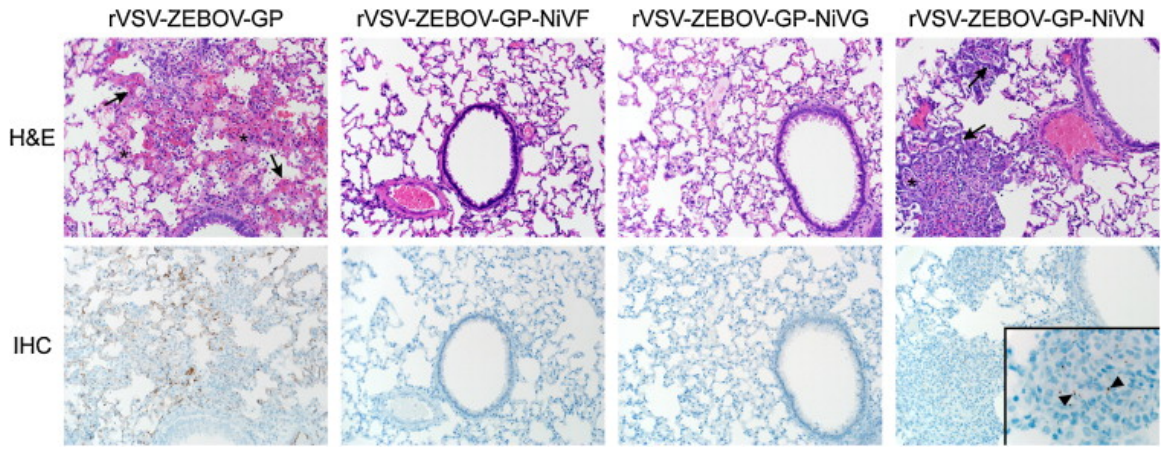

Figure 5-4: Vaccination reduces Nipah virus pathology.

Four hamsters per group were euthanized 5 days post challenge and lung sections were stained with H&E (top panel) for histopathology evaluation and IHC targeting NiV N protein for virus replication (bottom panel). Infected lungs showed thickening of the alveolar septae (arrows) by congestion, fibrin, edema, and small numbers of inflammatory cells. Alveolar spaces are filled with fibrin, edema, and inflammatory cells (asterisk). Inset in IHC panel demonstrates positive staining of NiV N-antigen (arrow heads). Images were taken at a magnification of 200× and inset at 1000×.

Staining for histological analysis was performed on lung tissue derived from the same 4 animals euthanized 5 days post challenge. All rVSV-ZEBOV-GP vaccinated control animals developed multifocal interstitial pneumonia characterized by thickening of the alveolar septae by small to moderate numbers of macrophages, fewer neutrophils, congestion, fibrin and edema (Figure 5-4). Occasionally, small numbers of inflammatory cells, fibrin and edema filled the adjacent alveolar spaces. There was also multifocal pleural mesothelial hyperplasia. Alveolar and arteriolar endothelial cells and pulmonary arteriolar smooth muscle cells demonstrated diffuse viral antigen by IHC staining (Figure 5-4). Most animals (three out of four) in the partially protected rVSV-ZEBOV-GP-NiVN group developed pneumonia similar to that found in controls. These hamsters had rare and weak multifocal viral antigen staining, primarily within mononuclear cells in areas of pneumonia. All animals in the completely protected groups (rVSV-ZEBOV-GP-NiVF and rVSV-ZEBOV-GP-NiVG) showed no lesions and were negative for viral antigen by IHC staining (Figure 5-4).

Passive serum transfer protects naïve animals from Nipah virus infection

To test whether antibodies elicited by the rVSV vectors alone can afford protection against NiV challenge, we performed a passive transfer experiment. Groups of 18 hamsters were vaccinated with 10^5 PFU i.p. of one of the rVSV vectors. After 28 days, sera were collected and pooled for each group. Pooled sera from rVSV-ZEBOV-GP-NiVF and rVSV-ZEBOV-GP-NiVG had neutralization titers of 200 and 400, respectively, whereas sera collected from the rVSV-ZEBOV-GP and rVSV-ZEBOV-GP-NiVN vaccinated groups were negative. Groups of six naïve hamsters were administered i.p. 1 mL of pooled serum the day prior to and the day following NiV challenge (1000

LD_{50}). All animals, except one, that received serum without neutralizing activity (rVSV-ZEBOV-GP and rVSV-ZEBOV-GP-NiVN) had to be euthanized according to protocol (Figure 5-5). All animals that received serum displaying neutralizing activity (rVSV-ZEBOV-GP-NiVF- or rVSV-ZEBOV-GP-NiVG) were completely protected from NiV challenge with no signs of disease.

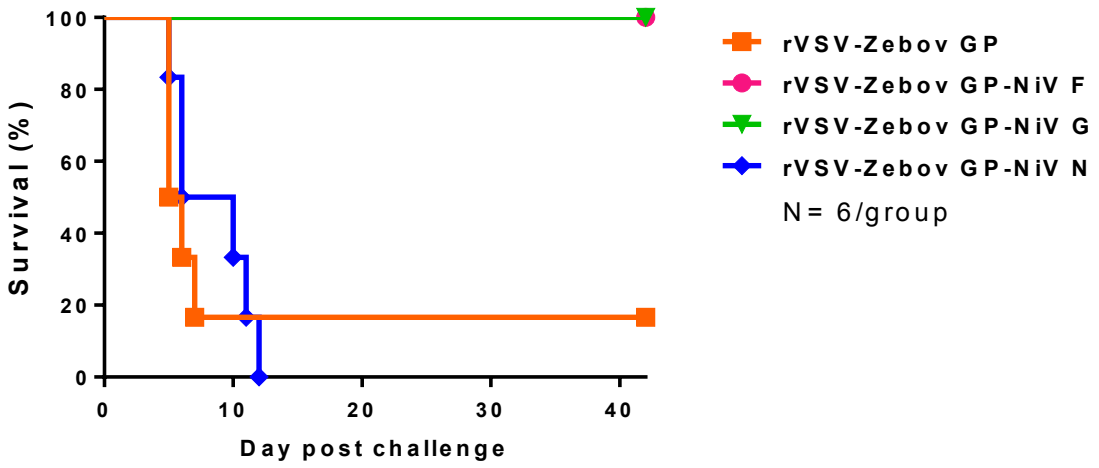

Figure 5-5: Passive serum transfer protects naïve hamsters from Nipah virus challenge. **Serum was collected from groups of 18 hamsters 28 days after vaccination with 10^5 PFU of the specific vaccine vectors. One day prior to, and 1 day post challenge with 1000 LD_{50} of NiV, groups of six naïve hamsters were given 1 mL of sera from immunized animals and monitored for 42 days for signs of disease**.

Discussion

Over the past decade, multiple distinct NiV vaccine approaches have been developed and evaluated in different animal models, including DNA vaccines, subunit vaccines (virus-like particles, soluble G protein), replication-deficient vectors as well as replication-competent vectors. Several of these approaches have only been evaluated for their ability to elicit immune responses, whereas others have been used to evaluate protective efficacy against NiV challenge in different animal models (49, 54, 99, 105–110, 112, 113, 115, 116, 155, 156).

With the exception of three recent studies, all vaccine approaches thus far have required a boosting immunization scheme for immunogenicity and/or efficacy and are therefor less likely to be useful for ring vaccination approaches in an outbreak situation. The three new studies include an adenovirus-associated virus vector expressing NiV G (108), replication-incompetent VSV pseudotypes expressing NiV G or F proteins (113) and a VSV virion with F and G that can undergo a single round of replication that was produced by co-infection of two VSV pseudotypes , one expressing F and one expressing G (114). The adenovirus-associated virus vector approach used relatively high vaccine doses, and the VSV approaches are based on replication-deficient pseudotype particles produced by plasmid transfections, both of which may be challenging in regards to vaccine production.

Our goal was to develop a fast-acting, single-dose NiV vaccine suitable for use as a ring vaccination approach during outbreaks as they currently occur in Bangladesh. We chose live-attenuated rVSV vectors as our platform due to their ease of genetic modification and their subsequent efficient and cost-effective manufacturing. We

preferred a replication-competent vaccine as those generally provide better durability when compared to a replication-incompetent vaccine approaches, eliciting faster and more effective innate and adaptive immune responses (166). Replication-competent vaccine approaches, however, are commonly associated with safety concerns, but all of our previous vaccine work using the rVSV platform, including immunization of several immune-compromised animal species, has assigned this approach a good safety record (159, 167). Noteworthy, a live-attenuated rVSV-based vaccine vector was approved for use in a human laboratory exposure to Ebola virus (168). Among commonly used replicating vaccine vectors, VSV provides advantages over similar platforms, such as the limited pre-existing immunity against VSV in the human population and the only rare and mild human disease caused by VSV, which is largely an animal pathogen (169, 170). To further limit VSV immunity and pathogenicity, we removed VSV-G, the major target for neutralizing antibodies and a key VSV virulence factor (170). VSV-G was replaced in the vaccine vector by ZEBOV-GP to overcome the lack of a functional surface protein for virus entry. Virus entry cannot be achieved by any of the chosen NiV antigens, because henipavirus cell entry is dependent on the presence of both G and F proteins (149). The ZEBOV-GP was particularly chosen for its known targeting of important immune cells, such as mononuclear phagocytotic and antigen presenting cells (160, 165, 171). Targeting of these cells allows for their strong stimulation and better antigen presentation by MHC class I and II pathways, and thus leads to more potent innate and adaptive immune responses (172, 173).

In order to characterize the mechanism of protection afforded by the rVSV-based vaccine vectors, we examined the importance of the humoral immune responses.

Previously it has been demonstrated that protection against NiV challenge can be afforded by passive serum transfer that contains neutralizing antibodies (99). Additionally, m102.4, a human neutralizing monoclonal antibody, can protect against NiV and Hendra virus in several animal models (54, 103). The rVSV vaccine vectors expressing NiV F or G both induced glycoprotein-specific antibody responses that conferred complete protection against NiV challenge in a serum transfer study. Neutralizing antibody responses are most likely key for protection, as serum transfer of N-specific antibodies did not show any protective effect, even though the role of non-neutralizing glycoprotein-specific antibodies for protection cannot be excluded. VSV is known to also elicit strong cellular immune responses (166, 174, 175). The role of cellular immune responses mediated through rVSV vectors is supported here by the partial protection achieved through vaccination with the rVSV vector expressing NiV N as well as the lack of protection in serum transfer experiments using sera with N-specific non-neutralizing antibodies. Therefore, these new rVSV vectors might be stronger vaccine candidates than vaccine platforms that more selectively trigger humoral immune responses, such as subunit protein vaccines (109, 110, 155).

Conclusions

Here we describe a vaccine approach and mechanism of protection that could be used to control NiV infections and spread in outbreak situation if used in a ring vaccination approach. Recent outbreaks have involved increased human-to-human transmission events, most often seen in family members or healthcare workers (67). Due to the ease in identifying high-risk individuals, those in close contact with patients, fast-acting, single-dose vaccines, like the rVSV vectors here, would be advantageous for

targeted use during outbreaks over vaccines that need multiple injections and thus require more time between vaccination and protection. Another advantage of replication-competent rVSVs has been its efficacy upon use peri-exposure, allowing for simultaneous vaccination and treatment in outbreak situations (159, 160, 165, 176, 177). Future studies are aimed to assess time to immunity and peri-exposure treatment efficacy of these new rVSV NiV vectors as well as efficacy studies in a second animal model to fulfill FDA requirements for licensing.

Acknowledgments

This work is fully published in *Vaccine*, 2014 May 7;32(22):2637-44. doi: 10.1016/j.vaccine.2014.02.087 (178).

http://www.sciencedirect.com/science/article/pii/S0264410X14003144

This work was supported by the Division of Intramural Research (DIR), National Institutes of Allergy and Infection Diseases (NIAID), National Institutes of Health (NIH).

The authors would like to thank Dan Long, Rebecca Rosenke, and Tina Thomas (Rocky Mountain Veterinary Branch, DIR, NIAID, NIH) for histopathology work, Elaine Haddock (DIR, NIAID, NIH) for BSL4 technical assistance and Anita Mora (DIR, NIAID, NIH) for graphics.

Conflict of Interest

All authors declare no conflict of interest.

CHAPTER 6 GENERAL DISCUSSION AND CONCLUSIONS

Nipah virus is a zoonotic pathogen that causes disease in humans in Asia. The initial outbreak of Nipah virus originated in Malaysia and caused over 100 human deaths as well as the culling of over 1 million pigs (26). Subsequent outbreaks have been localized to Bangladesh and India causing almost annual outbreaks. In the case of Nipah and Hendra viruses infection, there is no known treatment, infection is often fatal (~70% CFR), and may cause relapsing encephalitis (27, 78). Like many other emerging infectious diseases, Nipah virus emerged from a spill-over event from reservoir (bats) to domestic animals/livestock (pigs), followed by humans infection (sometimes human-to-human transmission). Today, with the increase in land use causing human encroachment and deforestation the interface between human/wildlife is increasing leading to the increase prevalence of new human pathogens (179–181). Factors like human bushmeat consumption, climate change, movement of animal species, increased population and shrinking wilderness habitat all play a role in increased interaction between wildlife and humans (182–185). Over the years, examples of increased spillover has been seen with the emergence of human immunodeficiency virus (HIV), chikungunya virus, influenza, and Middle East respiratory syndrome coronavirus to name a few (186). Research should focus on this interface, studying emerging and reemerging pathogens in a one-health approach including both human and veterinary studies.

Focusing on multidisciplinary studies during the Nipah outbreak in Malaysia, we see effects on human health, livestock health, and damage to the economy all caused by the outbreak. Nipah virus was found to be a bat-borne pathogen that spilled over into pigs in Malaysia (32, 34). Once the connection between bats-pigs-humans was made, action

was taken to reduced interactions between species; this led to the end of the outbreak and spread of the virus (26). However, this was after the virus spread to Singapore and caused more than 250 cases, and left many with relapsing encephalitis (76). Beside the human impact, the outbreak halted animal trade, closed many farms, and lead to the culling of over 1 million pigs, thus causing great economic loss. The virus reemerged in Bangladesh in 2001 and causes small outbreaks there and in neighboring India on an almost yearly basis. These outbreaks are thought to be caused by human-bat interactions and often are linked to the harvesting and drinking of date palm sap (44, 131). After this connection was made steps were made to reduce bat-human contact and bat-date palm sap interactions; the effects are still under review but appear to be reducing cases (41, 187). Another factor causing concern over Nipah virus is the large host range of the reservoir species and the detection of Nipah-like sequences in bats in Thailand, Africa, and Australia further emphasizing the importance of Nipah virus and strengthen the need to study this zoonotic pathogen (2, 38–40, 68, 188). The study of this virus has led to reduced infectious, however outbreaks still occur and further research into Nipah virus needs to be completed to further understand viral infection, develop therapies or vaccines, as well as manage future outbreaks more efficiently. To contribute to completing these goals, we 1) studied variations of the virus strains, comparing them in animals; 2) better defined pathology in important cell types; and 3) developed and tested vaccine candidates for future use during outbreaks.

Specifically we studied the outcome of infection with both Nipah strains in cell culture and in the hamster model focusing on pathogenesis and the host immune response. The strains were isolated from geographically and temporary separate

outbreaks(28, 125). Epidemiologic data and disease progression during outbreaks differs between strains. The current understanding of Nipah virus pathogenesis has come from human autopsies and experimental work with the Malaysian strain of Nipah virus. We infected hamster cells with both strains and found that Nipah Malaysia replicated faster and had more cytopathic effect (CPE) and syncytia formation compared to the Bangladesh strain. In the hamster model there was also a slight difference between strains. Overall there is a delay (about 2 days) in Nipah Bangladesh disease progression, including time to death, virus replication, pathology and immune response, compared to Malaysia infected animals. Overall infection with either strain resulted in similar disease and outcome in hamsters. This data hints that discrepancies in human life style, cultural differences, and quality of health care between the two countries could account for the differences in epidemiology reported rather than the differences in sequence (73, 189).

We also studied infection in the microvasculature, a major target of Nipah virus infection. Specifically, we focused on studying Nipah infection in endothelial cells (EC) and smooth muscle cells (SMC) using both animal models and primary human cell culture. We found that in hamster and African green monkey tissue Nipah virus antigen was detected in EC lining small vessels in the lung as well as the surrounding SMC. EC positive for Nipah virus antigen often showed signs of pathogenesis including syncytia formation, while SMC were infected but showed no negative effect from infection. Similarly to *in vivo* data, studies in primary human EC and SMC showed permissibility to infection and only CPE in EC. Further experiments showed that only a small fraction of SMC were infected in culture even though viral titers produced were high. This led us to hypothesize that entry into the cell and/ or spread to neighboring cells could be the

limiting factor/s in SMC infection. In testing the ability of SMC to fuse we found that infected SMC could fuse with non-infected EC, thus proving the ability of SMC to form syncytia after infection. To test entry as the limiting factor we analyzed receptor expression and found that SMC express little to no ephrin B2/B3 on the surface. The exact mechanism of viral entry in SMC need to be further studied; this data suggests that cells could become infected by other means, be it macropinocytosis or a second receptor.

After studying pathogenesis, we focused on creating a countermeasure that would protect from infection/disease. We created recombinant vesicular stomatitis virus based vaccines expressing Nipah virus antigens (glycoprotein, fusion protein, or nucleoprotein) and tested their efficacy in the hamster model. The glycoprotein and fusion protein group's showed no signs of disease or weight loss after infection and were completely protected from disease. Nucleoprotein vaccinated animals were partially protected with 2 out of 6 showing no clinical disease. As expected, control animals showed signs of disease and succumb to infection. In tissues we found that vaccination against Nipah reduced viral replication and antigen detection compared to control. This data supported the efficacy of our vaccines. In order to better understand the mechanisms of protection we did a passive transfer into naïve animals, which provided complete protection in vaccines that elicited neutralizing antibodies (F and G). Taken together this data suggest that neutralizing antibodies are enough to provide protection but that other cellular responses add to protection. This study showed that our vaccine was efficacious and that the VSV backbone is a strong inducer of antibodies and cellular responses that strengthen protection.

In conclusion, this work further elucidated pathology caused by Nipah virus infection and developed and testing of a potential vaccine candidate. We were the first to describe experimental infection of animals with Nipah Bangladesh as well as directly compare the strains under an experimental setting. Our work set the ground work for future experiments with the Bangladesh strain including further strain comparison in other animal models (190), transmission studies (51), and vaccine testing. Before this work little was known about Nipah infection in smooth muscle cells. Previous works have documented positive antigen staining in these cells but no work had yet studied their role in pathology and viral replication. Our work fills this gap of knowledge as well as leads to some interesting questions for further study. In this work we also describe a potent single dose vaccine that fully protects hamsters. This vaccine differs from previously published vaccines by eliciting a fast strong immune response after a single dose. Together our study adds to the fields understanding of Nipah virus pathology as well as proposes a possible vaccine candidate for use against disease, contributing to future management and treatment of outbreaks.

REFERENCES

1. **Wang L-F, Harcourt BH, Yu M, Tamin A, Rota PA, Bellini WJ, Eaton BT**. 2001. Molecular biology of Hendra and Nipah viruses. Microbes Infect. **3**:279–287.

2. **Marsh GA, de Jong C, Barr JA, Tachedjian M, Smith C, Middleton D, Yu M, Todd S, Foord AJ, Haring V, Payne J, Robinson R, Broz I, Crameri G, Field HE, Wang L-F**. 2012. Cedar virus: a novel Henipavirus isolated from Australian bats. PLoS Pathog. **8**:e1002836.

3. **Goldsmith CS, Whistler T, Rollin PE, Ksiazek TG, Rota PA, Bellini WJ, Daszak P, Wong K., Shieh W-J, Zaki SR**. 2003. Elucidation of Nipah virus morphogenesis and replication using ultrastructural and molecular approaches. Virus Res. **92**:89–98.

4. **Chua KB, Bellini WJ, Rota PA, Harcourt BH, Tamin A, Lam SK, Ksiazek TG, Rollin PE, Zaki SR, Shieh W, Goldsmith CS, Gubler DJ, Roehrig JT, Eaton B, Gould AR, Olson J, Field H, Daniels P, Ling AE, Peters CJ, Anderson LJ, Mahy BW**. 2000. Nipah virus: a recently emergent deadly paramyxovirus. Science (80-.). **288**:1432–5.

5. **Rota PA, Lo MK**. 2012. Molecular virology of the henipaviruses. Curr. Top. Microbiol. Immunol. **359**:41–58.

6. 2007. Fields Virology, 5th edition, 5th ed. Lippincott Williams & Wilkins, Philadelphia.

7. **Bonaparte MI, Dimitrov AS, Bossart KN, Crameri G, Mungall BA, Bishop KA, Choudhry V, Dimitrov DS, Wang L-F, Eaton BT, Broder CC**. 2005. Ephrin-B2 ligand is a functional receptor for Hendra virus and Nipah virus. Proc. Natl. Acad. Sci. U. S. A. **102**:10652–7.

8. **Negrete OA, Levroney EL, Aguilar HC, Bertolotti-Ciarlet A, Nazarian R, Tajyar S, Lee B**. 2005. EphrinB2 is the entry receptor for Nipah virus, an emergent deadly paramyxovirus. Nature **436**:401–5.

9. **Flanagan JG, Vanderhaeghen P**. 1998. The ephrins and Eph receptors in neural development. Annu. Rev. Neurosci. **21**:309–45.

10. **Erbar S, Diederich S, Maisner A**. 2008. Selective receptor expression restricts Nipah virus infection of endothelial cells. Virol. J. **5**:142.

11. **Augustin HG, Reiss Y**. 2003. EphB receptors and ephrinB ligands: regulators of vascular assembly and homeostasis. Cell Tissue Res. **314**:25–31.

12. **Negrete OA, Wolf MC, Aguilar HC, Enterlein S, Wang W, Mühlberger E, Su S V, Bertolotti-Ciarlet A, Flick R, Lee B**. 2006. Two key residues in ephrinB3 are critical for its use as an alternative receptor for Nipah virus. PLoS Pathog. **2**:e7.

13. **Pernet O, Pohl C, Ainouze M, Kweder H, Buckland R**. 2009. Nipah virus entry can occur by macropinocytosis. Virology **395**:298–311.

14. **Xu K, Rockx B, Xie Y, Debuysscher BL, Fusco DL, Zhu Z, Chan Y-P, Xu Y, Luu T, Cer RZ, Feldmann H, Mokashi V, Dimitrov DS, Bishop-Lilly KA, Broder CC, Nikolov DB**. 2013. Crystal Structure of the Hendra Virus Attachment G Glycoprotein Bound to a Potent Cross-Reactive Neutralizing Human Monoclonal Antibody. PLoS Pathog. **9**:e1003684.

15. **Harrison MS, Sakaguchi T, Schmitt AP**. 2010. Paramyxovirus assembly and budding: building particles that transmit infections. Int. J. Biochem. Cell Biol. **42**:1416–29.

16. **Whelan SPJ, Barr JN, Wertz GW**. 2004. Transcription and replication of nonsegmented negative-strand RNA viruses. Curr. Top. Microbiol. Immunol. **283**:61–119.

17. **Maisner A, Neufeld J, Weingartl H**. 2009. Organ- and endotheliotropism of Nipah virus infections in vivo and in vitro. Thromb. Haemost. **102**:1014–23.

18. **Diederich S, Moll M, Klenk H-D, Maisner A**. 2005. The nipah virus fusion protein is cleaved within the endosomal compartment. J. Biol. Chem. **280**:29899–903.

19. **Patch JR, Crameri G, Wang L-F, Eaton BT, Broder CC**. 2007. Quantitative analysis of Nipah virus proteins released as virus-like particles reveals central role for the matrix protein. Virol. J. **4**:1.

20. **Wang YE, Park A, Lake M, Pentecost M, Torres B, Yun TE, Wolf MC, Holbrook MR, Freiberg AN, Lee B**. 2010. Ubiquitin-regulated nuclear-cytoplasmic trafficking of the Nipah virus matrix protein is important for viral budding. PLoS Pathog. **6**:e1001186.

21. **Chua KB**. 2012. Introduction: Nipah virus--discovery and origin. Curr. Top. Microbiol. Immunol. **359**:1–9.

22. **Chua KB**. 2010. Epidemiology, surveillance and control of Nipah virus infections in Malaysia. Malays. J. Pathol. **32**:69–73.

23. **Chua KB**. 2010. Risk factors, prevention and communication strategy during Nipah virus outbreak in Malaysia. Malays. J. Pathol. **32**:75–80.

24. **Chua KB**. 2003. Nipah virus outbreak in Malaysia. J. Clin. Virol. **26**:265–275.

25. 1999. Outbreak of Hendra-like virus--Malaysia and Singapore, 1998-1999. MMWR. Morb. Mortal. Wkly. Rep. **48**:265–9.

26. 1999. Update: outbreak of Nipah virus--Malaysia and Singapore, 1999. MMWR. Morb. Mortal. Wkly. Rep. **48**:335–7.

27. **Chua KB, Goh KJ, Wong KT, Kamarulzaman A, Tan PS, Ksiazek TG, Zaki SR, Paul G, Lam SK, Tan CT**. 1999. Fatal encephalitis due to Nipah virus among pig-farmers in Malaysia. Lancet **354**:1257–9.

28. **Harcourt BH, Lowe L, Tamin A, Liu X, Bankamp B, Bowden N, Rollin PE, Comer JA, Ksiazek TG, Hossain MJ, Gurley ES, Breiman RF, Bellini WJ, Rota PA**. 2005. Genetic characterization of Nipah virus, Bangladesh, 2004. Emerg. Infect. Dis. **11**:1594–7.

29. **AbuBakar S, Chang L-Y, Ali ARM, Sharifah SH, Yusoff K, Zamrod Z**. 2004. Isolation and molecular identification of Nipah virus from pigs. Emerg. Infect. Dis. **10**:2228–30.

30. **Parashar UD, Sunn LM, Ong F, Mounts AW, Arif MT, Ksiazek TG, Kamaluddin MA, Mustafa AN, Kaur H, Ding LM, Othman G, Radzi HM, Kitsutani PT, Stockton PC, Arokiasamy J, Gary HE, Anderson LJ**. 2000. Case-control study of risk factors for human infection with a new zoonotic paramyxovirus, Nipah virus, during a 1998-1999 outbreak of severe encephalitis in Malaysia. J. Infect. Dis. **181**:1755–9.

31. **Amal NM, Lye MS, Ksiazek TG, Kitsutani PD, Hanjeet KS, Kamaluddin MA, Ong F, Devi S, Stockton PC, Ghazali O, Zainab R, Taha MA, N M Amal MSL**. 2000. Risk factors for Nipah virus transmission, Port Dickson, Negeri Sembilan, Malaysia: results from a hospital-based case-control study. Southeast Asian J. Trop. Med. Public Health **31**:301 – 6.

32. **Enserink M**. 2000. Emerging diseases. Malaysian researchers trace Nipah virus outbreak to bats. Science **289**:518–9.

33. **Luby SP, Hossain MJ, Gurley ES, Ahmed BN, Banu S, Khan SU, Homaira N, Rota PA, Rollin PE, Comer JA, Kenah E, Ksiazek TG, Rahman M**. 2009. Recurrent zoonotic transmission of Nipah virus into humans, Bangladesh, 2001-2007. Emerg. Infect. Dis. **15**:1229–35.

34. **Yob JM, Field H, Rashdi AM, Morrissy C, van der Heide B, Rota P, bin Adzhar A, White J, Daniels P, Jamaluddin A, Ksiazek T**. 2001. Nipah virus infection in bats (order Chiroptera) in peninsular Malaysia. Emerg. Infect. Dis. **7**:439–41.

35. **Chua KB**. 2003. A novel approach for collecting samples from fruit bats for isolation of infectious agents. Microbes Infect. **5**:487–490.

36. **Chua KB, Koh CL, Hooi PS, Wee KF, Khong JH, Chua BH, Chan YP, Lim ME, Lam SK**. 2002. Isolation of Nipah virus from Malaysian Island flying-foxes. Microbes Infect. **4**:145–51.

37. **Middleton DJ, Weingartl HM**. 2012. Henipaviruses in their natural animal hosts. Curr. Top. Microbiol. Immunol. **359**:105–21.

38. **Wacharapluesadee S, Boongird K, Wanghongsa S, Ratanasetyuth N, Supavonwong P, Saengsen D, Gongal GN, Hemachudha T**. 2010. A longitudinal study of the prevalence of Nipah virus in Pteropus lylei bats in Thailand: evidence for seasonal preference in disease transmission. Vector Borne Zoonotic Dis. **10**:183–90.

39. **Hayman DTS, Suu-Ire R, Breed AC, McEachern JA, Wang L, Wood JLN, Cunningham AA**. 2008. Evidence of henipavirus infection in West African fruit bats. PLoS One **3**:e2739.

40. **Drexler JF, Corman VM, Gloza-Rausch F, Seebens A, Annan A, Ipsen A, Kruppa T, Müller MA, Kalko EK V, Adu-Sarkodie Y, Oppong S, Drosten C**. 2009. Henipavirus RNA in African bats. PLoS One **4**:e6367.

41. **Khan MSU, Hossain J, Gurley ES, Nahar N, Sultana R, Luby SP**. 2010. Use of infrared camera to understand bats' access to date palm sap: implications for preventing Nipah virus transmission. Ecohealth **7**:517–25.

42. **Reynes J-M, Counor D, Ong S, Faure C, Seng V, Molia S, Walston J, Georges-Courbot MC, Deubel V, Sarthou J-L**. 2005. Nipah virus in Lyle's flying foxes, Cambodia. Emerg. Infect. Dis. **11**:1042–7.

43. **Mohd Nor MN, Gan CH, Ong BL**. 2000. Nipah virus infection of pigs in peninsular Malaysia. Rev. Sci. Tech. **19**:160–5.

44. **Luby SP, Gurley ES, Hossain MJ**. 2009. Transmission of human infection with Nipah virus. Clin. Infect. Dis. **49**:1743–8.

45. **Torres-Velez FJ, Shieh W-J, Rollin PE, Morken T, Brown C, Ksiazek TG, Zaki SR**. 2008. Histopathologic and immunohistochemical characterization of Nipah virus infection in the guinea pig. Vet. Pathol. **45**:576–85.

46. **Middleton DJ, Westbury HA, Morrissy CJ, van der Heide BM, Russell GM, Braun MA, Hyatt AD**. 2002. Experimental Nipah virus infection in pigs and cats. J. Comp. Pathol. **126**:124–36.

47. **Williamson MM, Torres-Velez FJ**. 2010. Henipavirus: a review of laboratory animal pathology. Vet. Pathol. **47**:871–80.

48. **Weingartl HM, Berhane Y, Czub M**. 2009. Animal models of henipavirus infection: a review. Vet. J. **181**:211–20.

49. **Weingartl HM, Berhane Y, Caswell JL, Loosmore S, Audonnet J-C, Roth JA, Czub M**. 2006. Recombinant nipah virus vaccines protect pigs against challenge. J. Virol. **80**:7929–38.

50. **Wong KT, Grosjean I, Brisson C, Blanquier B, Fevre-Montange M, Bernard A, Loth P, Georges-Courbot M-C, Chevallier M, Akaoka H, Marianneau P, Lam SK, Wild TF, Deubel V**. 2003. A golden hamster model for human acute Nipah virus infection. Am. J. Pathol. **163**:2127–37.

51. **De Wit E, Bushmaker T, Scott D, Feldmann H, Munster VJ**. 2011. Nipah virus transmission in a hamster model. PLoS Negl. Trop. Dis. **5**:e1432.

52. **De Wit E, Prescott J, Falzarano D, Bushmaker T, Scott D, Feldmann H, Munster VJ**. 2014. Foodborne transmission of nipah virus in Syrian hamsters. PLoS Pathog. **10**:e1004001.

53. **Rockx B, Brining D, Kramer J, Callison J, Ebihara H, Mansfield K, Feldmann H**. 2011. Clinical outcome of henipavirus infection in hamsters is determined by the route and dose of infection. J. Virol. **85**:7658–71.

54. **Bossart KN, Zhu Z, Middleton D, Klippel J, Crameri G, Bingham J, McEachern JA, Green D, Hancock TJ, Chan Y-P, Hickey AC, Dimitrov DS, Wang L-F, Broder CC**. 2009. A neutralizing human monoclonal antibody protects against lethal disease in a new ferret model of acute nipah virus infection. PLoS Pathog. **5**:e1000642.

55. **Marianneau P, Guillaume V, Wong T, Badmanathan M, Looi RY, Murri S, Loth P, Tordo N, Wild F, Horvat B, Contamin H**. 2010. Experimental infection of squirrel monkeys with nipah virus. Emerg. Infect. Dis. **16**:507–10.

56. **Geisbert TW, Daddario-DiCaprio KM, Hickey AC, Smith MA, Chan Y-P, Wang L-F, Mattapallil JJ, Geisbert JB, Bossart KN, Broder CC**. 2010. Development of an acute and highly pathogenic nonhuman primate model of Nipah virus infection. PLoS One **5**:e10690.

57. **Ali R, Mounts AW, Parashar UD, Sahani M, Lye MS, Isa MM, Balathevan K, Arif MT, Ksiazek TG**. 2001. Nipah virus among military personnel involved in pig culling during an outbreak of encephalitis in Malaysia, 1998-1999. Emerg. Infect. Dis. **7**:759–61.

58. **Mounts AW, Kaur H, Parashar UD, Ksiazek TG, Cannon D, Arokiasamy JT, Anderson LJ, Lye MS**. 2001. A cohort study of health care workers to assess nosocomial transmissibility of Nipah virus, Malaysia, 1999. J. Infect. Dis. **183**:810–3.

59. **Tan K, Sarji SA, Tan C, Abdullah B, Chong HT, Thayaparan T, Koh C-N**. 2000. Patients with asymptomatic Nipah virus infection may have abnormal cerebral MR imaging. Neurol. J. southwest Asia **5**:69–73.

60. **Rahman MMA, Hossain MJ, Sultana S, Homaira N, Khan SU, Gurley ES, Rollin PE, Lo MK, Comer JA, Lowe L, Rota PA, Ksiazek TG, Kenah E, Sharker Y, Luby SP**. 2012. Date palm sap linked to Nipah virus outbreak in Bangladesh, 2008. Vector Borne Zoonotic Dis. **12**:65–72.

61. **Nahar N, Sultana R, Gurley ES, Hossain MJ, Luby SP**. 2010. Date palm sap collection: exploring opportunities to prevent Nipah transmission. Ecohealth **7**:196–203.

62. **Luby SP, Gurley ES**. 2012. Epidemiology of henipavirus disease in humans. Curr. Top. Microbiol. Immunol. **359**:25–40.

63. **Montgomery JM, Hossain MJ, Gurley E, Carroll GDS, Croisier A, Bertherat E, Asgari N, Formenty P, Keeler N, Comer J, Bell MR, Akram K, Molla AR, Zaman K, Islam MR, Wagoner K, Mills JN, Rollin PE, Ksiazek TG, Breiman RF**. 2008. Risk factors for Nipah virus encephalitis in Bangladesh. Emerg. Infect. Dis. **14**:1526–32.

64. **Fogarty R, Halpin K, Hyatt AD, Daszak P, Mungall BA**. 2008. Henipavirus susceptibility to environmental variables. Virus Res. **132**:140–4.

65. **Blum LS, Khan R, Nahar N, Breiman RF**. 2009. In-Depth Assessment of an Outbreak of Nipah Encephalitis with Person-to-Person Transmission in Bangladesh: Implications for Prevention and Control Strategies. Am J Trop Med Hyg **80**:96–102.

66. **Homaira N, Rahman M, Hossain MJ, Epstein JH, Sultana R, Khan MSU, Podder G, Nahar K, Ahmed B, Gurley ES, Daszak P, Lipkin WI, Rollin PE, Comer JA, Ksiazek TG, Luby SP**. 2010. Nipah virus outbreak with person-to-person transmission in a district of Bangladesh, 2007. Epidemiol. Infect. **138**:1630–6.

67. **Gurley ES, Montgomery JM, Hossain MJ, Bell M, Azad AK, Islam MR, Molla MAR, Carroll DS, Ksiazek TG, Rota PA, Lowe L, Comer JA, Rollin P, Czub M, Grolla A, Feldmann H, Luby SP, Woodward JL, Breiman RF**. 2007. Person-to-person transmission of Nipah virus in a Bangladeshi community. Emerg. Infect. Dis. **13**:1031–7.

68. **Luby SP**. 2013. The pandemic potential of Nipah virus. Antiviral Res. **100**:38–43.

69. **Chadha MS, Comer JA, Lowe L, Rota PA, Rollin PE, Bellini WJ, Ksiazek TG, Mishra A**. 2006. Nipah virus-associated encephalitis outbreak, Siliguri, India. Emerg. Infect. Dis. **12**:235–40.

70. **Sazzad HMS, Hossain MJ, Gurley ES, Ameen KMH, Parveen S, Islam MS, Faruque LI, Podder G, Banu SS, Lo MK, Rollin PE, Rota PA, Daszak P, Rahman M, Luby SP**. 2013. Nipah virus infection outbreak with nosocomial and corpse-to-human transmission, Bangladesh. Emerg. Infect. Dis. **19**:210–7.

71. **Tan CT, Tan KS**. 2001. Nosocomial transmissibility of Nipah virus. J. Infect. Dis. **184**:1367.

72. **Clayton BA, Middleton D, Bergfeld J, Haining J, Arkinstall R, Wang L, Marsh GA**. 2012. Transmission routes for nipah virus from Malaysia and Bangladesh. Emerg. Infect. Dis. **18**:1983–93.

73. **Hossain MJ, Gurley ES, Montgomery JM, Bell M, Carroll DS, Hsu VP, Formenty P, Croisier A, Bertherat E, Faiz MA, Azad AK, Islam R, Molla MAR, Ksiazek TG, Rota PA, Comer JA, Rollin PE, Luby SP, Breiman RF**. 2008. Clinical presentation of nipah virus infection in Bangladesh. Clin. Infect. Dis. **46**:977–84.

74. **Goh KJ, Tan CT, Chew NK, Tan PS, Kamarulzaman A, Sarji SA, Wong KT, Abdullah BJ, Chua KB, Lam SK**. 2000. Clinical features of Nipah virus encephalitis among pig farmers in Malaysia. N. Engl. J. Med. **342**:1229–35.

75. **Wong KT, Shieh W-J, Kumar S, Norain K, Abdullah W, Guarner J, Goldsmith CS, Chua KB, Lam SK, Tan CT, Goh KJ, Chong HT, Jusoh R, Rollin PE, Ksiazek TG, Zaki SR**. 2002. Nipah virus infection: pathology and pathogenesis of an emerging paramyxoviral zoonosis. Am. J. Pathol. **161**:2153–67.

76. **Paton NI, Leo YS, Zaki SR, Auchus AP, Lee KE, Ling AE, Chew SK, Ang B, Rollin PE, Umapathi T, Sng I, Lee CC, Lim E, Ksiazek TG**. 1999. Outbreak of Nipah-virus infection among abattoir workers in Singapore. Lancet **354**:1253–6.

77. **Sarji SA, Abdullah BJ, Goh KJ, Tan CT, Wong KT**. 2000. MR imaging features of Nipah encephalitis. AJR. Am. J. Roentgenol. **175**:437–42.

78. **Tan CT, Goh KJ, Wong KT, Sarji SA, Chua KB, Chew NK, Murugasu P, Loh YL, Chong HT, Tan KS, Thayaparan T, Kumar S, Jusoh MR**. 2002. Relapsed and late-onset Nipah encephalitis. Ann. Neurol. **51**:703–8.

79. **Sejvar JJ, Hossain J, Saha SK, Gurley ES, Banu S, Hamadani JD, Faiz MA, Siddiqui FM, Mohammad QD, Mollah AH, Uddin R, Alam R, Rahman R,**

Tan CT, Bellini W, Rota P, Breiman RF, Luby SP. 2007. Long-term neurological and functional outcome in Nipah virus infection. Ann. Neurol. **62**:235–42.

80. **Hooper P, Zaki S, Daniels P, Middleton D**. 2001. Comparative pathology of the diseases caused by Hendra and Nipah viruses. Microbes Infect. **3**:315–22.

81. **Abdullah S, Chang L, Rahmat K, Goh KJ, Tin C**. 2012. Late-onset Nipah virus encephalitis 11 years after the initial outbreak : A case report. Neurol. Asia **17**:71–74.

82. **Pernet O, Wang YE, Lee B**. 2012. Henipavirus receptor usage and tropism. Curr. Top. Microbiol. Immunol. **359**:59–78.

83. **Mathieu C, Pohl C, Szecsi J, Trajkovic-Bodennec S, Devergnas S, Raoul H, Cosset F-L, Gerlier D, Wild TF, Horvat B**. 2011. Nipah virus uses leukocytes for efficient dissemination within a host. J. Virol. **85**:7863–71.

84. **Vigant F, Lee B**. 2011. Hendra and nipah infection: pathology, models and potential therapies. Infect. Disord. Drug Targets **11**:315–36.

85. **Chong HT, Kamarulzaman A, Tan CT, Goh KJ, Thayaparan T, Kunjapan SR, Chew NK, Chua KB, Lam SK**. 2001. Treatment of acute Nipah encephalitis with ribavirin. Ann. Neurol. **49**:810–3.

86. **Snell NJC**. 2004. Ribavirin therapy for Nipah virus infection. J. Virol. **78**:10211.

87. **Aljofan M, Porotto M, Moscona A, Mungall BA**. 2008. Development and validation of a chemiluminescent immunodetection assay amenable to high throughput screening of antiviral drugs for Nipah and Hendra virus. J. Virol. Methods **149**:12–9.

88. **Aljofan M, Saubern S, Meyer AG, Marsh G, Meers J, Mungall BA**. 2009. Characteristics of Nipah virus and Hendra virus replication in different cell lines and their suitability for antiviral screening. Virus Res. **142**:92–9.

89. **Wright PJ, Crameri G, Eaton BT**. 2005. RNA synthesis during infection by Hendra virus: an examination by quantitative real-time PCR of RNA accumulation, the effect of ribavirin and the attenuation of transcription. Arch. Virol. **150**:521–32.

90. **Freiberg AN, Worthy MN, Lee B, Holbrook MR**. 2010. Combined chloroquine and ribavirin treatment does not prevent death in a hamster model of Nipah and Hendra virus infection. J. Gen. Virol. **91**:765–72.

91. **Georges-Courbot MC, Contamin H, Faure C, Loth P, Baize S, Leyssen P, Neyts J, Deubel V**. 2006. Poly(I)-poly(C12U) but not ribavirin prevents death in a hamster model of Nipah virus infection. Antimicrob. Agents Chemother. **50**:1768–72.

92. **Rockx B, Bossart KN, Feldmann F, Geisbert JB, Hickey AC, Brining D, Callison J, Safronetz D, Marzi A, Kercher L, Long D, Broder CC, Feldmann H, Geisbert TW**. 2010. A novel model of lethal Hendra virus infection in African green monkeys and the effectiveness of ribavirin treatment. J. Virol. **84**:9831–9.

93. **Porotto M, Doctor L, Carta P, Fornabaio M, Greengard O, Kellogg GE, Moscona A**. 2006. Inhibition of hendra virus fusion. J. Virol. **80**:9837–49.

94. **Porotto M, Yokoyama CC, Palermo LM, Mungall B, Aljofan M, Cortese R, Pessi A, Moscona A**. 2010. Viral entry inhibitors targeted to the membrane site of action. J. Virol. **84**:6760–8.

95. **Bossart KN, Mungall BA, Crameri G, Wang L-F, Eaton BT, Broder CC**. 2005. Inhibition of Henipavirus fusion and infection by heptad-derived peptides of the Nipah virus fusion glycoprotein. Virol. J. **2**:57.

96. **Porotto M, Carta P, Deng Y, Kellogg GE, Whitt M, Lu M, Mungall BA, Moscona A**. 2007. Molecular determinants of antiviral potency of paramyxovirus entry inhibitors. J. Virol. **81**:10567–74.

97. **Porotto M, Rockx B, Yokoyama CC, Talekar A, Devito I, Palermo LM, Liu J, Cortese R, Lu M, Feldmann H, Pessi A, Moscona A**. 2010. Inhibition of Nipah virus infection in vivo: targeting an early stage of paramyxovirus fusion activation during viral entry. PLoS Pathog. **6**:e1001168.

98. **Steffen DL, Xu K, Nikolov DB, Broder CC**. 2012. Henipavirus mediated membrane fusion, virus entry and targeted therapeutics. Viruses **4**:280–308.

99. **Guillaume V, Contamin H, Loth P, Georges-Courbot M-C, Lefeuvre A, Marianneau P, Chua KB, Lam SK, Buckland R, Deubel V, Wild TF**. 2004. Nipah virus: vaccination and passive protection studies in a hamster model. J. Virol. **78**:834–40.

100. **Guillaume V, Contamin H, Loth P, Grosjean I, Courbot MCG, Deubel V, Buckland R, Wild TF**. 2006. Antibody prophylaxis and therapy against Nipah virus infection in hamsters. J. Virol. **80**:1972–8.

101. **Zhu Z, Dimitrov AS, Bossart KN, Crameri G, Bishop KA, Choudhry V, Mungall BA, Feng Y-RY, Choudhary A, Zhang M-Y, Wang L-F, Xiao X, Eaton BT, Broder CC, Dimitrov DS**. 2006. Potent neutralization of Hendra and Nipah viruses by human monoclonal antibodies. J. Virol. **80**:891–9.

102. **Zhu Z, Bossart KN, Bishop KA, Crameri G, Dimitrov AS, McEachern JA, Feng Y, Middleton D, Wang L-F, Broder CC, Dimitrov DS**. 2008. Exceptionally potent cross-reactive neutralization of Nipah and Hendra viruses by a human monoclonal antibody. J. Infect. Dis. **197**:846–53.

103. **Bossart KN, Geisbert TW, Feldmann H, Zhu Z, Feldmann F, Geisbert JB, Yan L, Feng Y-R, Brining D, Scott D, Wang Y, Dimitrov AS, Callison J, Chan Y-P, Hickey AC, Dimitrov DS, Broder CC, Rockx B**. 2011. A neutralizing human monoclonal antibody protects african green monkeys from hendra virus challenge. Sci. Transl. Med. **3**:105ra103.

104. **Geisbert TW, Mire CE, Geisbert JB, Chan Y-P, Agans KN, Feldmann F, Fenton KA, Zhu Z, Dimitrov DS, Scott DP, Bossart KN, Feldmann H, Broder CC**. 2014. Therapeutic Treatment of Nipah Virus Infection in Nonhuman Primates with a Neutralizing Human Monoclonal Antibody. Sci. Transl. Med. **6**:242ra82–242ra82.

105. **Kong D, Wen Z, Su H, Ge J, Chen W, Wang X, Wu C, Yang C, Chen H, Bu Z**. 2012. Newcastle disease virus-vectored Nipah encephalitis vaccines induce B and T cell responses in mice and long-lasting neutralizing antibodies in pigs. Virology **432**:327–35.

106. **Defang GN, Khetawat D, Broder CC, Quinnan G V**. 2010. Induction of neutralizing antibodies to Hendra and Nipah glycoproteins using a Venezuelan equine encephalitis virus in vivo expression system. Vaccine **29**:212–20.

107. **Wang X, Ge J, Hu S, Wang Q, Wen Z, Chen H, Bu Z**. 2006. Efficacy of DNA immunization with F and G protein genes of Nipah virus. Ann. N. Y. Acad. Sci. **1081**:243–5.

108. **Ploquin A, Szécsi J, Mathieu C, Guillaume V, Barateau V, Ong KC, Wong KT, Cosset F-L, Horvat B, Salvetti A**. 2013. Protection against henipavirus infection by use of recombinant adeno-associated virus-vector vaccines. J. Infect. Dis. **207**:469–78.

109. **Mungall BA, Middleton D, Crameri G, Bingham J, Halpin K, Russell G, Green D, McEachern J, Pritchard LI, Eaton BT, Wang L-F, Bossart KN, Broder CC**. 2006. Feline model of acute nipah virus infection and protection with a soluble glycoprotein-based subunit vaccine. J. Virol. **80**:12293–302.

110. **McEachern JA, Bingham J, Crameri G, Green DJ, Hancock TJ, Middleton D, Feng Y-R, Broder CC, Wang L-F, Bossart KN**. 2008. A recombinant subunit vaccine formulation protects against lethal Nipah virus challenge in cats. Vaccine **26**:3842–52.

111. **Pallister JA, Klein R, Arkinstall R, Haining J, Long F, White JR, Payne J, Feng Y-R, Wang L-F, Broder CC, Middleton D**. 2013. Vaccination of ferrets with a recombinant G glycoprotein subunit vaccine provides protection against Nipah virus disease for over 12 months. Virol. J. **10**:237.

112. **Chattopadhyay A, Rose JK**. 2011. Complementing defective viruses that express separate paramyxovirus glycoproteins provide a new vaccine vector approach. J. Virol. **85**:2004–11.

113. **Lo MK, Bird BH, Chattopadhyay A, Drew CP, Martin BE, Coleman JD, Rose JK, Nichol ST, Spiropoulou CF**. 2013. Single-Dose Replication-Defective VSV-based Nipah Virus Vaccines Provide Protection from Lethal Challenge in Syrian Hamsters. Antiviral Res. **101**:26–9.

114. **Mire CE, Versteeg KM, Cross RW, Agans KN, Fenton KA, Whitt MA, Geisbert TW**. 2013. Single injection recombinant vesicular stomatitis virus vaccines protect ferrets against lethal Nipah virus disease. Virol. J. **10**:353.

115. **Yoneda M, Georges-Courbot M-C, Ikeda F, Ishii M, Nagata N, Jacquot F, Raoul H, Sato H, Kai C**. 2013. Recombinant measles virus vaccine expressing the Nipah virus glycoprotein protects against lethal Nipah virus challenge. PLoS One **8**:e58414.

116. **Walpita P, Barr J, Sherman M, Basler CF, Wang L**. 2011. Vaccine potential of Nipah virus-like particles. PLoS One **6**:e18437.

117. **Wild TF**. 2009. Henipaviruses: a new family of emerging Paramyxoviruses. Pathol. Biol. (Paris). **57**:188–96.

118. **Uppal PK**. 2000. Emergence of Nipah virus in Malaysia. Ann. N. Y. Acad. Sci. **916**:354–7.

119. **Field HE, Mackenzie JS, Daszak P**. 2007. Henipaviruses: emerging paramyxoviruses associated with fruit bats. Curr. Top. Microbiol. Immunol. **315**:133–59.

120. **Lo MK, Rota PA**. 2008. The emergence of Nipah virus, a highly pathogenic paramyxovirus. J. Clin. Virol. **43**:396–400.

121. **Hsu VP, Hossain MJ, Parashar UD, Ali MM, Ksiazek TG, Kuzmin I, Niezgoda M, Rupprecht C, Bresee J, Breiman RF**. 2004. Nipah virus encephalitis reemergence, Bangladesh. Emerg. Infect. Dis. **10**:2082–7.

122. **Bellini WJ, Harcourt BH, Bowden N, Rota PA**. 2005. Nipah virus: an emergent paramyxovirus causing severe encephalitis in humans. J. Neurovirol. **11**:481–7.

123. **Quddus R, Alam S, Majumdar MA, Anwar S, Zahid AKS, Khan M, Arif SM, Alam R, Siddique FM, Tan CT, Faiz MA**. 2004. A report of 4 patients with Nipah encephalitis from Rajbari district , Bangladesh in the January 2004 outbreak. Neurol. Asia **9**:33–37.

124. **Geisbert TW, Feldmann H, Broder CC**. 2012. Animal challenge models of henipavirus infection and pathogenesis. Curr. Top. Microbiol. Immunol. **359**:153–77.

125. **Harcourt BH, Tamin A, Ksiazek TG, Rollin PE, Anderson LJ, Bellini WJ, Rota PA**. 2000. Molecular characterization of Nipah virus, a newly emergent paramyxovirus. Virology **271**:334–49.

126. **Zivcec M, Safronetz D, Haddock E, Feldmann H, Ebihara H**. 2011. Validation of assays to monitor immune responses in the Syrian golden hamster (Mesocricetus auratus). J. Immunol. Methods **368**:24–35.

127. **Erbar S, Maisner A**. 2010. Nipah virus infection and glycoprotein targeting in endothelial cells. Virol. J. **7**:305.

128. **Weise C, Erbar S, Lamp B, Vogt C, Diederich S, Maisner A**. 2010. Tyrosine residues in the cytoplasmic domains affect sorting and fusion activity of the Nipah virus glycoproteins in polarized epithelial cells. J. Virol. **84**:7634–41.

129. **Wurth MA, Schowalter RM, Smith EC, Moncman CL, Dutch RE, McCann RO**. 2010. The actin cytoskeleton inhibits pore expansion during PIV5 fusion protein-promoted cell-cell fusion. Virology **404**:117–26.

130. **Harit AK, Ichhpujani RL, Gupta S, Gill KS, Lal S, Ganguly NK, Agarwal SP**. 2006. Nipah/Hendra virus outbreak in Siliguri, West Bengal, India in 2001. Indian J. Med. Res. **123**:553–60.

131. **Luby SP, Rahman M, Hossain MJ, Blum LS, Husain MM, Gurley E, Khan R, Ahmed B-N, Rahman S, Nahar N, Kenah E, Comer JA, Ksiazek TG**. 2006. Foodborne transmission of Nipah virus, Bangladesh. Emerg. Infect. Dis. **12**:1888–94.

132. **Chua KB, Lam SK, Goh KJ, Hooi PS, Ksiazek TG, Kamarulzaman A, Olson J, Tan CT**. 2001. The presence of Nipah virus in respiratory secretions and urine of patients during an outbreak of Nipah virus encephalitis in Malaysia. J. Infect. **42**:40–3.

133. **Lo MK, Miller D, Aljofan M, Mungall BA, Rollin PE, Bellini WJ, Rota PA**. 2010. Characterization of the antiviral and inflammatory responses against Nipah virus in endothelial cells and neurons. Virology **404**:78–88.

134. **Mathieu C, Guillaume V, Sabine A, Ong KC, Wong KT, Legras-Lachuer C, Horvat B**. 2012. Lethal Nipah virus infection induces rapid overexpression of CXCL10. PLoS One **7**:e32157.

135. **Teruya-Feldstein J, Jaffe ES, Burd PR, Kanegane H, Kingma DW, Wilson WH, Longo DL, Tosato G**. 1997. The role of Mig, the monokine induced by interferon-gamma, and IP-10, the interferon-gamma-inducible protein-10, in tissue necrosis and vascular damage associated with Epstein-Barr virus-positive lymphoproliferative disease. Blood **90**:4099–105.

136. **Sauty A, Dziejman M, Taha RA, Iarossi AS, Neote K, Garcia-Zepeda EA, Hamid Q, Luster AD**. 1999. The T cell-specific CXC chemokines IP-10, Mig, and I-TAC are expressed by activated human bronchial epithelial cells. J. Immunol. **162**:3549–58.

137. **Akira S, Hirano T, Taga T, Kishimoto T**. 1990. Biology of multifunctional cytokines: IL 6 and related molecules (IL 1 and TNF). FASEB J. **4**:2860–7.

138. **Stachowiak B, Weingartl HM**. 2012. Nipah virus infects specific subsets of porcine peripheral blood mononuclear cells. PLoS One **7**:e30855.

139. **Sundararajan A, Huan L, Richards KA, Marcelin G, Alam S, Joo H, Yang H, Webby RJ, Topham DJ, Sant AJ, Sangster MY**. 2012. Host differences in influenza-specific CD4 T cell and B cell responses are modulated by viral strain and route of immunization. PLoS One **7**:e34377.

140. **DeBuysscher BL, de Wit E, Munster VJ, Scott D, Feldmann H, Prescott J**. 2013. Comparison of the pathogenicity of Nipah virus isolates from Bangladesh and Malaysia in the Syrian hamster. PLoS Negl. Trop. Dis. **7**:e2024.

141. **Wong KT, Tan CT**. 2012. Clinical and pathological manifestations of human henipavirus infection. Curr. Top. Microbiol. Immunol. **359**:95–104.

142. **Jacoby RO, Johnson EA, Paturzo FX, Ball-Goodrich L**. 2000. Persistent Rat Virus Infection in Smooth Muscle of Euthymic and Athymic Rats. J. Virol. **74**:11841–11848.

143. **Tumilowicz JJ, Gawlik ME, Powell BB, Trentin JJ**. 1985. Replication of cytomegalovirus in human arterial smooth muscle cells. J. Virol. **56**:839–845.

144. **Lemström KB, Bruning JH, Bruggeman CA, Lautenschlager IT, Häyry PJ**. 1993. Cytomegalovirus infection enhances smooth muscle cell proliferation and intimal thickening of rat aortic allografts. J. Clin. Invest. **92**:549–58.

145. **Jenson HB, Montalvo EA, McClain KL, Ench Y, Heard P, Christy BA, Dewalt-Hagan PJ, Moyer MP**. 1999. Characterization of natural Epstein-Barr

virus infection and replication in smooth muscle cells from a leiomyosarcoma. J. Med. Virol. **57**:36–46.

146. **Burch GE, Harb JM**. 1973. Encephalomyocarditis (EMC) virus infection of the mouse aorta. Am. Heart J. **86**:669–675.

147. **MELNICK J**. 1983. CYTOMEGALOVIRUS ANTIGEN WITHIN HUMAN ARTERIAL SMOOTH MUSCLE CELLS. Lancet **322**:644–647.

148. **Biering SB, Huang A, Vu AT, Robinson LR, Bradel-Tretheway B, Choi E, Lee B, Aguilar HC**. 2012. N-Glycans on the Nipah virus attachment glycoprotein modulate fusion and viral entry as they protect against antibody neutralization. J. Virol. **86**:11991–2002.

149. **Aguilar HC, Iorio RM**. 2012. Henipavirus membrane fusion and viral entry. Curr. Top. Microbiol. Immunol. **359**:79–94.

150. **Gale NW, Baluk P, Pan L, Kwan M, Holash J, DeChiara TM, McDonald DM, Yancopoulos GD**. 2001. Ephrin-B2 selectively marks arterial vessels and neovascularization sites in the adult, with expression in both endothelial and smooth-muscle cells. Dev. Biol. **230**:151–60.

151. **Dhiman N, Jacobson RM, Poland GA**. Measles virus receptors: SLAM and CD46. Rev. Med. Virol. **14**:217–29.

152. **Campbell GR, Campbell JH, Manderson JA, Horrigan S, Rennick RE**. 1988. Arterial smooth muscle. A multifunctional mesenchymal cell. Arch. Pathol. Lab. Med. **112**:977–86.

153. **E Csonka PIB**. 1990. Influence of the measles virus on the proliferation and protein synthesis of aortic endothelial and smooth muscle cells. Acta Microbiol. Hung. **37**:193 – 200.

154. **Chong HT, Hossain MJ, Tan CT**. 2008. Differences in epidemiologic and clinical features of Nipah virus encephalitis between the Malaysian and Bangladesh outbreaks. Neurol. Asia **13**:23–26.

155. **Bossart KN, Rockx B, Feldmann F, Brining D, Scott D, LaCasse R, Geisbert JB, Feng Y-R, Chan Y-P, Hickey AC, Broder CC, Feldmann H, Geisbert TW**. 2012. A Hendra virus G glycoprotein subunit vaccine protects African green monkeys from Nipah virus challenge. Sci. Transl. Med. **4**:146ra107.

156. **Prescott J, de Wit E, Feldmann H, Munster VJ**. 2012. The immune response to Nipah virus infection. Arch. Virol. **157**:1635–41.

157. **Lawson ND, Stillman EA, Whitt MA, Rose JK**. 1995. Recombinant vesicular stomatitis viruses from DNA. Proc. Natl. Acad. Sci. U. S. A. **92**:4477–81.

158. **Cobleigh MA, Wei X, Robek MD**. 2013. A vesicular stomatitis virus-based therapeutic vaccine generates a functional CD8 T cell response to hepatitis B virus in transgenic mice. J. Virol. **87**:2969–73.

159. **Geisbert TW, Feldmann H**. 2011. Recombinant vesicular stomatitis virus-based vaccines against Ebola and Marburg virus infections. J. Infect. Dis. **204 Suppl** :S1075–81.

160. **Brown KS, Safronetz D, Marzi A, Ebihara H, Feldmann H**. 2011. Vesicular Stomatitis Virus-Based Vaccine Protects Hamsters against Lethal Challenge with Andes Virus. J. Virol. **85**:12781–12791.

161. **Anjeanette Roberts EKASPJFRPLBYKJKR, Roberts A, Kretzschmar E, Perkins AS, Forman J, Price R, Buonocore L, Kawaoka Y, Rose JK**. 1998. Vaccination with a Recombinant Vesicular Stomatitis Virus Expressing an Influenza Virus Hemagglutinin Provides Complete Protection from Influenza Virus Challenge. J. Virol. **72**:4704–4711.

162. **Steven R Wilson JHWLBAPJKRJDR**. 2008. Intranasal Immunization with Recombinant Vesicular Stomatitis Virus Expressing Murine Cytomegalovirus Glycoprotein B Induces Humoral and Cellular Immunity. Comp. Med. American Association for Laboratory Animal Science.

163. **Ito N, Takayama-Ito M, Yamada K, Hosokawa J, Sugiyama M, Minamoto N**. 2003. Improved recovery of rabies virus from cloned cDNA using a vaccinia virus-free reverse genetics system. Microbiol Immunol. **47**:613–7.

164. **Garbutt M, Liebscher R, Wahl-Jensen V, Jones S, Möller P, Wagner R, Volchkov V, Klenk H-D, Feldmann H, Ströher U**. 2004. Properties of replication-competent vesicular stomatitis virus vectors expressing glycoproteins of filoviruses and arenaviruses. J. Virol. **78**:5458–65.

165. **Tsuda Y, Safronetz D, Brown K, LaCasse R, Marzi A, Ebihara H, Feldmann H**. 2011. Protective efficacy of a bivalent recombinant vesicular stomatitis virus vaccine in the Syrian hamster model of lethal Ebola virus infection. J. Infect. Dis. **204 Suppl** :S1090–7.

166. **Kapadia SU, Rose JK, Lamirande E, Vogel L, Subbarao K, Roberts A**. 2005. Long-term protection from SARS coronavirus infection conferred by a single immunization with an attenuated VSV-based vaccine. Virology **340**:174–82.

167. **Mire CE, Miller AD, Carville A, Westmoreland S V, Geisbert JB, Mansfield KG, Feldmann H, Hensley LE, Geisbert TW**. 2012. Recombinant vesicular

stomatitis virus vaccine vectors expressing filovirus glycoproteins lack neurovirulence in nonhuman primates. PLoS Negl. Trop. Dis. **6**:e1567.

168. **Günther S, Feldmann H, Geisbert TW, Hensley LE, Rollin PE, Nichol ST, Ströher U, Artsob H, Peters CJ, Ksiazek TG, Becker S, ter Meulen J, Olschläger S, Schmidt-Chanasit J, Sudeck H, Burchard GD, Schmiedel S**. 2011. Management of accidental exposure to Ebola virus in the biosafety level 4 laboratory, Hamburg, Germany. J. Infect. Dis. **204 Suppl** :S785–90.

169. **Brody JA, Fischer GF, Peralta PH**. 1967. Vesicular stomatitis virus in Panama. Human serologic patterns in a cattle raising area. Am. J. Epidemiol. **86**:158–61.

170. **Lyles DS, Rupprecht CE**. 2007. Rhabdoviridae, p. 1364–1409. *In* Knipe, DM (ed.), Fields Virology, 5th ed. Lippincott Williams & Wilkins, Philadelphia, PA.

171. **Feldmann H, Geisbert TW**. 2011. Ebola haemorrhagic fever. Lancet **377**:849–62.

172. **Yewdell JW, Norbury CC, Bennink JR**. 1999. Mechanisms of exogenous antigen presentation by MHC class I molecules in vitro and in vivo: implications for generating CD8+ T cell responses to infectious agents, tumors, transplants, and vaccines. Adv. Immunol. **73**:1–77.

173. **Banchereau J, Steinman RM**. 1998. Dendritic cells and the control of immunity. Nature **392**:245–52.

174. **Palin A, Chattopadhyay A, Park S, Delmas G, Suresh R, Senina S, Perlin DS, Rose JK**. 2007. An optimized vaccine vector based on recombinant vesicular stomatitis virus gives high-level, long-term protection against Yersinia pestis challenge. Vaccine **25**:741–50.

175. **Schwartz JA, Buonocore L, Suguitan AL, Silaghi A, Kobasa D, Kobinger G, Feldmann H, Subbarao K, Rose JK**. 2010. Potent vesicular stomatitis virus-based avian influenza vaccines provide long-term sterilizing immunity against heterologous challenge. J. Virol. **84**:4611–8.

176. **Feldmann H, Jones SM, Daddario-DiCaprio KM, Geisbert JB, Ströher U, Grolla A, Bray M, Fritz EA, Fernando L, Feldmann F, Hensley LE, Geisbert TW**. 2007. Effective Post-Exposure Treatment of Ebola Infection. PLoS Pathog. **3**:e2.

177. **Geisbert TW, Hensley LE, Geisbert JB, Leung A, Johnson JC, Grolla A, Feldmann H**. 2010. Postexposure treatment of Marburg virus infection. Emerg. Infect. Dis. **16**:1119–22.

178. **Debuysscher BL, Scott D, Marzi A, Prescott J, Feldmann H**. 2014. Single-dose live-attenuated Nipah virus vaccines confer complete protection by eliciting antibodies directed against surface glycoproteins. Vaccine.

179. **Kruse H, Kirkemo A-M HK**. 2004. Wildlife as Source of Zoonotic Infections. Emerg. Infect. Dis. **10**.

180. **Cabello C C, Cabello C F**. 2008. Zoonoses with wildlife reservoirs: a threat to public health and the economy. Rev. Med. Chil. **136**:385–93.

181. **Taylor LH, Latham SM, Woolhouse ME**. 2001. Risk factors for human disease emergence. Philos. Trans. R. Soc. Lond. B. Biol. Sci. **356**:983–9.

182. **Bengis RG, Leighton FA, Fischer JR, Artois M, Mörner T, Tate CM**. 2004. The role of wildlife in emerging and re-emerging zoonoses. Rev. Sci. Tech. **23**:497–511.

183. **Brown C**. 2004. Emerging zoonoses and pathogens of public health significance--an overview. Rev. Sci. Tech. **23**:435–42.

184. **Sachan N, Singh VP**. 2010. Effect of climatic changes on the prevalence of zoonotic diseases. Vet. world **3**:519–522.

185. **ND W, P D, AM K, Burke D**. 2005. Bushmeat Hunting, Deforestation, and Prediction of Zoonotic Disease - Volume 11, Number 12—December 2005 - Emerging Infectious Disease journal - CDC. Emerg. Infect. Dis. **11**.

186. **ND W, P D, AM K, Burke D**. 2005. Bushmeat Hunting, Deforestation, and Prediction of Zoonotic Disease - Volume 11, Number 12—December 2005 - Emerging Infectious Disease journal - CDC. Emerg. Infect. Dis. **11**.

187. **Nahar N, Mondal UK, Sultana R, Hossain MJ, Khan MSU, Gurley ES, Oliveras E, Luby SP**. 2013. Piloting the use of indigenous methods to prevent Nipah virus infection by interrupting bats' access to date palm sap in Bangladesh. Health Promot. Int. **28**:378–86.

188. Bat Nipah Virus, Thailand - Volume 11, Number 12—December 2005 - Emerging Infectious Disease journal - CDC.

189. **Stone R**. 2011. Epidemiology. Breaking the chain in Bangladesh. Science **331**:1128–31.

190. **Dups J, Middleton D, Long F, Arkinstall R, Marsh GA, Wang L-F**. 2014. Subclinical infection without encephalitis in mice following intranasal exposure to Nipah virus-Malaysia and Nipah virus-Bangladesh. Virol. J. **11**:102.